

**The launching of a prolate-spheroidal body  
in a deep fluid and its descending trajectory**

By

**Bo Yang**

BS (Dalian University of Technology) 2013

A report submitted in partial satisfaction of the  
requirements for the degree of

Master of Science

in

Engineering - Mechanical Engineering

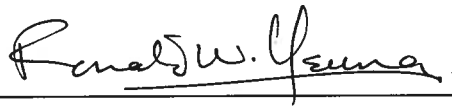
in the

Graduate Division

at

University of California, Berkeley

Committee in charge:

 *Ronald W. Yeung. April 9, 2015*

---

Professor Ronald W. Yeung, Chair



---

Professor Fai Ma

Spring 2015



---

# The launching of a prolate-spheroidal body in a deep fluid and its descending trajectory

---

Bo Yang  
May 13, 2015

## Abstract

In recent decades, a lot of attention has been paid to exploring the deep ocean environment and exploiting benthonic resources. Submarines and unmanned underwater vehicles (UUV) play an important role in this process. In the design stage of these underwater vehicles, it is of great interest to develop a hydrodynamic model, which could help predict their hydrodynamic performance and suggest potential control strategy. In this report, equations of motion for a submerged body of prolate-spheroidal shape are derived by including the consideration of gravitational force, buoyancy, hydrodynamic force. A fully coupled, time-dependent, and nonlinear system is developed. Then, a 4<sup>th</sup>-order Runge-Kutta integration method is used to solve it in MatLab. Instantaneous position, attitude, velocity, and angular velocity are obtained. Then, oscillation of trajectory descending is observed for a prolate spheroid under gravitational force and factors influencing the oscillation period are studied.

Master of Science in Mechanical Engineering  
University of California at Berkeley  
Berkeley, CA 94720-1740  
Professor Ronald W. Yeung, Chair



---

## ACKNOWLEDGMENT

I would like to thank Prof. Ronald W. Yeung for giving me the opportunity to work on this project and it is his patient guidance that enables the completion of this work. Many of my peers in the Computational Marine Mechanics Laboratory (CMML) who have provided support for this work, are truly appreciated. Of course, I acknowledge the understanding and support from my family and friends during the program.

The author is sponsored by Jaehne Graduate Scholarship in his first year of graduate program in UC Berkeley.



# CONTENTS

<b>List of Figures</b>	<b>vii</b>
<b>List of Tables</b>	<b>viii</b>
<b>1 Introduction</b>	<b>1</b>
1.1 Literature Review and Objectives . . . . .	1
1.2 Report Outline . . . . .	3
<b>2 Coordinate Systems and Coordinate Transformation</b>	<b>4</b>
2.1 Coordinate Systems and State Variables . . . . .	4
2.2 Transformation Matrix . . . . .	5
2.2.1 Derivation of $\mathbf{J}_1$ . . . . .	6
<b>3 Gravitational Force and Buoyancy</b>	<b>8</b>
3.1 Gravitational Force in Body Coordinate System . . . . .	8
3.2 Buoyancy in Body Coordinate System . . . . .	9
3.3 Forces Combination and Generalization . . . . .	9
<b>4 Hydrodynamic Force</b>	<b>11</b>
4.1 Added-mass Theory . . . . .	11
4.1.1 Assumptions and Expression of Hydrodynamic Force . . . . .	11
4.1.2 Hydrodynamic Force in terms of Velocity Potential . . . . .	12
4.1.3 Kirchhoff Decomposition . . . . .	13
4.1.4 Added Masses . . . . .	14
4.2 Added Masses for a Prolate Spheroid . . . . .	14
4.2.1 Symmetry Effects . . . . .	15
4.2.2 Analytical Solution for Added Mass of Prolate Spheroid . . . . .	17
4.3 Hydrodynamic Force and Moment for Prolate Spheroid . . . . .	18
4.4 Hydrodynamic Damping . . . . .	19
<b>5 Equations of Motion</b>	<b>20</b>
5.1 Equations of Motion . . . . .	20
5.2 Non-Dimensionalization . . . . .	24
5.3 Analysis of Equations of Motion and Numerical Computations . . . . .	27
5.3.1 Second-Order, Time-Dependent, Nonlinear, Fully coupled System . . . . .	27
5.3.2 Numerical Integration . . . . .	28
<b>6 Simplified Equations of Motion and Numerical Cases</b>	<b>30</b>
6.1 3-degree Freedom In-plane Motion . . . . .	30
6.2 Moving Forward with Oscillation . . . . .	31
6.3 In-plane Motion for Prolate Spheroid with Uniform Density Distribution . . . . .	34
6.4 Energy Conservation . . . . .	36
6.5 Oscillation Period Changes with Release Angle . . . . .	37
6.6 Oscillation Period Changes with Initial Velocity . . . . .	40
<b>7 Conclusions</b>	<b>43</b>
7.1 Summary and Conclusions . . . . .	43
7.2 Future Work . . . . .	43

<b>References</b>	<b>44</b>
<b>A <math>J_2</math></b>	<b>46</b>
<b>B Translational Motion and Rotational Motion</b>	<b>50</b>
B.1 Translational Motion . . . . .	50
B.2 Rotational Motion . . . . .	51
<b>C A Case of Non-uniform Mass Distribution</b>	<b>53</b>
<b>D 3-D Check</b>	<b>56</b>
<b>E MatLab Code</b>	<b>60</b>
E.1 Model Define . . . . .	60
E.2 Processing . . . . .	61
E.3 Post-processing . . . . .	65

# LIST OF FIGURES

1.1	David Bushnells Turtle [3] . . . . .	1
1.2	(a) Ohio class submarine [4] and (b) Russian submarine classes [5] . . . . .	1
1.3	(a) Alvin [7] and (b) Jiaolong [8] . . . . .	2
1.4	Bluefin 21 joining the searching of missing flight [11] . . . . .	2
2.1	Coordinate systems and standard notations [18] . . . . .	4
2.2	Rotation around $O'\hat{z}$ . . . . .	6
2.3	Rotation around $O'\hat{y}$ . . . . .	6
2.4	Rotation around $O'\hat{z}$ . . . . .	7
4.1	Prolate spheroid . . . . .	15
4.2	Transverse section . . . . .	16
6.1	Prolate-spheroidal rigid body with center of mass below center of buoyancy with initial condition as indicated . . . . .	32
6.2	Dimensionless position coordinates and Euler angles of Simulation 1 . . . . .	33
6.3	Free release with $-45^\circ$ . . . . .	34
6.4	Dimensionless position coordinates and Euler angles for Simulation 2 . . . . .	35
6.5	Dimensionless velocity in BFF for Simulation 2 . . . . .	35
6.6	Time history of $\bar{z}$ vs quadratic curve fit . . . . .	36
6.7	Dimensionless energy changes with time . . . . .	37
6.8	Histories of $\bar{x}$ for different release angles . . . . .	38
6.9	Dimensionless periods for change in horizontal position $\bar{x}$ with release angle $\theta_0$ . . . . .	38
6.10	Peaks of change in $\bar{x}$ with the release angle $\theta_0$ . . . . .	39
6.11	Histories of $\theta$ for different release angles . . . . .	39
6.12	Dimensionless periods for $\theta$ change with release angle' . . . . .	40
6.13	Histories of $\bar{x}$ when the release angle $= -\frac{\pi}{4}$ and initial speed is changed . . . . .	41
6.14	Histories of $\theta$ when fix the release angle and change initial speed . . . . .	41
6.15	Periods for $\theta$ vs initial Speed . . . . .	42
C.1	Distribution of density . . . . .	53
D.1	Case 1 . . . . .	56
D.2	Case 2 . . . . .	57
D.3	Case 3 . . . . .	57
D.4	Case 4 . . . . .	58
D.5	Dimensionless position in EFF and attitude . . . . .	58
D.6	Dimensionless velocity in BFF . . . . .	59

# LIST OF TABLES

2.1	Euler angles and fixed axes in three steps . . . . .	5
4.1	Symmetry of prolate spheroid . . . . .	15
5.1	Dimensions of variables . . . . .	24
5.2	Dimensionless variables . . . . .	25
6.1	Parameters of the model for Simulation 1 . . . . .	32
6.2	Parameters of the model for Simulation 2 . . . . .	34
D.1	Release attitudes of Four Cases . . . . .	56
D.2	Parameters of the model . . . . .	56



These streamline slender shapes are structurally efficient to resist high underwater pressure; and at the same time, it helps reduce hydrodynamic resistance. Today, submarine is still popular and important to navies of all countries. By 2014, United States, Russia, and China navies were equipped with 72, 63 and 69 submarines, respectively [6]. Other than military usage, there are small civilian submarines used for tourism, exploration and serving offshore industry.

Submersibles are known as being able to withstand high pressure and dive very deep to the ocean bottom. Because of this, they are widely used for ocean exploration and underwater archeology. Fig. 1.3 shows Alvin of United States and Jiaolong of China. Other well-known submersibles include Epaulard of France, Mir I and II of Russia, and Shinkai 6500 of Japan. All of them are not big in size and could accommodate a few people. Besides, they are not autonomous and need connecting to a support vessel to get replenishment. In addition to manned submersibles, there are also unmanned submersibles towed by ship having sensors for ocean exploration.

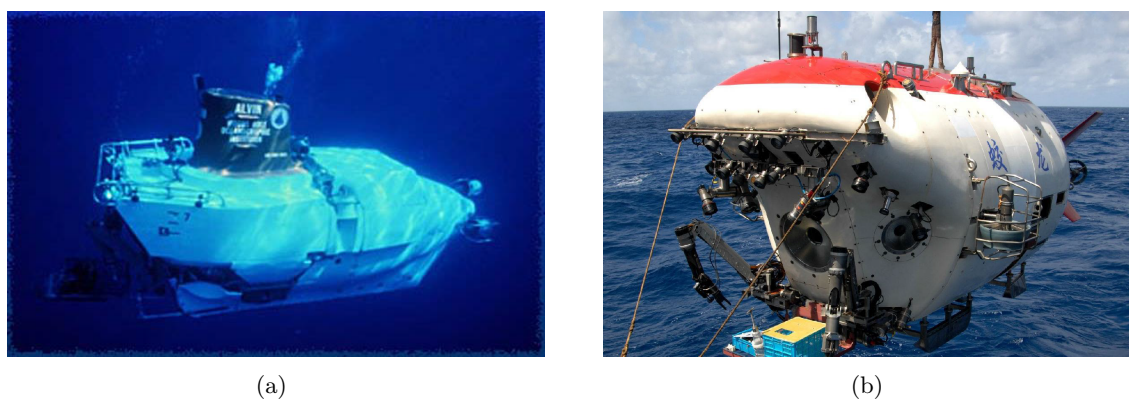


Figure 1.3: (a) Alvin [7] and (b) Jiaolong [8]

UUV can be divided into remotely operated underwater vehicle (ROV) and autonomous underwater vehicle (AUV). Early ROVs fabricated in middle 20th century were mainly used for military usage, such as uncovering torpedoes and mines. Later, it became widely used for offshore oil and gas industry when floating platform moved to deep ocean where divers could not reach.



Figure 1.4: Bluefin 21 joining the searching of missing flight [11]

There is a tether or an umbilical cable connecting ROV to supporting ship on the ocean surface, through which electricity power and control signal are delivered and information is exchanged [2, 9]. Different from ROV, AUV is a mobile robot equipped with a power source. It could travel relatively fast in designed route to accomplish predetermined tasks without requiring control input from crew. Torpedo is thought to be the first AUV; but the real design and development of AUVs began in 1960s [2]. AUVs have big advantages over other underwater vehicles as platforms for all kinds of sensors. Through the last five decades, the technology has quickly developed with support from navies [10]. With the maturity of this technology, it started to be used for ocean oceanography, off-

shore industry, and sea rescues. Fig. 1.4 shows Bluefin 21 being transported to join searching the missing Malaysia Airlines Flight 370 [11]. It is noted that torpedoes-like AUVs and submarines have similar shape since they both require relatively high cruise speed.

Conducting prototype or model test for submarine craft is a costly and time consuming process, especially because of the fact that geometry parameters need to be readjusted to satisfy different requirement. An accurate hydrodynamic model will be of great use to predict the hydrodynamic performance at the early state of design. It can give an insight for the interaction between vehicles and fluid and further suggest appropriate control strategies and parameters. Thus, there has been a lot of work on the equations of motion for underwater vehicles. Morton Gertier and Grant R. Hagen gave standard equations to simulate the trajectories of submarines in six degrees of freedom [12], which was revised by J. Feldman [13]. Thor I. Fossen developed detailed derivation of equations of motion in his book [14]. Meyer Nahon provided a simplified dynamics model by decomposing the vehicle into three constituent elements [15]. Besides, these equations are widely used AUV design process of [9, 16, 17].

## 1.2 REPORT OUTLINE

This report derives the equations of motion for a submerged rigid body (SB) of prolate-spheroidal shape and its motion is simulated by numerical methods. Firstly, earth-fixed and body-fixed coordinate systems are defined and twelve state variables are chosen to describe SB's instantaneous state. Coordinate transformation and relationship between position and velocity variables are derived. Then gravitational force and buoyancy are expressed in both frames; hydrodynamic force is modeled by using added mass theory, and viscosity is considered by including hydrodynamic damping. Acceleration and resultant force are related by Newton's second law and Euler equations. After nondimensionalization, dimensionless equations of motion are obtained. The motion is simulated by numerically integrating dimensionless, nonlinear and fully coupled equations of motion of 6 degrees of freedom. Finally, prolate-spheroidal rigid body's free descending under gravitational is studied. Oscillation is observed and factors influencing the oscillation are discussed.

## CHAPTER 2

### COORDINATE SYSTEMS AND COORDINATE TRANSFORMATION

In this study, the submerged body (SB) is able to have six degrees of freedom including three in translation and the other three in rotation. To describe the motion of SB properly, two right-handed Cartesian coordinate systems are introduced and transformations between the two are derived.

#### 2.1 COORDINATE SYSTEMS AND STATE VARIABLES

Two coordinate systems used here are earth-fixed frame (EFF) and body-fixed frame (BFF), as shown in Fig. 2.1.

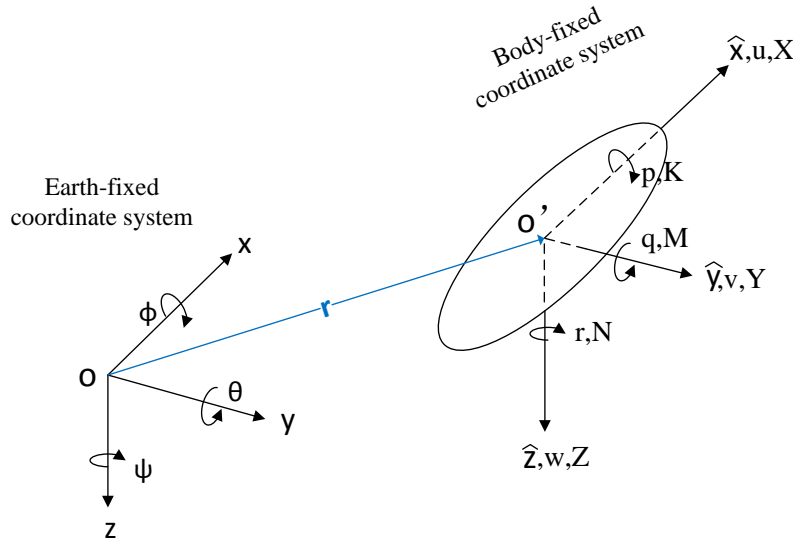


Figure 2.1: Coordinate systems and standard notations [18]

EFF is fixed on the earth. We refer this frame as  $Oxyz$ , as shown in Fig. 2.1 with  $Ox$  pointing north,  $Oy$  east, and  $Oz$  downward. BFF, notated as  $O'\hat{x}\hat{y}\hat{z}$ , is fixed on SB and can move and rotate with SB. This frame's origin  $O'$  is an arbitrary point on SB with  $O'\hat{x}$  pointing forward,  $O'\hat{y}$  portside, and  $O'\hat{z}$  downward.

Standard notation given in [18] is used here to describe SB's state. Position vector from  $O$  to  $O'$ , denoted as  $\mathbf{r}$ , is used to represent the SB's position and has expression of  $[x, y, z]^T$  in EFF. In terms of orientation, Euler angles  $\boldsymbol{\alpha} = [\phi, \theta, \psi]^T$  describe an arbitrary attitude of SB. Resultant force  $\mathbf{F}_r$ , translational velocity  $\mathbf{v}_{O'}$ , moment around  $O'$ ,  $\mathbf{M}_r$ , and angular velocity  $\boldsymbol{\omega}$  are expressed as  $[X, Y, Z]^T$ ,  $[u, v, w]^T$ ,  $[K, M, N]^T$ , and  $[p, q, r]^T$ , respectively in BFF.

Note that starting with EFF, any orientation of BFF can be obtained by a three-step rotation. In each step, we fix one axis and rotate the frame about that axis with an angle, which can be solved uniquely. For any orientation, there are twelve sets of three-step rotations and they can be divided into two groups depending on whether the fixed axes in step one and step three

are the same. The first group, named Classic Euler Angles, consisting of six conditions and in this group the same axis is fixed in step one and step three. The other group has the name of Tait-Bryan Angles, in which the body rotates about three different axes in three steps.

Classic Euler Angles	Tait-Bryan Angles
$\hat{x} - \hat{y} - \hat{x}$	$\hat{x} - \hat{y} - \hat{z}$
$\hat{x} - \hat{z} - \hat{x}$	$\hat{x} - \hat{z} - \hat{y}$
$\hat{y} - \hat{x} - \hat{y}$	$\hat{y} - \hat{x} - \hat{z}$
$\hat{y} - \hat{z} - \hat{y}$	$\hat{y} - \hat{z} - \hat{x}$
$\hat{z} - \hat{x} - \hat{z}$	$\hat{z} - \hat{x} - \hat{y}$
$\hat{z} - \hat{y} - \hat{z}$	$\hat{z} - \hat{y} - \hat{x}$

Table 2.1: Euler angles and fixed axes in three steps

All twelve sets of sequence shown in Tab. 2.1 could achieve an arbitrary orientation of SB; however, in most cases, different sets of rotation sequence need different and unique angular values. We choose  $\hat{z} - \hat{y} - \hat{x}$  as the fixed axes of rotation and the corresponding rotating angles are  $\psi - \theta - \phi$ .

## 2.2 TRANSFORMATION MATRIX

Until now, we have all twelve state variables including position vector  $\boldsymbol{\eta} \equiv [x, y, z, \phi, \theta, \psi]^T$  in inertia frame and velocity vector  $\boldsymbol{\nu} \equiv [u, v, w, p, q, r]^T$  in BFF. Transformation matrix  $\mathbf{J}(\boldsymbol{\alpha})$  could be derived to connect  $\dot{\boldsymbol{\eta}}$  and  $\boldsymbol{\nu}$

$$\dot{\boldsymbol{\eta}} = \mathbf{J}(\boldsymbol{\alpha})\boldsymbol{\nu} \quad (2.1)$$

The expression of  $\mathbf{J}(\boldsymbol{\alpha})$  is given in Eq. (2.2) and [14].

$$\mathbf{J}(\boldsymbol{\alpha}) = \begin{bmatrix} \mathbf{J}_1 & \mathbf{0}_{3 \times 3} \\ \mathbf{0}_{3 \times 3} & \mathbf{J}_2 \end{bmatrix} \quad (2.2)$$

$$= \begin{bmatrix} c(\theta)c(\psi) & s(\phi)s(\theta)c(\psi) - c(\phi)s(\psi) & s(\phi)s(\psi) + c(\phi)s(\theta)c(\psi) & 0 & 0 & 0 \\ c(\theta)s(\psi) & c(\phi)c(\psi) + s(\phi)s(\theta)s(\psi) & c(\phi)s(\theta)s(\psi) - s(\phi)c(\psi) & 0 & 0 & 0 \\ -s(\theta) & s(\phi)c(\theta) & c(\phi)c(\theta) & 0 & 0 & 0 \\ 0 & 0 & 0 & 1 & s(\phi)t(\theta) & c(\phi)t(\theta) \\ 0 & 0 & 0 & 0 & c(\phi) & -s(\phi) \\ 0 & 0 & 0 & 0 & \frac{s(\phi)}{c(\theta)} & \frac{c(\phi)}{c(\theta)} \end{bmatrix}$$

where  $c \equiv \cos$ ,  $s \equiv \sin$ , and  $t \equiv \tan$ .  $\mathbf{J}_1$  is the tensor that transforms a vector's expression in BFF into its expression in EFF and  $\mathbf{J}_2$  transforms angular velocities into time derivatives of Euler angles.  $\mathbf{J}_1$  and  $\mathbf{J}_2$  are rederived in the following section and in Appendix A, respectively.

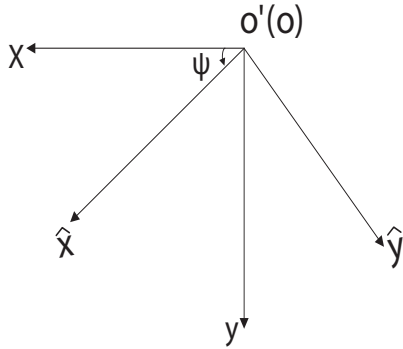
### 2.2.1 Derivation of $J_1$

Assume an arbitrary vector  $\mathbf{C}$  has expressions of  $[x, y, z]^T$  and  $[\hat{x}, \hat{y}, \hat{z}]^T$  in EFF and BFF, respectively.  $[x, y, z]^T$  equals to  $[\hat{x}, \hat{y}, \hat{z}]^T$  only if  $\boldsymbol{\alpha} = \mathbf{0}$  or  $\mathbf{C}$  itself is a zero vector. But an equation exists connecting these two expressions. Matrix  $\mathbf{T}$  is used to denote transformation from  $[x, y, z]^T$  to  $[\hat{x}, \hat{y}, \hat{z}]^T$

$$\begin{bmatrix} \hat{x} \\ \hat{y} \\ \hat{z} \end{bmatrix} = \mathbf{T} \cdot \begin{bmatrix} x \\ y \\ z \end{bmatrix}, \quad \begin{bmatrix} x \\ y \\ z \end{bmatrix} = \mathbf{J}_1 \cdot \begin{bmatrix} \hat{x} \\ \hat{y} \\ \hat{z} \end{bmatrix}, \quad \mathbf{J}_1 = \mathbf{T}^{-1} \quad (2.3)$$

$$\mathbf{T} = \mathbf{T}_\phi \cdot \mathbf{T}_\theta \cdot \mathbf{T}_\psi \quad (2.4)$$

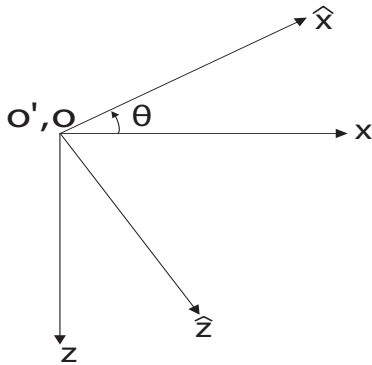
where  $\mathbf{T}_\psi$ ,  $\mathbf{T}_\theta$ , and  $\mathbf{T}_\phi$  are  $3 \times 3$  matrices representing effects due to rotations around z-axis, y-axis, and x-axis, respectively. They are shown in Figs. 2.2, 2.3, and 2.4.



$$\mathbf{T}_\psi = \begin{bmatrix} \cos(\psi) & \sin(\psi) & 0 \\ -\sin(\psi) & \cos(\psi) & 0 \\ 0 & 0 & 1 \end{bmatrix} \quad (2.5)$$

Figure 2.2: Rotation around  $O'\hat{z}$

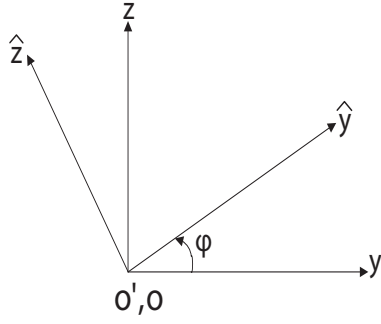
---



$$\mathbf{T}_\theta = \begin{bmatrix} \cos(\theta) & 0 & -\sin(\theta) \\ 0 & 1 & 0 \\ \sin(\theta) & 0 & \cos(\theta) \end{bmatrix} \quad (2.6)$$

Figure 2.3: Rotation around  $O'\hat{y}$

---



$$\mathbf{T}_\phi = \begin{bmatrix} 1 & 0 & 0 \\ 0 & \cos(\phi) & \sin(\phi) \\ 0 & -\sin(\phi) & \cos(\phi) \end{bmatrix} \quad (2.7)$$

 Figure 2.4: Rotation around  $O'\hat{z}$ 

$\mathbf{T}$  can be obtained by just multiplying  $\mathbf{T}_\phi$ ,  $\mathbf{T}_\theta$ , and  $\mathbf{T}_\psi$  together

$$\begin{aligned} \mathbf{T} &= \mathbf{T}_\phi \cdot \mathbf{T}_\theta \cdot \mathbf{T}_\psi \\ &= \begin{bmatrix} 1 & 0 & 0 \\ 0 & \cos(\phi) & \sin(\phi) \\ 0 & -\sin(\phi) & \cos(\phi) \end{bmatrix} \cdot \begin{bmatrix} \cos(\theta) & 0 & -\sin(\theta) \\ 0 & 1 & 0 \\ \sin(\theta) & 0 & \cos(\theta) \end{bmatrix} \cdot \begin{bmatrix} \cos(\psi) & \sin(\psi) & 0 \\ -\sin(\psi) & \cos(\psi) & 0 \\ 0 & 0 & 1 \end{bmatrix} \\ &= \begin{bmatrix} c(\theta)c(\psi) & c(\theta)s(\psi) & -s(\theta) \\ s(\phi)s(\theta)c(\psi) - c(\phi)s(\psi) & c(\phi)c(\psi) + s(\phi)s(\theta)s(\psi) & s(\phi)c(\theta) \\ s(\phi)s(\psi) + c(\phi)s(\theta)c(\psi) & c(\phi)s(\theta)s(\psi) - s(\phi)c(\psi) & c(\phi)c(\theta) \end{bmatrix} \end{aligned} \quad (2.8)$$

$$\mathbf{J}_1 = \mathbf{T}^{-1} = \begin{bmatrix} c(\theta)c(\psi) & s(\phi)s(\theta)c(\psi) - c(\phi)s(\psi) & s(\phi)s(\psi) + c(\phi)s(\theta)c(\psi) \\ c(\theta)s(\psi) & c(\phi)c(\psi) + s(\phi)s(\theta)s(\psi) & c(\phi)s(\theta)s(\psi) - s(\phi)c(\psi) \\ -s(\theta) & s(\phi)c(\theta) & c(\phi)c(\theta) \end{bmatrix} \quad (2.9)$$

Derivation of  $\mathbf{J}_2$  can be found in Appendix A.

It should be noted that  $\mathbf{J}_2$  is not defined when  $\theta$  equals to  $\pm\frac{\pi}{2}$ . In case pitch angle is close to this value, another set of Euler angle representation is needed, which should have different singularity. An alternative way is four-parameter method based on Euler parameters [14].

## CHAPTER 3

### GRAVITATIONAL FORCE AND BUOYANCY

Outside forces, including body force and surface force, on a submerged body cause the motion of the body. In this chapter, gravitational force and buoyancy are first expressed in EFF, and then transformed into BFF through Eq. (2.3). In the end, two forces are combined together and expressed in generalized form.

#### 3.1 GRAVITATIONAL FORCE IN BODY COORDINATE SYSTEM

In EFF, gravitational force vector  $\mathbf{G}$  could be easily expressed as

$$\mathbf{G} = \begin{bmatrix} G_x \\ G_y \\ G_z \end{bmatrix} = \begin{bmatrix} 0 \\ 0 \\ mg \end{bmatrix} \quad (3.1)$$

where  $m$  is the mass of the SB and  $g$  is the magnitude of gravitational acceleration. The point of action of  $\mathbf{G}$  is located at the center of mass, we use  $\mathbf{r}_G$  to denote the vector from the origin of BFF ( $O'$ ) to the center of mass. For a rigid body, the expression of  $\mathbf{r}_G$  in BFF, shown in Eq. (3.2), does not change with time.

$$\mathbf{r}_G = [x_G, y_G, z_G]^T \quad (3.2)$$

$\mathbf{G}$ 's expression in BFF, denoted as  $[G_1, G_2, G_3]^T$ , could be obtain by letting coordinate system transformation tensor  $\mathbf{T}$  act on its expression in EFF Eq. (3.1)

$$\begin{aligned} \begin{bmatrix} G_1 \\ G_2 \\ G_3 \end{bmatrix} &= \mathbf{T} \cdot \begin{bmatrix} G_x \\ G_y \\ G_z \end{bmatrix} = \mathbf{T} \cdot \begin{bmatrix} 0 \\ 0 \\ mg \end{bmatrix} \\ &= \begin{bmatrix} c(\theta)c(\psi) & c(\theta)s(\psi) & -s(\theta) \\ c(\psi)s(\phi)s(\theta) - c(\phi)s(\psi) & c(\phi)c(\psi) + s(\phi)s(\theta)s(\psi) & c(\theta)s(\phi) \\ s(\phi)s(\psi) + c(\phi)c(\psi)s(\theta) & c(\phi)s(\theta)s(\psi) - c(\psi)s(\phi) & c(\phi)c(\theta) \end{bmatrix} \cdot \begin{bmatrix} 0 \\ 0 \\ mg \end{bmatrix} \\ &= mg \begin{bmatrix} -s(\theta) \\ c(\theta)s(\phi) \\ c(\phi)c(\theta) \end{bmatrix} \end{aligned} \quad (3.3)$$

### 3.2 BUOYANCY IN BODY COORDINATE SYSTEM

Similarly, in EFF, the expression of buoyancy force  $\mathbf{F}$  can be expressed as

$$\mathbf{F} = \begin{bmatrix} F_x \\ F_y \\ F_z \end{bmatrix} = \begin{bmatrix} 0 \\ 0 \\ -m_d g \end{bmatrix} \quad (3.4)$$

where  $m_d$  is SB's displacement mass and equals to the multiplication of volume and density of fluid. The acting point of the buoyancy  $\mathbf{F}$  is SB's centroid and  $\mathbf{r}_F$  is used to denote the vector from the origin of BFF ( $O'$ ) to the centroid. For a rigid body, the expression of  $\mathbf{r}_F$  in BFF, shown in Eq. (3.5), does not change with time either.

$$\mathbf{r}_F = [x_F, y_F, z_F]^T \quad (3.5)$$

$\mathbf{F}$ 's expression in BFF, denoted as  $[F_1, F_2, F_3]^T$ , could be derived through the same process as  $\mathbf{G}$  before

$$\begin{bmatrix} F_1 \\ F_2 \\ F_3 \end{bmatrix} = \mathbf{T} \cdot \begin{bmatrix} 0 \\ 0 \\ -m_d g \end{bmatrix} = -m_d g \begin{bmatrix} -s(\theta) \\ c(\theta)s(\phi) \\ c(\phi)c(\theta) \end{bmatrix} \quad (3.6)$$

### 3.3 FORCES COMBINATION AND GENERALIZATION

Gravitational force and buoyancy both have stable directions and magnitudes in EFF, so they have similar expressions. For simplicity, we combine them together resulting in a moment as a result of they acting on different points.

As mentioned above,  $\mathbf{G}$  acts on the center of mass, while  $\mathbf{F}$  acts on the body's centroid. These two points does not necessarily coincide with each other. If origin of EFF ( $O'$ ) is chosen as the reference point, the two forces will cause a moment, denoted as  $\mathbf{M}_{O'}$ .  $\mathbf{F}_t$  is used to represent the composite force. In BFF, it has the following expression

$$\mathbf{F}_t = (m - m_d)g \begin{bmatrix} -s(\theta) \\ c(\theta)s(\phi) \\ c(\phi)c(\theta) \end{bmatrix} \quad (3.7)$$

$$\begin{aligned} \mathbf{M}_{O'} &= \mathbf{r}_G \times \mathbf{G} + \mathbf{r}_F \times \mathbf{F} \\ &= g \begin{bmatrix} (m y_G - m_d y_F) c(\phi) c(\theta) - (m z_G - m_d z_F) c(\theta) s(\phi) \\ -(m x_G - m_d x_F) c(\phi) c(\theta) - (m z_G - m_d z_F) s(\theta) \\ (m x_G - m_d x_F) c(\theta) s(\phi) + (m y_G - m_d y_F) s(\theta) \end{bmatrix} \end{aligned} \quad (3.8)$$

In a further step, for simplicity of expression, combined forces and moments are written in

generalized form  $\tilde{\mathbf{F}}_{GF}$ .

$$\tilde{\mathbf{F}}_{GF} = \begin{bmatrix} \mathbf{F}_t \\ \mathbf{M}_{O'} \end{bmatrix} = g \begin{bmatrix} -(m - m_d)s(\theta) \\ (m - m_d)c(\theta)s(\phi) \\ (m - m_d)c(\phi)c(\theta) \\ (my_G - m_dy_F)c(\phi)c(\theta) - (mz_G - m_dz_F)c(\theta)s(\phi) \\ -(mx_G - m_dx_F)c(\phi)c(\theta) - (mz_G - m_dz_F)s(\theta) \\ (mx_G - m_dx_F)c(\theta)s(\phi) + (my_G - m_dy_F)s(\theta) \end{bmatrix} \quad (3.9)$$

If the origin of BFF is located at the centroid of SB,  $\mathbf{r}_F = \mathbf{0}$ , Eq. (3.9) yields

$$\tilde{\mathbf{F}}_{GF} = g \begin{bmatrix} -(m - m_d)s(\theta) \\ (m - m_d)c(\theta)s(\phi) \\ (m - m_d)c(\phi)c(\theta) \\ my_Gc(\phi)c(\theta) - mz_Gc(\theta)s(\phi) \\ -mx_Gc(\phi)c(\theta) - mz_Gs(\theta) \\ mx_Gc(\theta)s(\phi) + my_Gs(\theta) \end{bmatrix} \quad (3.10)$$

## CHAPTER 4

### HYDRODYNAMIC FORCE

In the previous chapter, the generalized form of two static forces, gravitational force and buoyancy, were obtained in Eq. (3.9). In this chapter, added-mass theory [19] for unsteady hydrodynamic forces and moments is introduced and the expressions for hydrodynamic forces and moments are developed in explicit form. Hydrodynamic damping is included at the end as an empirical corrections.

#### 4.1 ADDED-MASS THEORY

##### 4.1.1 Assumptions and Expression of Hydrodynamic Force

We assume SB moves in the deep ocean; thus free surface and ocean bottom boundary are considered to be far away and their influences are negligible. In this case, the body is considered to move in a fluid which is infinite in all directions. Added-mass theory can be adopted to calculate the hydrodynamic force and moment. Assuming the fluid is inviscid and irrotational, we have curl of velocity equals to zero everywhere.

$$\nabla \times \mathbf{v} = 0 \quad (4.1)$$

Here, velocity  $\mathbf{v}$  can be expressed as gradient of velocity potential, denoted as  $\Phi$ .

$$\mathbf{v} = \nabla\Phi \quad (4.2)$$

Starting from Euler Equations

$$\rho \left( \frac{\partial \mathbf{v}}{\partial t} + \mathbf{v} \cdot \nabla \mathbf{v} \right) = -\nabla p + \rho \mathbf{g} \quad (4.3)$$

Bernoulli Equation for irrotational flow could be derived as

$$\frac{p}{\rho} = -\Phi_t - \frac{1}{2} |\nabla\Phi|^2 + gz \quad (4.4)$$

where pressure is expressed in terms of velocity potential. The  $gz$  term, contributing to hydrostatic force, has been discussed in Chap. 3 as buoyancy. Hence we drop it and write Eq. (4.4) as

$$\frac{p}{\rho} = -\Phi_t - \frac{1}{2} |\nabla\Phi|^2 \quad (4.5)$$

where  $p$  is hydrodynamic pressure. Integration of  $P$  over the whole body's surface gives hydrodynamic force  $\mathbf{F}_d(t)$ . Hydrodynamic moment around the origin of BFF ( $O'$ ),  $\mathbf{M}_{dO'}$ , is integration of pressure multiplied by position vector over the surface.

$$\mathbf{F}_d(t) = \int_{B(t)} p \mathbf{n} dS \quad (4.6)$$

$$\mathbf{M}_{dO'}(t) = \int_{B(t)} p(\mathbf{r}_{O'} \times \mathbf{n}) dS \quad (4.7)$$

where  $B(t)$  is the object's surface changing with time,  $\mathbf{r}_{O'}$  is the position vector starting with origin of BFF ( $O'$ ), and  $\mathbf{n}$  is the normal vector pointing inwards body's surface.

### 4.1.2 Hydrodynamic Force in terms of Velocity Potential

As in [19], let us take volume  $V$  bounded by  $B(t)$  and a large sphere surface  $\Sigma_R$  as the control volume.  $\Sigma_R$  is fixed in the EBF with  $R \rightarrow \infty$ . Therefore, the total linear momentum of fluid in the control volume is

$$\mathbf{M} = \rho \int_V \mathbf{v} dV = \rho \int_V \nabla \Phi dV = \rho \int_{B(t) \cup \Sigma_R} \Phi \mathbf{n} dV \quad (4.8)$$

Applying momentum theorem on the control volume  $V$ , we can get

$$-\mathbf{F}_d(t) - \int_{\Sigma_R} p \mathbf{n} dS = \rho \int_{\Sigma_R} \Phi_t \mathbf{n} dS + \rho \frac{d}{dt} \int_{B(t)} \Phi \mathbf{n} dS + \rho \int_{\Sigma_R} (\mathbf{v} \cdot \mathbf{n}) \mathbf{n} dS \quad (4.9)$$

The first term on the left-hand side (LHS),  $-\mathbf{F}_d(t)$ , is the surface force of the body acting on fluid in control volume, the second term on LHS,  $\int_{\Sigma_R} p \mathbf{n} dS$ , is surface force fluid outside the control volume exerting on control volume. On the right-hand side (RHS), the first two terms represent time derivative of the momentum in the control volume and the last term shows the momentum efflux on boundary  $\Sigma_R$ .

Direct substitution of expression of  $p$  in Eq. (4.5) into Eq. (4.9) gives

$$\mathbf{F}_d(t) = -\rho \frac{d}{dt} \int_{B(t)} \Phi \mathbf{n} dS - \rho \int_{\Sigma_R} [\mathbf{v}(\mathbf{v} \cdot \mathbf{n}) - \frac{1}{2}(\mathbf{v} \cdot \mathbf{v})\mathbf{n}] dS \quad (4.10)$$

Velocity  $\mathbf{v}$  caused by motion of body has the order of  $R^{-3}$  as  $R \rightarrow \infty$ . Also it is known for sphere

$$\int dS = \int_0^{2\pi} \int_0^\pi R^2 \sin \theta d\theta d\phi \quad (4.11)$$

Thus,  $[\mathbf{v}(\mathbf{v} \cdot \mathbf{n}) - \frac{1}{2}(\mathbf{v} \cdot \mathbf{v})\mathbf{n}]$  has the order of  $R^{-6}$ , and its integration over  $\Sigma_R$  should have the order of  $R^{-4}$

$$\rho \int_{\Sigma_R} [\mathbf{v}(\mathbf{v} \cdot \mathbf{n}) - \frac{1}{2}(\mathbf{v} \cdot \mathbf{v})\mathbf{n}] dS = O\{R^{-4}\} \quad (4.12)$$

As  $R$  approaches infinity,  $O\{R^{-4}\}$  decays rapidly to zero. Thus for large  $R$ , the second term on the RHS of Eq. (4.10) can be dropped and finally we get a simple expression of hydrodynamic force,  $\mathbf{F}_d(t)$ , in terms of velocity potential  $\Phi$

$$\mathbf{F}_d(t) = -\rho \frac{d}{dt} \int_{B(t)} \Phi \mathbf{n} dS \quad (4.13)$$

Similarly, the total angular momentum around  $O'$  in control volume  $V$  has the following expression

$$\mathbf{L}_{O'} = \rho \int_V (\mathbf{r}_{O'} \times \mathbf{v}) dV = \rho \int_V (\mathbf{r}_{O'} \times \nabla \Phi) dV = \rho \int_{B(t) \cup \Sigma_R} \Phi (\mathbf{r}_{O'} \times \mathbf{n}) dS \quad (4.14)$$

After control volume analysis and substitution of  $p$ , we can obtain hydrodynamic moment  $\mathbf{M}_{dO'}(t)$  around  $O'$

$$\mathbf{M}_{dO'}(t) = -\rho \frac{d}{dt} \int_{B(t)} \Phi (\mathbf{r}_{O'} \times \mathbf{n}) dS - \rho \int_{\Sigma_R} [(\mathbf{v} \cdot \mathbf{n})(\mathbf{r}_{O'} \times \mathbf{v}) - \frac{1}{2}(\mathbf{v} \cdot \mathbf{v})(\mathbf{r}_{O'} \times \mathbf{n})] dS \quad (4.15)$$

Term  $\rho \int_{\Sigma_R} [(\mathbf{v} \cdot \mathbf{n})(\mathbf{r}_{O'} \times \mathbf{v}) - \frac{1}{2}(\mathbf{v} \cdot \mathbf{v})(\mathbf{r}_{O'} \times \mathbf{n})] dS$  has the order of  $R^{-3}$  and decays fast as  $R \rightarrow \infty$ . We drop it and finally obtain hydrodynamic moment expressed in terms of velocity potential

$$\mathbf{M}_{dO'}(t) = -\rho \frac{d}{dt} \int_{B(t)} \Phi(\mathbf{r}_{O'} \times \mathbf{n}) dS \quad (4.16)$$

### 4.1.3 Kirchoff Decomposition

As mentioned before,  $\mathbf{n}$  is the normal vector pointing inwards S; for a rigid body in BFF,  $\mathbf{n}$  does not depend on time. Also in either coordinate system, velocity at any point on body surface can be described by velocity at the origin,  $\mathbf{v}_{O'}$ , angular velocity,  $\boldsymbol{\omega}$ , and relative position vector,  $\mathbf{r}_{O'}$ , as

$$\mathbf{v} = \mathbf{v}_{O'} + \boldsymbol{\omega} \times \mathbf{r}_{O'} \quad (4.17)$$

Velocity potential  $\hat{\Phi}$  observed in BFF must satisfy the kinematic boundary condition

$$\mathbf{v} \cdot \mathbf{n}|_B = \left. \frac{\partial \hat{\Phi}}{\partial \hat{x}} n_1 + \frac{\partial \hat{\Phi}}{\partial \hat{y}} n_2 + \frac{\partial \hat{\Phi}}{\partial \hat{z}} n_3 \right|_B \quad (4.18)$$

where

$$\mathbf{v} \cdot \mathbf{n}|_B = \mathbf{v}_{O'} \cdot \mathbf{n} + (\boldsymbol{\omega} \times \mathbf{r}_{O'}) \cdot \mathbf{n} = \mathbf{v}_{O'} \cdot \mathbf{n} + \boldsymbol{\omega} \cdot (\mathbf{r}_{O'} \times \mathbf{n}) \quad (4.19)$$

So the boundary condition for  $\hat{\Phi}$  is:

$$\hat{\Phi}_1 n_1 + \hat{\Phi}_2 n_2 + \hat{\Phi}_3 n_3 \Big|_B = \left\{ \begin{array}{l} u_1 n_1 + u_2 n_2 + u_3 n_3 + \omega_1 [\hat{y} n_3 - \hat{z} n_2] \\ + \omega_2 [\hat{z} n_1 - \hat{x} n_3] + \omega_3 [\hat{x} n_2 - \hat{y} n_1] \end{array} \right\} \Big|_B \quad (4.20)$$

where subscripts 1, 2, and 3 represent a vector's component in directions  $O'\hat{x}$ ,  $O'\hat{y}$ , and  $O'\hat{z}$ , respectively. Above boundary condition suggests the Kirchoff Decomposition of  $\hat{\Phi}$

$$\hat{\Phi} = \sum_{i=1}^6 \phi_i u_i \quad (4.21)$$

where  $[u_4, u_5, u_6]^T \equiv [\omega_1, \omega_2, \omega_3]^T$  and  $\phi_i$  is called unit potential and defined as follows

$$\begin{aligned} \frac{\partial \phi_1}{\partial \mathbf{n}} &= n_1 & \frac{\partial \phi_4}{\partial \mathbf{n}} &= (\hat{y} n_3 - \hat{z} n_2) = n_4 \\ \frac{\partial \phi_2}{\partial \mathbf{n}} &= n_2 & \frac{\partial \phi_5}{\partial \mathbf{n}} &= (\hat{z} n_1 - \hat{x} n_3) = n_5 \\ \frac{\partial \phi_3}{\partial \mathbf{n}} &= n_3 & \frac{\partial \phi_6}{\partial \mathbf{n}} &= (\hat{x} n_2 - \hat{y} n_1) = n_6 \end{aligned} \quad (4.22)$$

in which,  $\frac{\partial}{\partial \mathbf{n}}$  denotes directional derivative in  $\mathbf{n}$ 's direction. It should be noted that  $[u_1, u_2, u_3, u_4, u_5, u_6]^T$  is the same as  $[u, v, w, p, q, r]^T$ , which is notation suggested by [18] and used in other chapters. In addition, unit potentials, according to their definitions in Eq. (4.22), only depend on SB's geometry property and does not change with time.

#### 4.1.4 Added Masses

Although  $\mathbf{F}_d(t)$  and  $\mathbf{M}_{dO'}(t)$  in Eqs. (4.13) and (4.16) are expressed in terms of velocity potential  $\Phi$  in EFF,  $\hat{\Phi}$  can replace  $\Phi$  and satisfies these two equations because  $\hat{\Phi}$ , same as  $\Phi$ , is velocity potential for the velocity relative to inertia frame. But it is observed in BFF

$$\mathbf{v} = \frac{\partial \hat{\Phi}}{\partial \hat{x}} \hat{\mathbf{e}}_1 + \frac{\partial \hat{\Phi}}{\partial \hat{y}} \hat{\mathbf{e}}_2 + \frac{\partial \hat{\Phi}}{\partial \hat{z}} \hat{\mathbf{e}}_3 \quad (4.23)$$

where  $[\hat{\mathbf{e}}_1, \hat{\mathbf{e}}_2, \hat{\mathbf{e}}_3]^T$  is the orthonormal basis of BFF. Expression of  $\hat{\Phi}$  was developed through analyzing kinematic boundary condition on body surface, shown in Eqs. (4.21) and (4.22). Substitution of  $\hat{\Phi}$ 's expression in terms of unit potential into  $\mathbf{F}_{d(t)}$  and  $\mathbf{M}_{dO'}(t)$  leads to

$$\mathbf{F}_d(t) = -\rho \frac{d}{dt} \left[ u_i \int_B \phi_i \frac{\partial \phi_j}{\partial n} dS \right] \hat{\mathbf{e}}_j \quad (4.24)$$

$$\mathbf{M}_{dO'}(t) = -\rho \frac{d}{dt} \left[ u_i \int_B \phi_i \frac{\partial \phi_{k+3}}{\partial n} dS \right] \hat{\mathbf{e}}_k \quad (4.25)$$

where  $i=1,2,\dots,6$ , and  $j,k=1,2,3$ .

Introducing the definition of added mass  $\mu_{ji}$  as

$$\mu_{ji} = \rho \int_B \phi_i \frac{\partial \phi_j}{\partial n} dS \quad (4.26)$$

we can write Eqs. (4.24) and (4.25) as

$$\mathbf{F}_d(t) = -\frac{d}{dt} [u_i \cdot \mu_{ji}] \hat{\mathbf{e}}_j \quad (4.27)$$

$$\mathbf{M}_{dO'}(t) = -\frac{d}{dt} [u_i \cdot \mu_{(k+3)i}] \hat{\mathbf{e}}_k \quad (4.28)$$

The final expressions of hydrodynamic force and moment are expressed as

$$\mathbf{F}_d(t) = -[\dot{u}_i(t)\mu_{ji} + u_i \varepsilon_{jkl} \omega_k \mu_{li}] \hat{\mathbf{e}}_j \quad (4.29)$$

$$\mathbf{M}_{dO'}(t) = -[\dot{u}_i(t)\mu_{j+3,i} + u_i \varepsilon_{jkl} \omega_k \mu_{l+3,i} + u_i \varepsilon_{jkl} u_k \mu_{li}] \hat{\mathbf{e}}_j \quad (4.30)$$

Here,  $\varepsilon_{ijk}$  is called alternating tensor and has the value of 1, 0, and -1 when  $i, j$ , and  $k$  are cyclic, repeated, and acyclic, respectively.

## 4.2 ADDED MASSES FOR A PROLATE SPHEROID

In section 4.1.2, hydrodynamic force and moment are developed in Eqs. (4.29) and (4.30). It is noted that  $\mathbf{F}_d$  and  $\mathbf{M}_{dO'}$  are decomposed into time-varying velocity and acceleration and time-independent added mass. Added mass only depends on SB's geometry and if added mass is given,  $\mathbf{F}_d$  and  $\mathbf{M}_{dO'}$  are only functions of velocity and acceleration. For object in shape of prolate spheroid, shown in Fig. 4.1, if origin of BFF is placed at the centroid, expression of added mass can be greatly simplified due to its symmetry and could be found in [20, 21].

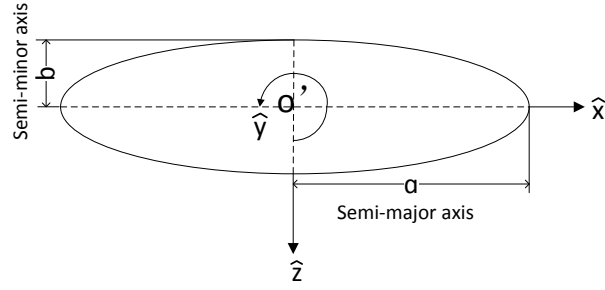


Figure 4.1: Prolate spheroid

### 4.2.1 Symmetry Effects

Prolate spheroid is symmetric about all three planes, as shown in Tab. 4.1

Symmetry	Plane
port-and-starboard	$O'\hat{x}\hat{z}$
fore-and-aft	$O'\hat{y}\hat{z}$
top-and-bottom	$O'\hat{x}\hat{y}$

Table 4.1: Symmetry of prolate spheroid

Because of the top-bottom symmetry, the components of the normal vector satisfy

$$\begin{aligned}
 n_1(\hat{x}, \hat{y}, \hat{z}) &= n_1(\hat{x}, \hat{y}, -\hat{z}) \\
 n_2(\hat{x}, \hat{y}, \hat{z}) &= n_2(\hat{x}, \hat{y}, -\hat{z}) \\
 n_3(\hat{x}, \hat{y}, \hat{z}) &= -n_3(\hat{x}, \hat{y}, -\hat{z}) \\
 n_4(\hat{x}, \hat{y}, \hat{z}) &= \hat{y}n_3 - \hat{z}n_2 = -n_4(\hat{x}, \hat{y}, -\hat{z}) \\
 n_5(\hat{x}, \hat{y}, \hat{z}) &= \hat{z}n_1 - \hat{x}n_3 = -n_5(\hat{x}, \hat{y}, -\hat{z}) \\
 n_6(\hat{x}, \hat{y}, \hat{z}) &= \hat{x}n_2 - \hat{y}n_1 = n_6(\hat{x}, \hat{y}, -\hat{z})
 \end{aligned} \tag{4.31}$$

According to the relationship between unit potential and components of normal vector expressed in Eqs. (4.22), the unit potentials at  $[\hat{x}, \hat{y}, \hat{z}]$  and  $[\hat{x}, \hat{y}, -\hat{z}]$  have the relation of

$$\begin{aligned}
 \phi_{1,2,6}(\hat{x}, \hat{y}, \hat{z}) &= \phi_{1,2,6}(\hat{x}, \hat{y}, -\hat{z}) \\
 \phi_{3,4,5}(\hat{x}, \hat{y}, \hat{z}) &= -\phi_{3,4,5}(\hat{x}, \hat{y}, -\hat{z})
 \end{aligned} \tag{4.32}$$

If we recall the definition of  $\mu_{ji}$  in Eqs. (4.26), the substitution and integration result in

$$\mu_{13} = \mu_{14} = \mu_{15} = \mu_{23} = \mu_{24} = \mu_{25} = \mu_{36} = \mu_{46} = \mu_{56} = 0 \tag{4.33}$$

Similarly, due to the fore-and-aft and port-and-starboard symmetries, we have

$$\begin{aligned}\mu_{12} = \mu_{13} = \mu_{14} = \mu_{25} = \mu_{35} = \mu_{45} = \mu_{26} = \mu_{36} = \mu_{46} = 0 \\ \mu_{12} = \mu_{23} = \mu_{25} = \mu_{14} = \mu_{34} = \mu_{45} = \mu_{16} = \mu_{36} = \mu_{56} = 0\end{aligned}\quad (4.34)$$

The added mass matrix,  $\boldsymbol{\mu}$ , is greatly simplified into a diagonal matrix

$$\boldsymbol{\mu} = \begin{bmatrix} \mu_{11} & 0 & 0 & 0 & 0 & 0 \\ 0 & \mu_{22} & 0 & 0 & 0 & 0 \\ 0 & 0 & \mu_{33} & 0 & 0 & 0 \\ 0 & 0 & 0 & \mu_{44} & 0 & 0 \\ 0 & 0 & 0 & 0 & \mu_{55} & 0 \\ 0 & 0 & 0 & 0 & 0 & \mu_{66} \end{bmatrix}\quad (4.35)$$

Besides, considering the fact that prolate spheroid is a solid of revolution about  $O'\hat{x}$  axis,  $O'\hat{y}$  and  $O'\hat{z}$  consist an arbitrarily set of base for the transverse middle plane that is perpendicular to  $O'\hat{x}$ . Also it can be seen that body with accelerations of the same magnitude along  $O'\hat{y}$  and  $O'\hat{z}$  undergo hydrodynamic forces of the same magnitude, so does hydrodynamic moments of rotating around  $O'\hat{y}$  and  $O'\hat{z}$ . According to the physical meaning of added mass, we have

$$\begin{aligned}\mu_{33} = \mu_{22} \\ \mu_{66} = \mu_{55}\end{aligned}\quad (4.36)$$

Furthermore, as mentioned above, prolate spheroid is a body of revolution about  $O'\hat{x}$  axis; hence each transverse section is in circular shape, as shown in Fig. 4.2

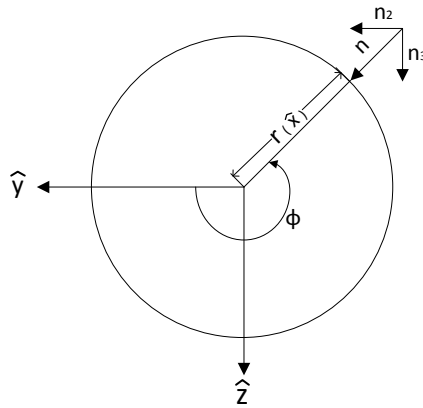


Figure 4.2: Transverse section

At any point  $(\hat{x}, \hat{y}, \hat{z})$  on SB's surface,  $n_4$  is expressed as

$$n_4(\hat{x}, \hat{y}, \hat{z}) = \hat{y}n_3 - \hat{z}n_2\quad (4.37)$$

where  $\hat{y}$ ,  $\hat{z}$ ,  $n_2$ , and  $n_3$  can be expressed in terms of radius  $r(\hat{x})$  and angle  $\phi$ .  $r(\hat{x})$  is a constant in each transverse section but changing with  $\hat{x}$

$$\begin{aligned}\hat{y} &= r(\hat{x}) \cdot \cos \phi \\ \hat{z} &= r(\hat{x}) \cdot \sin \phi \\ n_2 &= -\cos \phi \\ n_3 &= -\sin \phi\end{aligned}\tag{4.38}$$

Substitution of Eq. (4.38) into Eq. (4.37) gives  $n_4(\hat{x}, \hat{y}, \hat{z}) = 0$ ; thus  $\phi_4$  equals to zero.

$$\mu_{44} = \rho \int_{B(t)} \phi_4 \frac{\partial \phi_4}{\partial n} dS = 0\tag{4.39}$$

The final version of added mass matrix for prolate spheroid only has three independent variables  $\mu_{11}$ ,  $\mu_{33} = \mu_{22}$ , and  $\mu_{66} = \mu_{55}$ .

$$\boldsymbol{\mu} = \begin{bmatrix} \mu_{11} & 0 & 0 & 0 & 0 & 0 \\ 0 & \mu_{22} & 0 & 0 & 0 & 0 \\ 0 & 0 & \mu_{22} & 0 & 0 & 0 \\ 0 & 0 & 0 & 0 & 0 & 0 \\ 0 & 0 & 0 & 0 & \mu_{55} & 0 \\ 0 & 0 & 0 & 0 & 0 & \mu_{55} \end{bmatrix}\tag{4.40}$$

### 4.2.2 Analytical Solution for Added Mass of Prolate Spheroid

There are two geometry factor for a prolate spheroid, major axis  $2a$  and minor axis  $2b$ , shown in Fig. 4.1. Eccentricity of the meridian elliptical section, denoted as  $e$ , is defined as

$$e^2 \equiv 1 - \left(\frac{b}{a}\right)^2 = 1 - \bar{b}^2\tag{4.41}$$

Analytical solutions of  $\mu_{11}$ ,  $\mu_{22}$ , and  $\mu_{55}$  depend on  $a$ ,  $b$ , and density of fluid, which can be found in [20, 21]

$$\mu_{11} = \frac{k_1}{2 - k_2} \frac{4}{3} \pi \rho a b^2\tag{4.42a}$$

$$\mu_{22} = \frac{k_2}{2 - k_2} \frac{4}{3} \pi \rho a b^2\tag{4.42b}$$

$$\mu_{55} = -\frac{1}{5} \frac{(b^2 - a^2)^2 (k_2 - k_1)}{2(b^2 - a^2) + (b^2 + a^2)(k_2 - k_1)} \frac{4}{3} \pi \rho a b^2\tag{4.42c}$$

where  $k_1$  and  $k_2$  are two dimensionless factors

$$k_1 = \frac{2(1 - e^2)}{e^3} \left( \frac{1}{2} \ln \frac{1 + e}{1 - e} - e \right)\tag{4.43a}$$

$$k_2 = \frac{1}{e^2} - \frac{1-e^2}{2e^3} \ln \frac{1+e}{1-e} \quad (4.43b)$$

### 4.3 HYDRODYNAMIC FORCE AND MOMENT FOR PROLATE SPHEROID

Given fluid density and lengths of major and minor axes,  $\mu_{11}$ ,  $\mu_{22}$ , and  $\mu_{55}$  can be obtained through Eqs. (4.42). Substitution of simplified added mass  $\boldsymbol{\mu}$  in Eq. (4.40) into Eqs. (4.29) and (4.30) gives the expression of hydrodynamic force  $\mathbf{F}_d$  and moment  $\mathbf{M}_{dO'}$

$$\begin{aligned} \mathbf{F}_d &= F_{d1}\hat{\mathbf{e}}_1 + F_{d2}\hat{\mathbf{e}}_2 + F_{d3}\hat{\mathbf{e}}_3 \\ \mathbf{M}_{dO'} &= M_{d1}\hat{\mathbf{e}}_1 + M_{d2}\hat{\mathbf{e}}_2 + M_{d3}\hat{\mathbf{e}}_3 \end{aligned} \quad (4.44)$$

where

$$\begin{aligned} F_{d1} &= -\dot{u}_1\mu_{11} + \mu_{22}u_2\omega_3 - \mu_{33}u_3\omega_2 = -\dot{u}_1\mu_{11} + \mu_{22}[u_2\omega_3 - u_3\omega_2] \\ F_{d2} &= -\dot{u}_2\mu_{22} + u_3\omega_1\mu_{33} - u_1\omega_3\mu_{11} = \mu_{22}(u_3\omega_1 - \dot{u}_2) - u_1\omega_3\mu_{11} \\ F_{d3} &= -\dot{u}_3\mu_{22} + u_1\omega_2\mu_{11} - u_2\omega_1\mu_{22} = -\mu_{22}(\dot{u}_3 + u_2\omega_1) + u_1\omega_2\mu_{11} \\ M_{d1} &= 0 \\ M_{d2} &= \mu_{66}\omega_1\omega_3 - \mu_{55}\dot{\omega}_2 + u_1u_3\mu_{33} - u_1u_3\mu_{11} = \mu_{55}[\omega_1\omega_3 - \dot{\omega}_2] + u_1u_3[\mu_{22} - \mu_{11}] \\ M_{d3} &= -\mu_{66}\dot{\omega}_3 - \mu_{55}\omega_1\omega_2 + u_1u_2[\mu_{11} - \mu_{22}] = -\mu_{55}[\dot{\omega}_3 + \omega_1\omega_2] + u_1u_2[\mu_{11} - \mu_{22}] \end{aligned} \quad (4.45)$$

Generalized hydrodynamic force,  $\tilde{\mathbf{F}}_d$ , is shown below by combining hydrodynamic force and moment and replacing notation  $[u_1, u_2, u_3, \omega_1, \omega_2, \omega_3]^T$  with  $[u, v, w, p, q, r]^T$

$$\begin{aligned} \tilde{\mathbf{F}}_d &= - \begin{bmatrix} \mu_{11} & 0 & 0 & 0 & 0 & 0 \\ 0 & \mu_{22} & 0 & 0 & 0 & 0 \\ 0 & 0 & \mu_{22} & 0 & 0 & 0 \\ 0 & 0 & 0 & 0 & 0 & 0 \\ 0 & 0 & 0 & 0 & \mu_{55} & 0 \\ 0 & 0 & 0 & 0 & 0 & \mu_{55} \end{bmatrix} \cdot \begin{bmatrix} \dot{u} \\ \dot{v} \\ \dot{w} \\ \dot{p} \\ \dot{q} \\ \dot{r} \end{bmatrix} \\ &+ \begin{bmatrix} 0 & 0 & 0 & 0 & -\mu_{22}w & \mu_{22}v \\ 0 & 0 & 0 & \mu_{22}w & 0 & -\mu_{11}u \\ 0 & 0 & 0 & -\mu_{22}v & \mu_{11}u & 0 \\ 0 & 0 & 0 & 0 & 0 & 0 \\ \mu_{22}w & 0 & -\mu_{11}u & 0 & 0 & \mu_{55}p \\ -\mu_{22}v & \mu_{11}u & 0 & 0 & -\mu_{55}p & 0 \end{bmatrix} \cdot \begin{bmatrix} u \\ v \\ w \\ p \\ q \\ r \end{bmatrix} \end{aligned} \quad (4.46)$$

## 4.4 HYDRODYNAMIC DAMPING

In the previous three sections, added-mass theory was introduced and analytical solutions of added-mass for prolate spheroid was presented, based on which, expression of generalized hydrodynamic force is obtained in Eq. (4.46). In added-mass theory, fluid is assumed to be inviscid and the flow irrotational, but in the real condition, viscous effects might not be negligible. [14] suggests the following expression of hydrodynamic damping  $\tilde{\mathbf{F}}_{dp}$

$$\tilde{\mathbf{F}}_{dp} = \mathbf{D}(\boldsymbol{\nu}) \cdot \boldsymbol{\nu} \quad (4.47)$$

in which,  $\mathbf{D}(\boldsymbol{\nu})$  has four main components

$$\mathbf{D}(\boldsymbol{\nu}) \equiv \mathbf{D}_P(\boldsymbol{\nu}) + \mathbf{D}_S(\boldsymbol{\nu}) + \mathbf{D}_W(\boldsymbol{\nu}) + \mathbf{D}_M(\boldsymbol{\nu}) \quad (4.48)$$

where  $\mathbf{D}_P(\boldsymbol{\nu})$  represents potential damping effects,  $\mathbf{D}_S(\boldsymbol{\nu})$  represents linear and quadratic skin friction due to laminar and turbulent boundary layers, respectively,  $\mathbf{D}_W(\boldsymbol{\nu})$  is wave drift damping, and  $\mathbf{D}_M(\boldsymbol{\nu})$  is damping due to vortex shedding.

Since SB is symmetric about all three planes and moves in deep water, expression of  $\mathbf{D}(\boldsymbol{\nu})$  having linear and quadratic terms on diagonal can be used as a rough approximation of the damping effects [14, 22, 9].

$$\begin{aligned} \mathbf{D}(\boldsymbol{\nu}) = & \begin{bmatrix} X_u & 0 & 0 & 0 & 0 & 0 \\ 0 & Y_v & 0 & 0 & 0 & 0 \\ 0 & 0 & Z_w & 0 & 0 & 0 \\ 0 & 0 & 0 & K_p & 0 & 0 \\ 0 & 0 & 0 & 0 & M_q & 0 \\ 0 & 0 & 0 & 0 & 0 & N_r \end{bmatrix} - \begin{bmatrix} X_{u|u}|u| & 0 & 0 & 0 & 0 & 0 \\ 0 & Y_{v|v}|v| & 0 & 0 & 0 & 0 \\ 0 & 0 & Z_{w|w}|w| & 0 & 0 & 0 \\ 0 & 0 & 0 & K_{p|p}|p| & 0 & 0 \\ 0 & 0 & 0 & 0 & M_{q|q}|q| & 0 \\ 0 & 0 & 0 & 0 & 0 & N_{r|r}|r| \end{bmatrix} \\ = & \begin{bmatrix} X_u + X_{u|u}|u| & 0 & 0 & 0 & 0 & 0 \\ 0 & Y_v + Y_{v|v}|v| & 0 & 0 & 0 & 0 \\ 0 & 0 & Z_w + Z_{w|w}|w| & 0 & 0 & 0 \\ 0 & 0 & 0 & K_p + K_{p|p}|p| & 0 & 0 \\ 0 & 0 & 0 & 0 & M_q + M_{q|q}|q| & 0 \\ 0 & 0 & 0 & 0 & 0 & N_r + N_{r|r}|r| \end{bmatrix} \quad (4.49) \end{aligned}$$

In real, damping of a high-speed underwater vehicle is highly nonlinear and coupled [16]. Hydrodynamic damping coefficients need to be determined.

## CHAPTER 5

### EQUATIONS OF MOTION

In previous chapters, gravitational force, buoyancy, and hydrodynamic force were studied; this chapter will discuss the derivation of equations of motion, non-dimensionalization, and analysis of these equations.

#### 5.1 EQUATIONS OF MOTION

Newton's Second Law gives

$$\mathbf{F}_r = m\mathbf{a}_G \quad (5.1)$$

where  $\mathbf{F}_r$  is resultant force,  $m$  is the mass of SB and  $\mathbf{a}_G$  is the acceleration of SB's center of mass in an inertial frame of reference. The expression of  $\mathbf{a}_G$  shown in equation Eq. (5.2), is derived in Appendix B and can also be found in [14].

$$\mathbf{a}_G = \dot{\mathbf{v}}_{O'} + \boldsymbol{\omega} \times \mathbf{v}_{O'} + \dot{\boldsymbol{\omega}} \times \mathbf{r}_G + \boldsymbol{\omega} \times (\boldsymbol{\omega} \times \mathbf{r}_G) \quad (5.2)$$

where  $\mathbf{v}_{O'}$  is the velocity of BFF's origin measured in EFF, and  $\dot{\mathbf{v}}_{O'}$  is its time derivative with respect to BFF.  $\boldsymbol{\omega}$  is angular velocity of BFF about  $O'$ ,  $\dot{\boldsymbol{\omega}} = \dot{\boldsymbol{\omega}}$  is angular acceleration about  $O'$ , and  $\mathbf{r}_G$  is a vector pointing at center of mass from  $O'$ .

Similarly, torque and angular acceleration are connected by Euler equations Eq. (5.3).

$$\mathbf{M}_{r_{O'}} = \mathbf{I}_{O'}\dot{\boldsymbol{\omega}} + \boldsymbol{\omega} \times (\mathbf{I}_{O'}\boldsymbol{\omega}) + m\mathbf{r}_G \times (\dot{\mathbf{v}}_{O'} + \boldsymbol{\omega} \times \mathbf{v}_{O'}) \quad (5.3)$$

where  $\mathbf{M}_{r_{O'}}$  is resultant torque around  $O'$  and  $\mathbf{I}_{O'}$  is inertial tensor referred to BFF

$$\mathbf{I}_{O'} = \begin{bmatrix} I_x & -I_{xy} & -I_{xz} \\ -I_{yx} & I_y & -I_{yz} \\ -I_{zx} & -I_{zy} & I_z \end{bmatrix} \quad (5.4)$$

in which,

$$\begin{aligned} I_x &= \int (\hat{y}^2 + \hat{z}^2) dm \\ I_y &= \int (\hat{x}^2 + \hat{z}^2) dm \\ I_z &= \int (\hat{x}^2 + \hat{y}^2) dm \\ I_{xy} &= I_{yx} = \int \hat{x}\hat{y} dm \\ I_{xz} &= I_{zx} = \int \hat{x}\hat{z} dm \\ I_{yz} &= I_{zy} = \int \hat{y}\hat{z} dm \end{aligned} \quad (5.5)$$

In BFF,  $\mathbf{v}_{O'}$ ,  $\dot{\mathbf{v}}_{O'}$ ,  $\boldsymbol{\omega}$ ,  $\dot{\boldsymbol{\omega}}$ , and  $\mathbf{r}_G$  are expressed as

$$\mathbf{v}_{O'} = \begin{bmatrix} u \\ v \\ w \end{bmatrix}, \quad \dot{\mathbf{v}}_{O'} = \begin{bmatrix} \dot{u} \\ \dot{v} \\ \dot{w} \end{bmatrix}, \quad \boldsymbol{\omega} = \begin{bmatrix} p \\ q \\ r \end{bmatrix}, \quad \dot{\boldsymbol{\omega}} = \begin{bmatrix} \dot{p} \\ \dot{q} \\ \dot{r} \end{bmatrix}, \quad \mathbf{r}_G = \begin{bmatrix} x_G \\ y_G \\ z_G \end{bmatrix} \quad (5.6)$$

Substitution of all variables' expressions in Eqs. (5.4) and (5.6) into Eqs. (5.2) and (5.3) results in

$$\begin{bmatrix} \mathbf{F}_r \\ \mathbf{M}_{r_{O'}} \end{bmatrix} = \tilde{\mathbf{M}} \cdot \begin{bmatrix} \dot{u} \\ \dot{v} \\ \dot{w} \\ \dot{p} \\ \dot{q} \\ \dot{r} \end{bmatrix} + \left[ \begin{array}{c|c} \mathbf{0}_{3 \times 3} & \mathbf{D}_{12} \\ \hline \mathbf{D}_{21} & \mathbf{D}_{22} \end{array} \right] \cdot \begin{bmatrix} u \\ v \\ w \\ p \\ q \\ r \end{bmatrix} \quad (5.7)$$

where

$$\tilde{\mathbf{M}} = \begin{bmatrix} m & 0 & 0 & 0 & mz_G & -my_G \\ 0 & m & 0 & -mz_G & 0 & mx_G \\ 0 & 0 & m & my_G & -mx_G & 0 \\ 0 & -mz_G & my_G & I_x & -I_{xy} & -I_{xz} \\ mz_G & 0 & -mx_G & -I_{yx} & I_y & -I_{yz} \\ -my_G & mx_G & 0 & -I_{zx} & -I_{zy} & I_z \end{bmatrix} \quad (5.8a)$$

$$\mathbf{D}_{12} = \begin{bmatrix} m(y_G q + z_G r) & -m(x_G q - w) & -m(x_G r + v) \\ -m(y_G p + w) & m(z_G r + x_G p) & -m(y_G r - u) \\ -m(z_G p - v) & -m(z_G q + u) & m(x_G p + y_G q) \end{bmatrix} \quad (5.8b)$$

$$\mathbf{D}_{21} = \begin{bmatrix} -m(y_G q + z_G r) & m(y_G p + w) & m(z_G p - v) \\ m(x_G q - w) & -m(z_G r + x_G p) & m(z_G q + u) \\ m(x_G r + v) & m(y_G r - u) & -m(x_G p + y_G q) \end{bmatrix} \quad (5.8c)$$

$$\mathbf{D}_{22} = \begin{bmatrix} 0 & -I_{yz}q - I_{xz}p + I_z r & I_{yz}r + I_{xy}p - I_y q \\ I_{yz}q + I_{xz}p - I_z r & 0 & -I_{xz}r - I_{xy}q + I_x p \\ -I_{yz}r - I_{xy}p + I_y q & I_{xz}r + I_{xy}q - I_x p & 0 \end{bmatrix} \quad (5.8d)$$

Resultant force and torque consist of four components: gravitational force, buoyancy, hy-

drodynamic force, and hydrodynamic damping, shown in Eq. (5.9).

$$\begin{bmatrix} \mathbf{F}_r \\ \mathbf{M}_{r_{O'}} \end{bmatrix} = \tilde{\mathbf{F}}_{GF} + \tilde{\mathbf{F}}_d + \tilde{\mathbf{F}}_{dp} \quad (5.9)$$

Combination of Eqs. (5.7) and (5.9) gives

$$\tilde{\mathbf{F}}_{GF} + \tilde{\mathbf{F}}_d + \tilde{\mathbf{F}}_{dp} = \tilde{\mathbf{M}} \cdot \begin{bmatrix} \dot{u} \\ \dot{v} \\ \dot{w} \\ \dot{p} \\ \dot{q} \\ \dot{r} \end{bmatrix} + \left[ \begin{array}{c|c} \mathbf{0}_{3 \times 3} & \mathbf{D}_{12} \\ \hline \mathbf{D}_{21} & \mathbf{D}_{22} \end{array} \right] \cdot \begin{bmatrix} u \\ v \\ w \\ p \\ q \\ r \end{bmatrix} \quad (5.10)$$

Substitution of  $\tilde{\mathbf{F}}_{GF}$ ,  $\tilde{\mathbf{F}}_d$ , and  $\tilde{\mathbf{F}}_{dp}$  in Eqs. (3.10), (4.46), (4.47), and (4.49) into Eq. (5.10) results in the final equations of motion.

$$\mathbf{M} \cdot \begin{bmatrix} \dot{u} \\ \dot{v} \\ \dot{w} \\ \dot{p} \\ \dot{q} \\ \dot{r} \end{bmatrix} = \left[ \begin{array}{c|c} \mathbf{\Lambda}_{11} & \mathbf{\Lambda}_{12} \\ \hline \mathbf{\Lambda}_{21} & \mathbf{\Lambda}_{22} \end{array} \right] \cdot \begin{bmatrix} u \\ v \\ w \\ p \\ q \\ r \end{bmatrix} + g \begin{bmatrix} -(m - m_d)s(\theta) \\ (m - m_d)c(\theta)s(\phi) \\ (m - m_d)c(\phi)c(\theta) \\ m(y_Gc(\phi)c(\theta) - z_Gc(\theta)s(\phi)) \\ -m(x_Gc(\phi)c(\theta) + z_Gs(\theta)) \\ m(x_Gc(\theta)s(\phi) + y_Gs(\theta)) \end{bmatrix} \quad (5.11)$$

where

$$\mathbf{M} = \begin{bmatrix} m + \mu_{11} & 0 & 0 & 0 & mz_G & -my_G \\ 0 & m + \mu_{22} & 0 & -mz_G & 0 & mx_G \\ 0 & 0 & m + \mu_{22} & my_G & -mx_G & 0 \\ 0 & -mz_G & my_G & I_x & -I_{xy} & -I_{xz} \\ mz_G & 0 & -mx_G & -I_{yx} & I_y + \mu_{55} & -I_{yz} \\ -my_G & mx_G & 0 & -I_{zx} & -I_{zy} & I_z + \mu_{55} \end{bmatrix} \quad (5.12a)$$

$$\mathbf{\Lambda}_{11} = \begin{bmatrix} -(X_u + X_{u|u}|u|) & 0 & 0 \\ 0 & -(Y_v + Y_{v|v}|v|) & 0 \\ 0 & 0 & -(Z_w + Z_{w|w}|w|) \end{bmatrix} \quad (5.12b)$$

$$\mathbf{\Lambda}_{12} = \begin{bmatrix} -m(y_G q + z_G r) & m(x_G q - w) - \mu_{22} w & m(x_G r + v) + \mu_{22} v \\ m(y_G p + w) + \mu_{22} w & -m(z_G r + x_G p) & m(y_G r - u) - \mu_{11} u \\ m(z_G p - v) - \mu_{22} v & m(z_G q + u) + \mu_{11} u & -m(x_G p + y_G q) \end{bmatrix} \quad (5.12c)$$

$$\mathbf{\Lambda}_{21} = \begin{bmatrix} m(y_G q + z_G r) & -m(y_G p + w) & -m(z_G p - v) \\ -m(x_G q - w) + \mu_{22} w & m(z_G r + x_G p) & -m(z_G q + u) - \mu_{11} u \\ -m(x_G r + v) - \mu_{22} v & -m(y_G r - u) + \mu_{11} u & m(x_G p + y_G q) \end{bmatrix} \quad (5.12d)$$

$$\mathbf{\Lambda}_{22} = \begin{bmatrix} -(K_p + K_{p|p}|p|) & I_{yz} q + I_{xz} p - I_z r & -I_{yz} r - I_{xy} p + I_y q \\ -I_{yz} q - I_{xz} p + I_z r & -(M_q + M_{q|q}|q|) & I_{xz} r + I_{xy} q - I_x p + \mu_{55} p \\ I_{yz} r + I_{xy} p - I_y q & -I_{xz} r - I_{xy} q + I_x p - \mu_{55} p & -(N_r + N_{r|r}|r|) \end{bmatrix} \quad (5.12e)$$

## 5.2 NON-DIMENSIONALIZATION

In previous section, Eq. (5.10) was derived to describe SB's motion. In this section, dimensions of all the variables will be checked and Eq. (5.10) will be rewritten in its dimensionless form. All variables included in this problem are listed in Tab. 5.1 and they are expressed in terms of basic dimensions: M(mass), T(time), and L(length).

Variables	Dimensions	Variables	Dimensions	Variables	Dimensions
$2a$	[L]	$2b$	[L]	$x$	[L]
$y$	[L]	$z$	[L]	$x_G$	[L]
$y_G$	[L]	$z_G$	[L]	$m$	[M]
$m_d$	[L]	$\mu_{11}$	[M]	$\mu_{22}$	[M]
$I_x$	[ML <sup>2</sup> ]	$I_{xy}$	[ML <sup>2</sup> ]	$I_{xz}$	[ML <sup>2</sup> ]
$I_{yx}$	[ML <sup>2</sup> ]	$I_y$	[ML <sup>2</sup> ]	$I_{yz}$	[ML <sup>2</sup> ]
$I_{zx}$	[ML <sup>2</sup> ]	$I_{zy}$	[ML <sup>2</sup> ]	$I_z$	[ML <sup>2</sup> ]
$\mu_{55}$	[ML <sup>2</sup> ]	$\phi$	[I]	$\theta$	[I]
$\psi$	[I]	$g$	[LT <sup>-2</sup> ]	$u$	[LT <sup>-1</sup> ]
$v$	[LT <sup>-1</sup> ]	$w$	[LT <sup>-1</sup> ]	$p$	[T <sup>-1</sup> ]
$q$	[T <sup>-1</sup> ]	$r$	[T <sup>-1</sup> ]	$\dot{u}$	[LT <sup>-2</sup> ]
$\dot{v}$	[LT <sup>-2</sup> ]	$\dot{w}$	[LT <sup>-2</sup> ]	$\dot{p}$	[T <sup>-2</sup> ]
$\dot{q}$	[T <sup>-2</sup> ]	$\dot{r}$	[T <sup>-2</sup> ]	$X_u$	[MT <sup>-1</sup> ]
$Y_v$	[MT <sup>-1</sup> ]	$Z_w$	[MT <sup>-1</sup> ]	$K_p$	[ML <sup>2</sup> T <sup>-1</sup> ]
$M_q$	[ML <sup>2</sup> T <sup>-1</sup> ]	$N_r$	[ML <sup>2</sup> T <sup>-1</sup> ]	$X_{u u }$	[ML <sup>-1</sup> ]
$Y_{v v }$	[ML <sup>-1</sup> ]	$Z_{w w }$	[ML <sup>-1</sup> ]	$K_{p p }$	[ML <sup>2</sup> ]
$M_{q q }$	[ML <sup>2</sup> ]	$N_{r r }$	[ML <sup>2</sup> ]		

Table 5.1: Dimensions of variables

Here,  $\phi$ ,  $\theta$ , and  $\psi$  themselves are dimensionless and [I] is used to denote this property.

Length of the major axis  $2a$ , displacement mass  $m_d$ , and gravitational acceleration  $g$  are chosen as the three principal variables. Then, all the variables in Tab. 5.1 can be expressed in terms of these three principal variables. Dimensionless form of all the variables could be obtained

through dividing them by combination of those three bases, as shown in Tab. 5.2.

Dimensionless variables	Expressions	Dimensionless variables	Expressions	Dimensionless variables	Expressions
$\bar{b}$	$\frac{2b}{2a}$	$\bar{x}$	$\frac{x}{2a}$	$\bar{y}$	$\frac{y}{2a}$
$\bar{z}$	$\frac{z}{2a}$	$\bar{x}_G$	$\frac{x_G}{2a}$	$\bar{y}_G$	$\frac{y_G}{2a}$
$\bar{z}_G$	$\frac{z_G}{2a}$	$\bar{m}$	$\frac{m}{m_d}$	$\bar{\mu}_{11}$	$\frac{\mu_{11}}{m_d}$
$\bar{\mu}_{22}$	$\frac{\mu_{22}}{m_d}$	$\bar{I}_x$	$\frac{I_x}{4m_d a^2}$	$\bar{I}_{xy}$	$\frac{I_{xy}}{4m_d a^2}$
$\bar{I}_{xz}$	$\frac{I_{xz}}{4m_d a^2}$	$\bar{I}_{yx}$	$\frac{I_{yx}}{4m_d a^2}$	$\bar{I}_y$	$\frac{I_y}{4m_d a^2}$
$\bar{I}_{yz}$	$\frac{I_{yz}}{4m_d a^2}$	$\bar{I}_{zx}$	$\frac{I_{zx}}{4m_d a^2}$	$\bar{I}_{zy}$	$\frac{I_{zy}}{4m_d a^2}$
$\bar{I}_z$	$\frac{I_z}{4m_d a^2}$	$\bar{\mu}_{55}$	$\frac{\mu_{55}}{4m_d a^2}$	$\phi$	$\phi$
$\theta$	$\theta$	$\psi$	$\psi$	$\bar{t}$	$\frac{t}{\sqrt{\frac{2a}{g}}}$
$\bar{u}$	$\frac{u}{\sqrt{2ga}}$	$\bar{v}$	$\frac{v}{\sqrt{2ga}}$	$\bar{w}$	$\frac{w}{\sqrt{2ga}}$
$\bar{p}$	$\frac{p}{\sqrt{\frac{g}{2a}}}$	$\bar{q}$	$\frac{q}{\sqrt{\frac{g}{2a}}}$	$\bar{r}$	$\frac{r}{\sqrt{\frac{g}{2a}}}$
$\dot{\bar{u}}$	$\frac{\dot{u}}{g}$	$\dot{\bar{v}}$	$\frac{\dot{v}}{g}$	$\dot{\bar{w}}$	$\frac{\dot{w}}{g}$
$\dot{\bar{p}}$	$\frac{\dot{p}}{\frac{g}{2a}}$	$\dot{\bar{q}}$	$\frac{\dot{q}}{\frac{g}{2a}}$	$\dot{\bar{r}}$	$\frac{\dot{r}}{\frac{g}{2a}}$
$\bar{X}_u$	$m_d \sqrt{\frac{g}{2a}}$	$\bar{Y}_v$	$m_d \sqrt{\frac{g}{2a}}$	$\bar{Z}_w$	$m_d \sqrt{\frac{g}{2a}}$
$\bar{K}_p$	$2m_d a \sqrt{2ga}$	$\bar{M}_q$	$2m_d a \sqrt{2ga}$	$\bar{N}_r$	$2m_d a \sqrt{2ga}$
$\bar{X}_{u u}$	$\frac{m_d}{2a}$	$\bar{Y}_{v v}$	$\frac{m_d}{2a}$	$\bar{Z}_{w w}$	$\frac{m_d}{2a}$
$\bar{K}_{p p}$	$4m_d a$	$\bar{M}_{q q}$	$4m_d a$	$\bar{N}_{r r}$	$4m_d a$

Table 5.2: Dimensionless variables

Expressions of  $\mu_{11}$ ,  $\mu_{22}$ , and  $\mu_{55}$  for body in shape of prolate spheroid are expressed in Eqs. (4.42) and (4.43), also SB's displacement mass  $m_d$  has the expression

$$m_d = \frac{4}{3}\pi\rho ab^2 \quad (5.13)$$

Dimensionless added mass is obtained as

$$\bar{\mu}_{11} = \frac{\mu_{11}}{m_d} = \frac{k_1}{2 - k_2} \quad (5.13a)$$

$$\bar{\mu}_{33} = \bar{\mu}_{22} = \frac{\mu_{22}}{m_d} = \frac{k_2}{2 - k_2} \quad (5.13b)$$

$$\bar{\mu}_{66} = \bar{\mu}_{55} = \frac{\mu_{55}}{4m_d a^2} = -\frac{1}{20} \frac{(\bar{b}^2 - 1)^2 (k_2 - k_1)}{2(\bar{b}^2 - 1) + (\bar{b}^2 + 1)(k_2 - k_1)} \quad (5.13c)$$

in which,  $k_1$  and  $k_2$  were defined in Eq. (4.43).

Substitution of all dimensional variables in Tab. 5.2 into Eq. (5.10) leads to the dimensionless equations of motion, as shown in Eq. (5.14) below.

$$\bar{\mathbf{M}} \cdot \begin{bmatrix} \bar{u} \\ \bar{v} \\ \bar{w} \\ \bar{p} \\ \bar{q} \\ \bar{r} \end{bmatrix} = \begin{bmatrix} \bar{\Lambda}_{11} & \bar{\Lambda}_{12} \\ \bar{\Lambda}_{21} & \bar{\Lambda}_{22} \end{bmatrix} \cdot \begin{bmatrix} \bar{u} \\ \bar{v} \\ \bar{w} \\ \bar{p} \\ \bar{q} \\ \bar{r} \end{bmatrix} + \begin{bmatrix} -(\bar{m} - 1)s(\theta) \\ (\bar{m} - 1)c(\theta)s(\phi) \\ (\bar{m} - 1)c(\phi)c(\theta) \\ \bar{m}\bar{y}_G c(\phi)c(\theta) - \bar{m}\bar{z}_G c(\theta)s(\phi) \\ -\bar{m}\bar{x}_G c(\phi)c(\theta) - \bar{m}\bar{z}_G s(\theta) \\ \bar{m}\bar{x}_G c(\theta)s(\phi) + \bar{m}\bar{y}_G s(\theta) \end{bmatrix} \quad (5.14)$$

where

$$\bar{\mathbf{M}} = \begin{bmatrix} \bar{m} + \bar{\mu}_{11} & 0 & 0 & 0 & \bar{m}\bar{z}_G & -\bar{m}\bar{y}_G \\ 0 & \bar{m} + \bar{\mu}_{22} & 0 & -\bar{m}\bar{z}_G & 0 & \bar{m}\bar{x}_G \\ 0 & 0 & \bar{m} + \bar{\mu}_{22} & \bar{m}\bar{y}_G & -\bar{m}\bar{x}_G & 0 \\ 0 & -\bar{m}\bar{z}_G & \bar{m}\bar{y}_G & \bar{I}_x & -\bar{I}_{xy} & -\bar{I}_{xz} \\ \bar{m}\bar{z}_G & 0 & -\bar{m}\bar{x}_G & -\bar{I}_{yx} & \bar{I}_y + \bar{\mu}_{55} & -\bar{I}_{yz} \\ -\bar{m}\bar{y}_G & \bar{m}\bar{x}_G & 0 & -\bar{I}_{zx} & -\bar{I}_{zy} & \bar{I}_z + \bar{\mu}_{55} \end{bmatrix} \quad (5.15a)$$

$$\bar{\Lambda}_{11} = \begin{bmatrix} -(\bar{X}_u + \bar{X}_{u|u}|u|) & 0 & 0 \\ 0 & -(\bar{Y}_v + \bar{Y}_{v|v}|v|) & 0 \\ 0 & 0 & -(\bar{Z}_w + \bar{Z}_{w|w}|w|) \end{bmatrix} \quad (5.15b)$$

$$\bar{\Lambda}_{12} = \begin{bmatrix} -\bar{m}(\bar{y}_G \bar{q} + \bar{z}_G \bar{r}) & \bar{m}(\bar{x}_G \bar{q} - \bar{w}) - \bar{\mu}_{22} \bar{w} & \bar{m}(\bar{x}_G \bar{r} + \bar{v}) + \bar{\mu}_{22} \bar{v} \\ \bar{m}(\bar{y}_G \bar{p} + \bar{w}) + \bar{\mu}_{22} \bar{w} & -\bar{m}(\bar{z}_G \bar{r} + \bar{x}_G \bar{p}) & \bar{m}(\bar{y}_G \bar{r} - \bar{u}) - \bar{\mu}_{11} \bar{u} \\ \bar{m}(\bar{z}_G \bar{p} - \bar{v}) - \bar{\mu}_{22} \bar{v} & \bar{m}(\bar{z}_G \bar{q} + \bar{u}) + \bar{\mu}_{11} \bar{u} & -\bar{m}(\bar{x}_G \bar{p} + \bar{y}_G \bar{q}) \end{bmatrix} \quad (5.15c)$$

$$\bar{\Lambda}_{21} = \begin{bmatrix} \bar{m}(\bar{y}_G \bar{q} + \bar{z}_G \bar{r}) & -\bar{m}(\bar{y}_G \bar{p} + \bar{w}) & -\bar{m}(\bar{z}_G \bar{p} - \bar{v}) \\ -\bar{m}(\bar{x}_G \bar{q} - \bar{w}) + \bar{\mu}_{22} \bar{w} & \bar{m}(\bar{z}_G \bar{r} + \bar{x}_G \bar{p}) & -\bar{m}(\bar{z}_G \bar{q} + \bar{u}) - \bar{\mu}_{11} \bar{u} \\ -\bar{m}(\bar{x}_G \bar{r} + \bar{v}) - \bar{\mu}_{22} \bar{v} & -\bar{m}(\bar{y}_G \bar{r} - \bar{u}) + \bar{\mu}_{11} \bar{u} & \bar{m}(\bar{x}_G \bar{p} + \bar{y}_G \bar{q}) \end{bmatrix} \quad (5.15d)$$

$$\bar{\Lambda}_{22} = \begin{bmatrix} -(\bar{K}_p + \bar{K}_{p|p}|\bar{p}|) & \bar{I}_{yz} \bar{q} + \bar{I}_{xz} \bar{p} - \bar{I}_z \bar{r} & -\bar{I}_{yz} \bar{r} - \bar{I}_{xy} \bar{p} + \bar{I}_y \bar{q} \\ -\bar{I}_{yz} \bar{q} - \bar{I}_{xz} \bar{p} + \bar{I}_z \bar{r} & -(\bar{M}_q + \bar{M}_{q|q}|\bar{q}|) & \bar{I}_{xz} \bar{r} + \bar{I}_{xy} \bar{q} - \bar{I}_x \bar{p} + \bar{\mu}_{55} \bar{p} \\ \bar{I}_{yz} \bar{r} + \bar{I}_{xy} \bar{p} - \bar{I}_y \bar{q} & -\bar{I}_{xz} \bar{r} - \bar{I}_{xy} \bar{q} + \bar{I}_x \bar{p} - \bar{\mu}_{55} \bar{p} & -(\bar{N}_r + \bar{N}_{r|r}|\bar{r}|) \end{bmatrix} \quad (5.15e)$$

It is noted that  $\bar{M}$  is a symmetric matrix.

### 5.3 ANALYSIS OF EQUATIONS OF MOTION AND NUMERICAL COMPUTATIONS

#### 5.3.1 Second-Order, Time-Dependent, Nonlinear, Fully coupled System

As claimed in Chap. 2, twelve variables are needed to describe the instantaneous state of SB's motion. They are dimensionless position vector  $\bar{\eta}$  expressed in EFF as  $[\bar{x}, \bar{y}, \bar{z}, \phi, \theta, \psi]^T$  and dimensionless velocity vector  $\bar{\nu}$  expressed in BFF as  $[\bar{u}, \bar{v}, \bar{w}, \bar{p}, \bar{q}, \bar{r}]^T$ .

Recalling Eq. (2.1) and Eq. (5.14), we derive their dimensionless forms as

$$\dot{\bar{\eta}} = \mathbf{J}(\boldsymbol{\alpha}) \bar{\nu} \quad (5.16)$$

$$\bar{M} \ddot{\bar{\nu}} = \bar{\Lambda} \bar{\nu} + \mathbf{T}(\bar{\eta}) \quad (5.17)$$

where

$$\bar{\Lambda} = \begin{bmatrix} \bar{\Lambda}_{11} & \bar{\Lambda}_{12} \\ \bar{\Lambda}_{21} & \bar{\Lambda}_{22} \end{bmatrix} \quad \mathbf{T}(\bar{\eta}) = \begin{bmatrix} -(\bar{m} - 1)s(\theta) \\ (\bar{m} - 1)c(\theta)s(\phi) \\ (\bar{m} - 1)c(\phi)c(\theta) \\ \bar{m}\bar{y}_G c(\phi)c(\theta) - \bar{m}\bar{z}_G c(\theta)s(\phi) \\ -\bar{m}\bar{x}_G c(\phi)c(\theta) - \bar{m}\bar{z}_G s(\theta) \\ \bar{m}\bar{x}_G c(\theta)s(\phi) + \bar{m}\bar{y}_G s(\theta) \end{bmatrix} \quad (5.18)$$

This system is nonlinear because some terms contain square of velocities and trigonometrical function of the Euler angles. It is noted that  $\bar{\Lambda}$  is a function of  $\boldsymbol{\alpha}$ , which changes over time; hence the system is time-dependent. Besides, the fact that  $\bar{\Lambda}_{12}$  and  $\bar{\Lambda}_{21}$  does not equal to 0 indicates the coupling of translational motion and rotational motion. As a result, the system is so complicated that an explicit analytical solution of SB's motion can not obtained. Numerical integration as an alternative way has to be used.

For a general case, this system have the following independent inputs:

- Properties of SB

$$\bar{m}, \quad \bar{b}, \quad \bar{\boldsymbol{\mu}}, \quad [\bar{x}_G, \bar{y}_G, \bar{z}_G], \quad \begin{bmatrix} \bar{I}_x & -\bar{I}_{xy} & -\bar{I}_{xz} \\ -\bar{I}_{yx} & \bar{I}_y & -\bar{I}_{yz} \\ -\bar{I}_{zx} & -\bar{I}_{zy} & \bar{I}_z \end{bmatrix}$$

- Initial position and attitude

$$[\bar{x}_0, \bar{y}_0, \bar{z}_0, \phi_0, \theta_0, \psi_0]$$

- Initial velocity

$$[\bar{u}_0, \bar{v}_0, \bar{w}_0, \bar{p}_0, \bar{q}_0, \bar{r}_0]$$

If we adjust one of the variables above, the moving trajectory will be changed.

### 5.3.2 Numerical Integration

As the system is completely defined, given twelve state variables at time  $t$ , time derivative of the velocity vector can be calculated using equations of motion (Eq. (5.14)). Meanwhile, time derivative of the position vector can be obtained by applying transformation matrix on velocity vector (Eq. (2.1)). **4<sup>th</sup>-order Runge-Kutta** method is used for integration over time and obtain twelve state variables in each time step.

$$\bar{\dot{\boldsymbol{\eta}}} = \mathbf{J}(\boldsymbol{\alpha})\bar{\boldsymbol{\nu}} \quad (5.19)$$

$$\bar{\mathbf{M}}\bar{\boldsymbol{\nu}} = \bar{\boldsymbol{\Lambda}}\bar{\boldsymbol{\nu}} + \mathbf{T}(\bar{\boldsymbol{\eta}}) \quad (5.20)$$

Define functions  $f_1$  and  $f_2$  such that

$$\bar{\boldsymbol{\nu}}(\bar{t}) = \bar{\mathbf{M}}^{-1}(\bar{\boldsymbol{\Lambda}}\bar{\boldsymbol{\nu}} + \mathbf{T}(\bar{\boldsymbol{\eta}})) = f_1(t, \bar{\boldsymbol{\nu}}(\bar{t}), \bar{\boldsymbol{\eta}}(\bar{t})) \quad (5.21)$$

$$\bar{\dot{\boldsymbol{\eta}}} = \mathbf{J}(\boldsymbol{\alpha})\bar{\boldsymbol{\nu}} = f_2(\bar{\boldsymbol{\nu}}(\bar{t}), \bar{\boldsymbol{\eta}}(\bar{t})) \quad (5.22)$$

which represents the dimensionless equations of motion and transformation matrix.  $d\bar{t}$  is time step. Apply **4<sup>th</sup> order Runge-Kutta method**:

$$\bar{\boldsymbol{\nu}}(\bar{t} + d\bar{t}) = \bar{\boldsymbol{\nu}}(\bar{t}) + \frac{d\bar{t}}{6}(k_1 + 2k_2 + 2k_3 + k_4) + O(dt^4) \quad (5.23)$$

$$\bar{\boldsymbol{\eta}}(\bar{t} + d\bar{t}) = \bar{\boldsymbol{\eta}}(\bar{t}) + \frac{d\bar{t}}{6}(k_5 + 2k_6 + 2k_7 + k_8) + O(dt^4) \quad (5.24)$$

where  $O(dt^4)$  is the error, which is 4<sup>th</sup> order of  $dt$  and

$$\begin{aligned} k_1 &= f_1(\bar{\boldsymbol{\nu}}(\bar{t}), \bar{\boldsymbol{\eta}}(\bar{t})); & k_5 &= f_2(\bar{\boldsymbol{\nu}}(\bar{t}), \bar{\boldsymbol{\eta}}(\bar{t})) \\ k_2 &= f_1(\bar{\boldsymbol{\nu}}(\bar{t}) + \frac{d\bar{t}}{2}k_1, \bar{\boldsymbol{\eta}}(\bar{t}) + \frac{d\bar{t}}{2}k_5); & k_6 &= f_2(\bar{\boldsymbol{\nu}}(\bar{t}) + \frac{d\bar{t}}{2}k_1, \bar{\boldsymbol{\eta}}(\bar{t}) + \frac{d\bar{t}}{2}k_5) \\ k_3 &= f_1(\bar{\boldsymbol{\nu}}(\bar{t}) + \frac{d\bar{t}}{2}k_2, \bar{\boldsymbol{\eta}}(\bar{t}) + \frac{d\bar{t}}{2}k_6); & k_7 &= f_2(\bar{\boldsymbol{\nu}}(\bar{t}) + \frac{d\bar{t}}{2}k_2, \bar{\boldsymbol{\eta}}(\bar{t}) + \frac{d\bar{t}}{2}k_6) \\ k_4 &= f_1(\bar{\boldsymbol{\nu}}(\bar{t}) + k_3d\bar{t}, \bar{\boldsymbol{\eta}}(\bar{t}) + k_7d\bar{t}); & k_8 &= f_2(\bar{\boldsymbol{\nu}}(\bar{t}) + k_3d\bar{t}, \bar{\boldsymbol{\eta}}(\bar{t}) + k_7d\bar{t}) \end{aligned}$$

Time step is chosen to be small enough to have convergent results and all instantaneous state variables can be obtained. The numerical scheme is implemented in commercial software MatLab and the code could be found in Appendix E. A 3-dimension test case is shown in Appendix D.

## CHAPTER 6

### SIMPLIFIED EQUATIONS OF MOTION AND NUMERICAL CASES

#### 6.1 3-DEGREE FREEDOM IN-PLANE MOTION

Intuition tells us if the mass distribution and initial conditions are all symmetric about the  $Oxz$  plane, SB should stay on this plane and the number of degrees of freedom will be reduced to three. We will demonstrate that in this section.

First, assuming symmetry of density distribution about  $O'\hat{x}\hat{z}$  plane is kept, according to Eqs. (5.5) and (C.1)(a-d), we can derive

$$\begin{aligned} \bar{x}_G \neq 0, \bar{z}_G \neq 0, \bar{y}_G &= 0 \\ \bar{I}_{xz} &= \bar{I}_{zx} \neq 0 \\ \bar{I}_{xy} = \bar{I}_{yx} = \bar{I}_{yz} = \bar{I}_{zy} &= 0 \end{aligned} \quad (6.1)$$

and moment of inertia tensor is simplified to be

$$\mathbf{I}_{O'} = \begin{bmatrix} \bar{I}_x & 0 & -\bar{I}_{xz} \\ 0 & \bar{I}_y & 0 \\ -\bar{I}_{zx} & 0 & \bar{I}_z \end{bmatrix} \quad (6.2)$$

Dimensionless acceleration at  $\bar{t}$  can be obtained by putting above zeros into the dimensionless equations of motion of Eqs. (5.16) and (5.17)

$$\left\{ \begin{array}{l} (\bar{m} + \bar{\mu}_{11})\bar{u} + \bar{m}\bar{z}_G\bar{q} = \bar{m}\bar{x}_G\bar{q}^2 - (\bar{m} + \bar{\mu}_{22})\bar{w}\bar{q} - (\bar{m} - 1)\sin(\theta) \\ \boxed{(\bar{m} + \bar{\mu}_{22})\bar{v} - \bar{m}\bar{z}_G\bar{p} + \bar{m}\bar{x}_G\bar{r} = 0} \\ (\bar{m} + \bar{\mu}_{22})\bar{w} - \bar{m}\bar{x}_G\bar{q} = \bar{m}\bar{z}_G\bar{q}^2 + (\bar{m} + \bar{\mu}_{11})\bar{q}\bar{u} + (\bar{m} - 1)\cos\theta \\ \boxed{-\bar{m}\bar{z}_G\bar{v} + \bar{I}_x\bar{p} - \bar{I}_{xz}\bar{r} = 0} \\ (\bar{I}_y + \bar{\mu}_{55})\bar{q} + \bar{m}\bar{z}_G\bar{u} - \bar{m}\bar{x}_G\bar{w} = \bar{m}\bar{x}_G\bar{q}\bar{u} + (\bar{\mu}_{22} - \bar{\mu}_{11})\bar{w}\bar{u} - \bar{m}\bar{z}_G\bar{q}\bar{w} - \bar{m}(\bar{x}_G\cos\theta + \bar{z}_G\sin\theta) \\ \boxed{\bar{m}\bar{x}_G\bar{v} - \bar{I}_{zx}\bar{p} + (\bar{I}_z + \bar{\mu}_{55})\bar{r} = 0} \end{array} \right. \quad (6.3)$$

From the above three boxed equations, we can derive that  $\bar{v} = \bar{p} = \bar{r} = 0$ , i.e., no transverse translation and rotation about  $\hat{x}$  and  $\hat{y}$  axes.

In addition, assume that SB is released in the  $Oxz$  plane; transformation matrix  $\mathbf{J}$  in Eq. (2.2) can be simplified and dimensionless time derivative of position is expressed as

$$\begin{bmatrix} \dot{\bar{x}} \\ \dot{\bar{y}} \\ \dot{\bar{z}} \end{bmatrix} = \begin{bmatrix} \cos\theta & 0 & \sin\theta \\ 0 & 1 & 0 \\ -\sin\theta & 0 & \cos\theta \end{bmatrix} \cdot \begin{bmatrix} \bar{u} \\ \bar{v} \\ \bar{w} \end{bmatrix}; \quad \begin{bmatrix} \dot{\bar{\phi}} \\ \dot{\bar{\theta}} \\ \dot{\bar{\psi}} \end{bmatrix} = \begin{bmatrix} 1 & 0 & \tan\theta \\ 0 & 1 & 0 \\ 0 & 0 & \frac{1}{\cos\theta} \end{bmatrix} \cdot \begin{bmatrix} \bar{p} \\ \bar{q} \\ \bar{r} \end{bmatrix} \quad (6.4)$$

Since

$$\bar{v} = \bar{p} = \bar{r} = 0$$

it could be proved that

$$\bar{y} = \bar{\phi} = \bar{\psi} = 0$$

Thus we conclude

$$\begin{aligned} \phi = \psi = \bar{v} = \bar{p} = \bar{r} = 0 \\ \implies \bar{\phi} = \bar{\psi} = \bar{v} = \bar{p} = \bar{r} = 0 \end{aligned}$$

Six degrees of freedom are reduced to three and the system is simplified to 6 ODEs as follows for surge  $\bar{u}$ , heave  $\bar{w}$ , pitch  $\bar{q}$ , displacements in the  $\bar{x}$ ,  $\bar{y}$  directions and  $\theta$  attitude.

$$\left\{ \begin{array}{l} (\bar{m} + \bar{\mu}_{11})\bar{\dot{u}} + \bar{m}\bar{z}_G\bar{\dot{q}} = \bar{m}\bar{x}_G\bar{q}^2 - (\bar{m} + \bar{\mu}_{22})\bar{w}\bar{q} - (\bar{m} - 1)\sin\theta \\ (\bar{m} + \bar{\mu}_{22})\bar{\dot{w}} - \bar{m}\bar{x}_G\bar{\dot{q}} = \bar{m}\bar{z}_G\bar{q}^2 + (\bar{m} + \bar{\mu}_{11})\bar{q}\bar{u} + (\bar{m} - 1)\cos\theta \\ (\bar{I}_y + \bar{\mu}_{55})\bar{\dot{q}} + \bar{m}\bar{z}_G\bar{\dot{u}} - \bar{m}\bar{x}_G\bar{\dot{w}} = \bar{m}\bar{x}_G\bar{q}\bar{u} + (\bar{\mu}_{22} - \bar{\mu}_{11})\bar{w}\bar{u} - \bar{m}\bar{z}_G\bar{q}\bar{w} - \bar{m}(\bar{x}_G\cos\theta + \bar{z}_G\sin\theta) \\ \bar{\dot{\theta}} = \bar{q} \\ \bar{\dot{x}} = \bar{u}\cos\theta + \bar{w}\sin\theta \\ \bar{\dot{z}} = -\bar{u}\sin\theta + \bar{w}\cos\theta \end{array} \right. \quad (6.5)$$

SB will move in  $Oxz$  plane as expected.

## 6.2 MOVING FORWARD WITH OSCILLATION

In the case that weight equals to buoyancy  $m/m_d = 1$  and the center of mass is below the center of buoyancy  $\bar{z}_G < 0$ ,

$$\bar{m} = 1, \quad \bar{x}_G = 0, \quad \bar{z}_G < 0$$

the system can be further simplified to:

$$\left\{ \begin{array}{l} (1 + \bar{\mu}_{11})\bar{\dot{u}} + \bar{z}_G\bar{\dot{q}} = -(1 + \bar{\mu}_{22})\bar{w}\bar{q} \\ (1 + \bar{\mu}_{22})\bar{\dot{w}} = \bar{z}_G\bar{q}^2 + (1 + \bar{\mu}_{11})\bar{q}\bar{u} \\ (\bar{I}_y + \bar{\mu}_{55})\bar{\dot{q}} + \bar{z}_G\bar{\dot{u}} = (\bar{\mu}_{22} - \bar{\mu}_{11})\bar{w}\bar{u} - \bar{z}_G\bar{q}\bar{w} - \bar{z}_G\sin\theta \\ \bar{\dot{\theta}} = \bar{q} \\ \bar{\dot{x}} = \bar{u}\cos\theta + \bar{w}\sin\theta \\ \bar{\dot{z}} = -\bar{u}\sin\theta + \bar{w}\cos\theta \end{array} \right. \quad (6.6)$$

If the perturbations of the velocities are small, the high-order nonlinear terms can be neglected. In addition, assuming that  $\theta$  is a small angle, so that  $\sin\theta \approx \theta$  is valid, the system could be linearized as

$$(\bar{I}_y + \bar{\mu}_{55})\bar{\ddot{\theta}} = -\bar{z}_G\theta \quad (6.7)$$

Solution of the system is a trigonometric function, which indicates that the prolate-spheroidal body oscillates while moving forward; the dimensionless period of the oscillation is

$$\bar{P} = 2\pi \sqrt{\frac{\bar{I}_y + \bar{\mu}_{55}}{\bar{z}_G}} \quad (6.8)$$

**Simulation 1** The simulation setting as follows:

Properties	Values
Major Axis( $m$ )	0.24
Minor Axis( $m$ )	0.024
Density of SB $[\rho_1, \rho_2, \rho_3, \rho_4]$ ( $kg/m^3$ )	[698.6, 698.6, 1298.6, 1298.6]
Density of Water( $kg/m^3$ )	998.6
$[x_0, y_0, z_0, \phi_0, \theta_0, \psi_0]$ ( $m$ or $I$ )	$[0, 0, 0, 0, -\frac{\pi}{24}, 0]$
$[u_0, v_0, w_0, p_0, q_0, r_0]$ ( $m/s$ or $s^{-1}$ )	$[0.1 \cos(-\frac{\pi}{24}), 0, 0.1 \sin(-\frac{\pi}{24}), 0, 0, 0]$

Table 6.1: Parameters of the model for Simulation 1

Density distribution follows the description in Appendix C with  $\rho_1, \rho_2, \rho_3$  and  $\rho_4$  given in Tab. 6.1. Other parameters are also defined in Tab. 6.1; initial conditions are depicted in Fig. 6.1

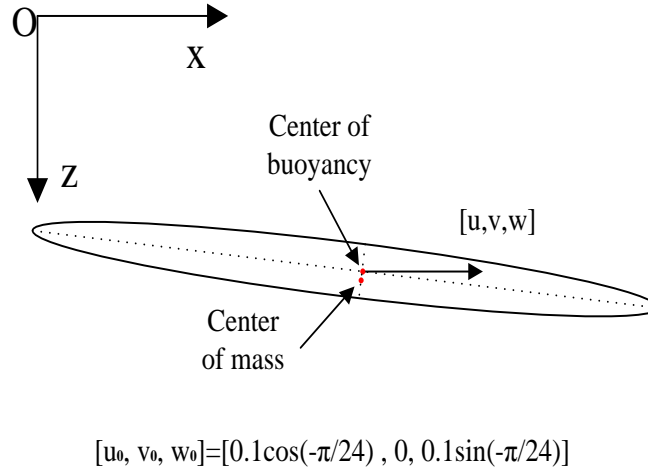


Figure 6.1: Prolate-spheroidal rigid body with center of mass below center of buoyancy with initial condition as indicated

According to Eqs. (C.7), (C.8), and (5.14),

$$\bar{I}_y = 0.0505, \quad \bar{\mu}_{55} = 0.0446, \quad \bar{z}_G = 0.0056, \quad (6.9)$$

Substituting them in Eq. (6.8) gives the estimated period

$$\bar{P} \approx 26.1635 \quad (6.10)$$

The time-histories of the dimensionless position coordinates  $(\bar{x}, \bar{y})$  and Euler angles are shown in Fig. 6.2. The time step is  $10^{-5}$  second and the simulation time is 15 seconds. Dimensionless oscillation period is about 32 when nonlinear terms are considered. Compared with 26.1635, we can see that three degrees of freedom are heavily coupled and nonlinear terms are significant and can not be ignored even with very small initial velocity. Numerical experiment shows if the initial velocity is chosen to be 0, the dimensionless period will be very close to the estimated one given by Eq. (6.8).

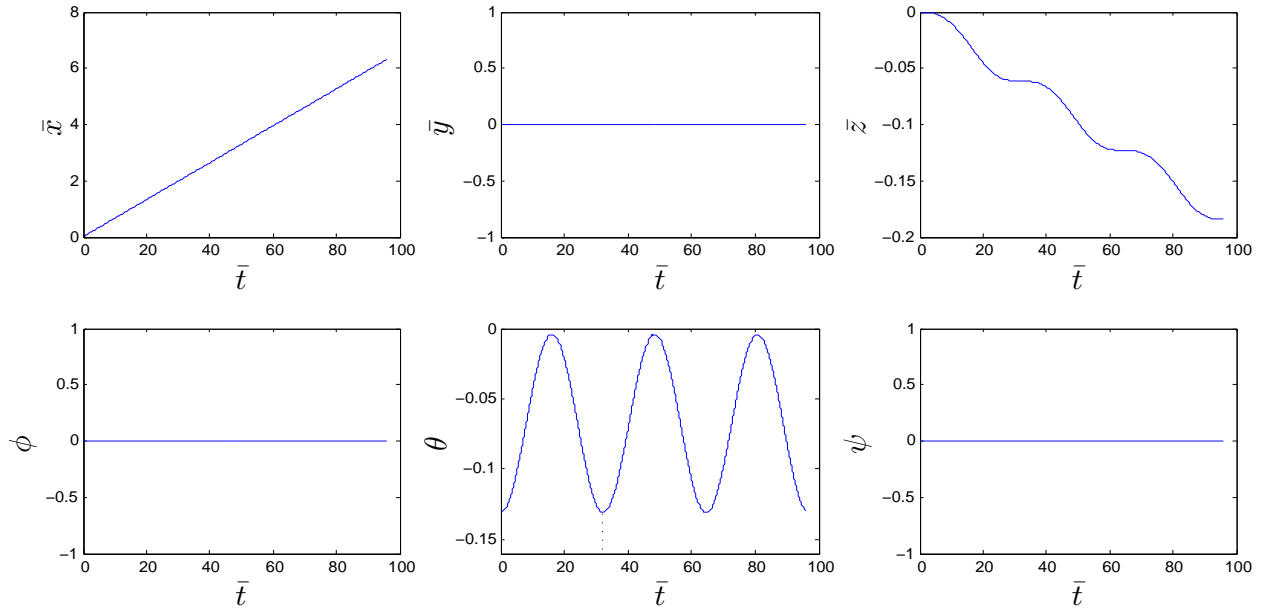


Figure 6.2: Dimensionless position coordinates and Euler angles of Simulation 1

Here, time-history of  $\bar{x}$  shown in Fig. 6.2 is not linear and  $\bar{x}$  in Eq. (6.6) is not a constant, it seems to be linear just because the fluctuation of horizontal velocity is very small.

### 6.3 IN-PLANE MOTION FOR PROLATE SPHEROID WITH UNIFORM DENSITY DISTRIBUTION

If prolate-spheroidal rigid body is assumed to have uniform density distribution, according to Eq. (C.1), we can derive  $x_G = z_G = 0$ . The system can be simplified to:

$$\begin{cases} \bar{u} = \frac{1}{\bar{m} + \bar{\mu}_{11}} [-(\bar{m} + \bar{\mu}_{22})\bar{w}\bar{q} - (\bar{m} - 1)\sin\theta] \\ \bar{w} = \frac{1}{\bar{m} + \bar{\mu}_{22}} [(\bar{m} + \bar{\mu}_{11})\bar{q}\bar{u} + (\bar{m} - 1)\cos\theta] \\ \bar{q} = \frac{1}{I_y + \bar{\mu}_{55}} [(\bar{\mu}_{22} - \bar{\mu}_{11})\bar{w}\bar{u}] \\ \bar{\theta} = \bar{q} \\ \bar{x} = \bar{u}\cos\theta + \bar{w}\sin\theta \\ \bar{z} = -\bar{u}\sin\theta + \bar{w}\cos\theta \end{cases} \quad (6.11)$$

The expression of  $\bar{q}$  in Eq. (6.11) shows that gravitational force and buoyancy contribute to zero moment and angular acceleration is only a result of the coupling term of the translational velocity in the plane, which is known as unsteady Munk moment. Although the given conditions greatly simplified the equations of motion, the system is still a second-order, time-dependent, nonlinear, and coupled dynamic system, which needs to be solved numerically.

**Simulation 2** The simulation setting for this testing case is as follows:

Geometry and physical parameters of the model are defined in Tab. 6.2. The prolate-spheroidal rigid body has a uniform density that is set to be slightly greater than standard fresh water. It is released in zero initial velocity and  $-45^\circ$  of  $\theta$ , as shown in Fig. 6.3.

Properties	Values
Major Axis	0.24 m
Minor Axis	0.024 m
Density of SB	1050 kg/m <sup>3</sup>
Density of Water	998.6 kg/m <sup>3</sup>
$[x_0, y_0, z_0, \phi_0, \theta_0, \psi_0]$	$[0, 0, 0, 0, -\frac{\pi}{4}, 0]$
$[u_0, v_0, w_0, p_0, q_0, r_0]$	$[0, 0, 0, 0, 0, 0]$

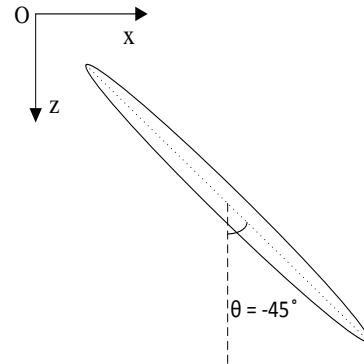


Figure 6.3: Free release with  $-45^\circ$

Table 6.2: Parameters of the model for Simulation 2

Time step is chosen to be  $10^{-5}$  second and simulation period is from 0 to 4.5 seconds.

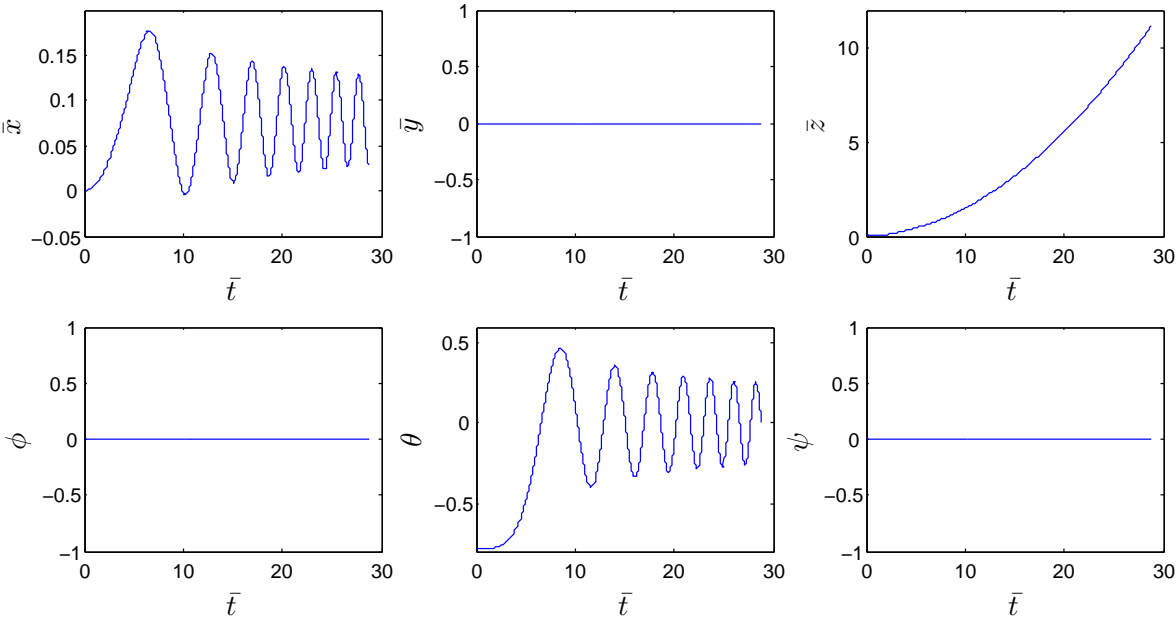


Figure 6.4: Dimensionless position coordinates and Euler angles for Simulation 2

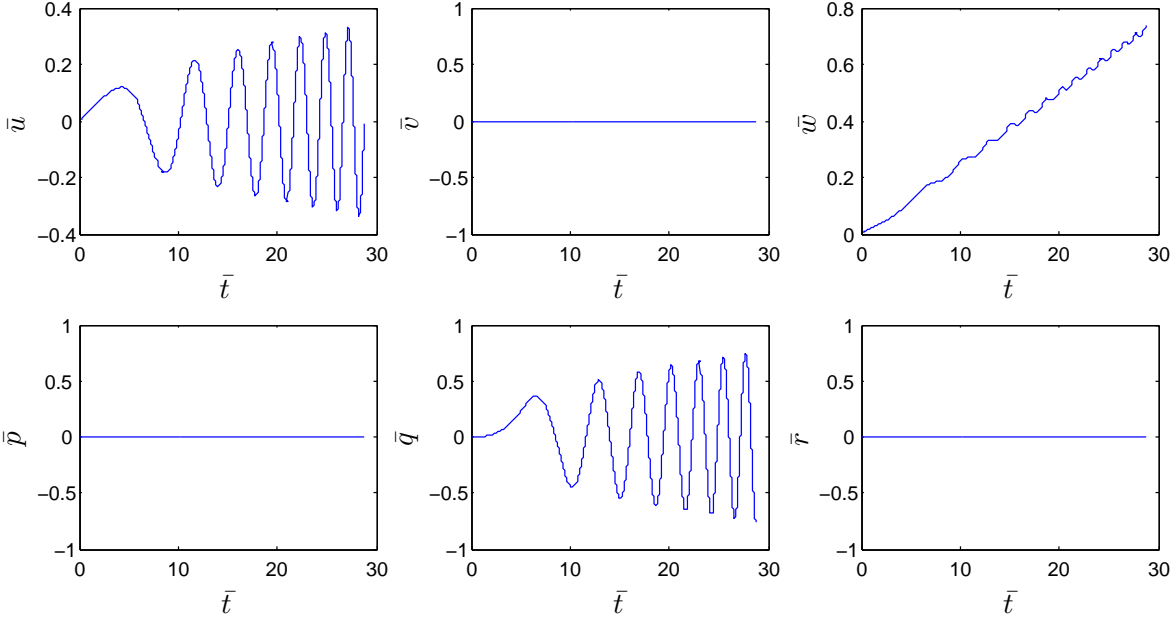


Figure 6.5: Dimensionless velocity in BFF for Simulation 2

Fig. 6.4 shows the historical responses of dimensionless position coordinates and Euler angles, from which we note that three degrees of freedom  $\bar{x}$ ,  $\bar{z}$ ,  $\theta$  are not zeros and the other three stay at zero. It should be noted that time-history of  $\bar{z}$  is not a quadratic function as shown in Fig. 6.6. It looks close to a quadratic line, because the fluctuation of vertical velocity is relatively

small.  $\bar{x}$  is observed to be oscillating around a positive number, which means instead of gliding down, the prolate spheroid actually is wiggling down like a leaf falling in the air.

Fig. 6.5 represents the historical responses of dimensionless velocity in BFF. Putting Eq. (6.11), Figs. 6.3, 6.4, and 6.5 together, it is noted that, at the beginning,  $\bar{u}$  and  $\bar{w}$  in BFF start to increase under gravitational force; then positive  $\bar{u}$  and  $\bar{w}$  lead to positive Munk moment and hence positive angular velocity  $\bar{q}$ , because added mass  $\bar{\mu}_{22}$  is larger than  $\bar{\mu}_{11}$ . That positive  $\bar{q}$  comes back and results in negative  $\bar{u}$  and the body ends up with oscillating horizontally.

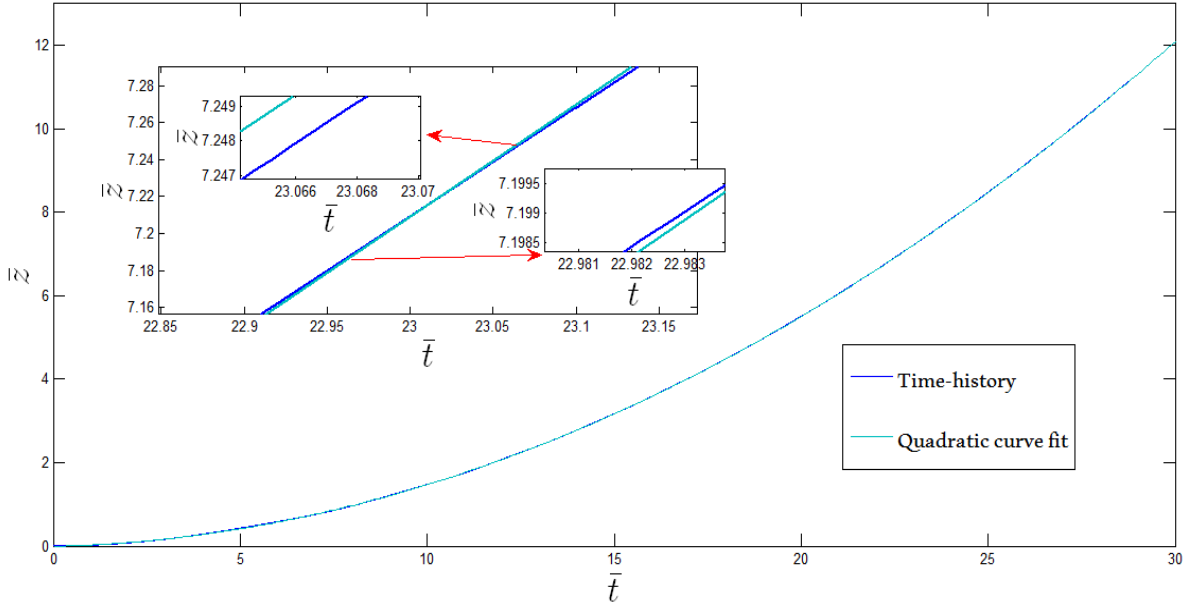


Figure 6.6: Time history of  $\bar{z}$  vs quadratic curve fit

## 6.4 ENERGY CONSERVATION

In the case that viscous effects are not considered, there will be no damping terms dissipating energy hence total energy including kinetic energy and potential energy should be conserved. Eq. (6.12) expresses kinetic energy of the system by considering both the mass of rigid body and added mass. Eq. (6.13) gives the expression of gravitational potential energy of the system.

$$K = \frac{1}{2} [(m + \mu_{11})u^2 + (m + \mu_{22})v^2 + (m + \mu_{22})w^2 + I_x p^2 + (I_y + \mu_{55})q^2 + (I_z + \mu_{55})r^2 + 2I_{xy}pq + 2I_{yz}qr + 2I_{xz}pr] \quad (6.12)$$

$$P = -(m - m_d)gz \quad (6.13)$$

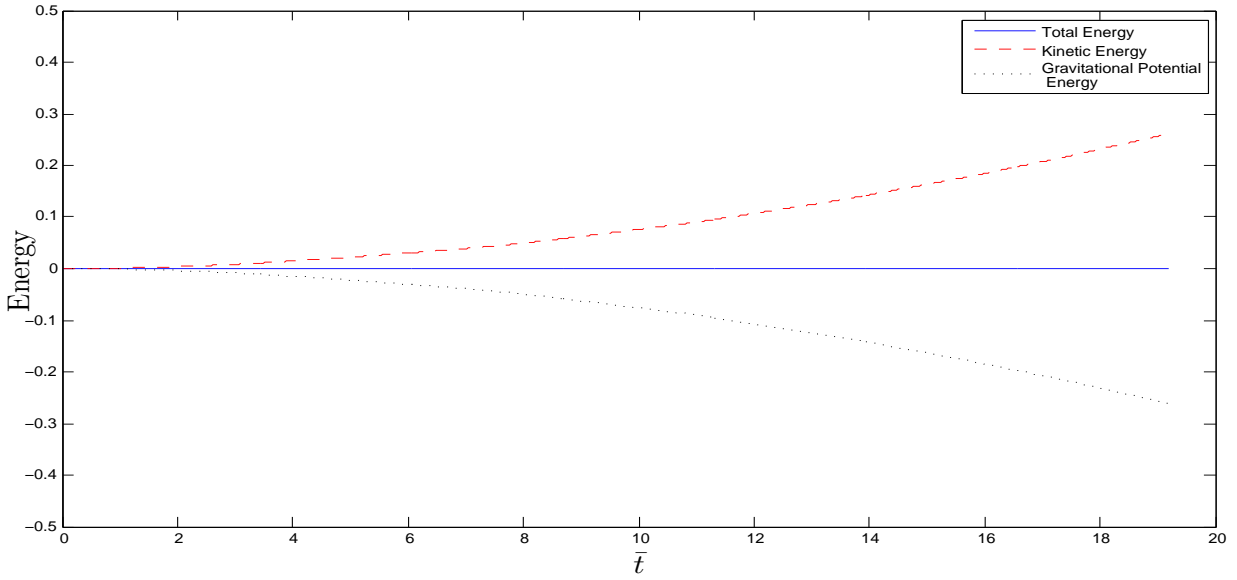


Figure 6.7: Dimensionless energy changes with time

Total energy is the sum of kinetic and potential energy. Nondimensionlizing it by  $2m_dga$  lead to

$$\bar{T} = \frac{K + P}{2m_dga} \quad (6.14)$$

$$= \frac{1}{2} [(\bar{m} + \bar{\mu}_{11})\bar{u}^2 + (\bar{m} + \bar{\mu}_{22})\bar{v}^2 + (\bar{m} + \bar{\mu}_{22})\bar{w}^2 + \bar{I}_x\bar{p}^2 + (\bar{I}_y + \bar{\mu}_{55})\bar{q}^2 + (\bar{I}_z + \bar{\mu}_{55})\bar{r}^2 + 2\bar{I}_{xy}\bar{p}\bar{q} + 2\bar{I}_{yz}\bar{q}\bar{r} + 2\bar{I}_{xz}\bar{p}\bar{r}] - (\bar{m} - \bar{m}_d)\bar{z} \quad (6.15)$$

Fig. 6.7 shows the dimensionless kinetic energy, gravitation potential energy, and total energy for **simulation 2**. We can see that, during falling, gravitational potential energy is transformed into kinematic energy resulting in conserved total energy.

## 6.5 OSCILLATION PERIOD CHANGES WITH RELEASE ANGLE

In previous sections, it was shown that prolate spheroid would oscillate horizontally instead of gliding down. This section would discuss the influence of release angle on the oscillation period.

### Simulation 3

Prolate spheroid is released with zero initial velocity and all the model parameters are the same as **Simulation 2** except for the release angle  $\theta_0$ . Recall Eq. 6.11 as the control equations for this simulation. Fig. 6.8 shows the histories of  $\bar{x}$ . Period is defined to be the time between two adjacent peaks, for example, first period represents time between the first peak and second peak. In algorithm, times corresponding to two adjacent peaks of amplitude are found and subtraction gives us the period length.

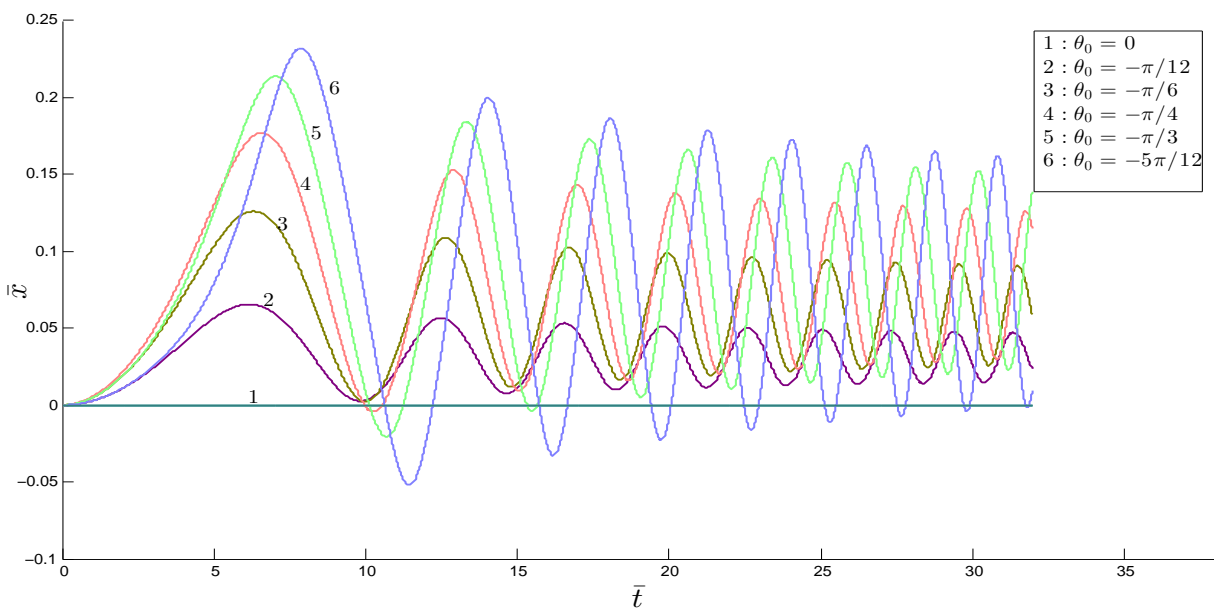


Figure 6.8: Histories of  $\bar{x}$  for different release angles

Fig. 6.9 illustrates that periods change with release angle. It is noted that the first few periods for different release angles are almost the same, i.e. changing release angle has little influence on the period of horizontal oscillation. On the other hand, different periods are of different lengths, for example the first period of all cases is about 6.3 and the second period is about 4.05.

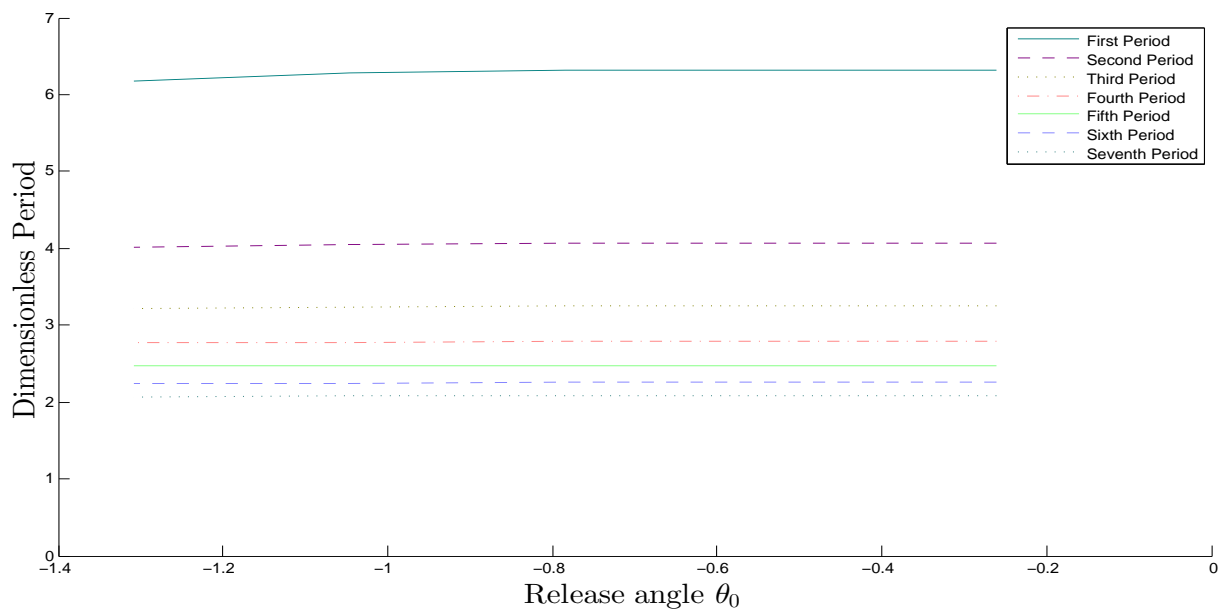


Figure 6.9: Dimensionless periods for change in horizontal position  $\bar{x}$  with release angle  $\theta_0$

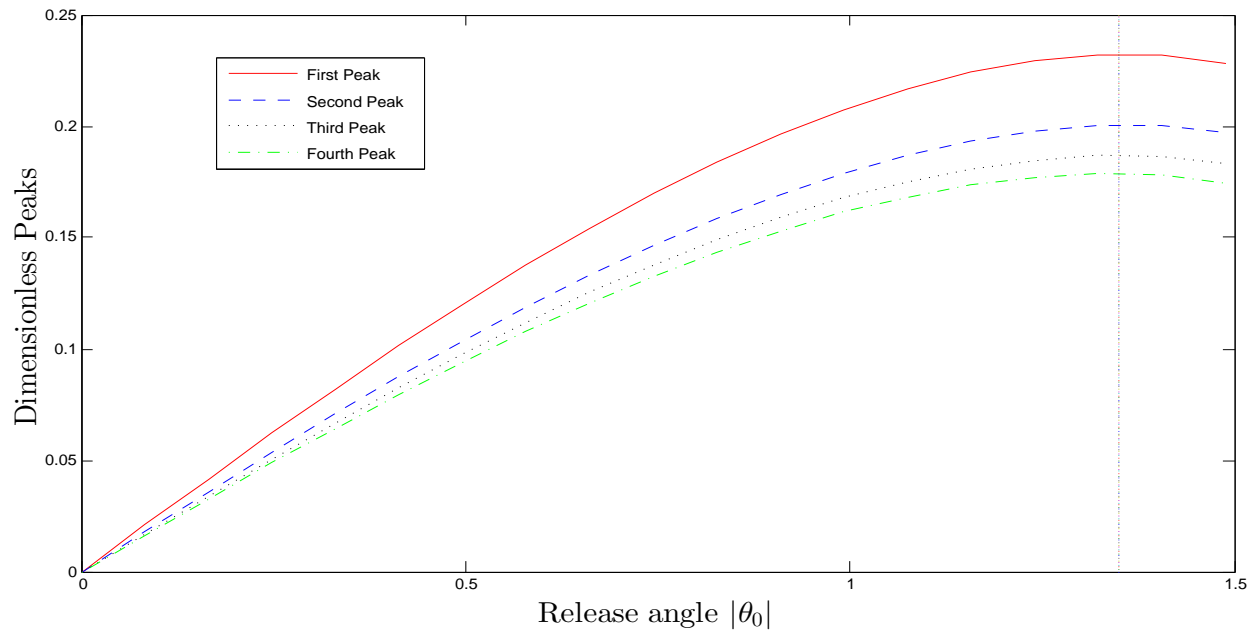


Figure 6.10: Peaks of change in  $\bar{x}$  with the release angle  $\theta_0$

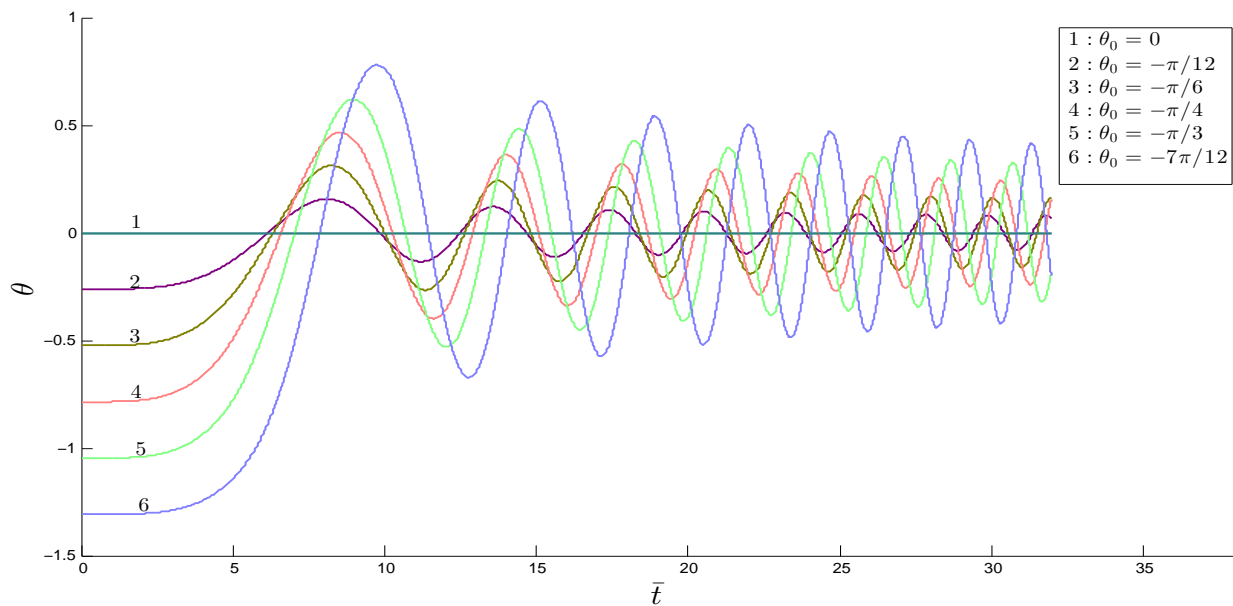


Figure 6.11: Histories of  $\theta$  for different release angles

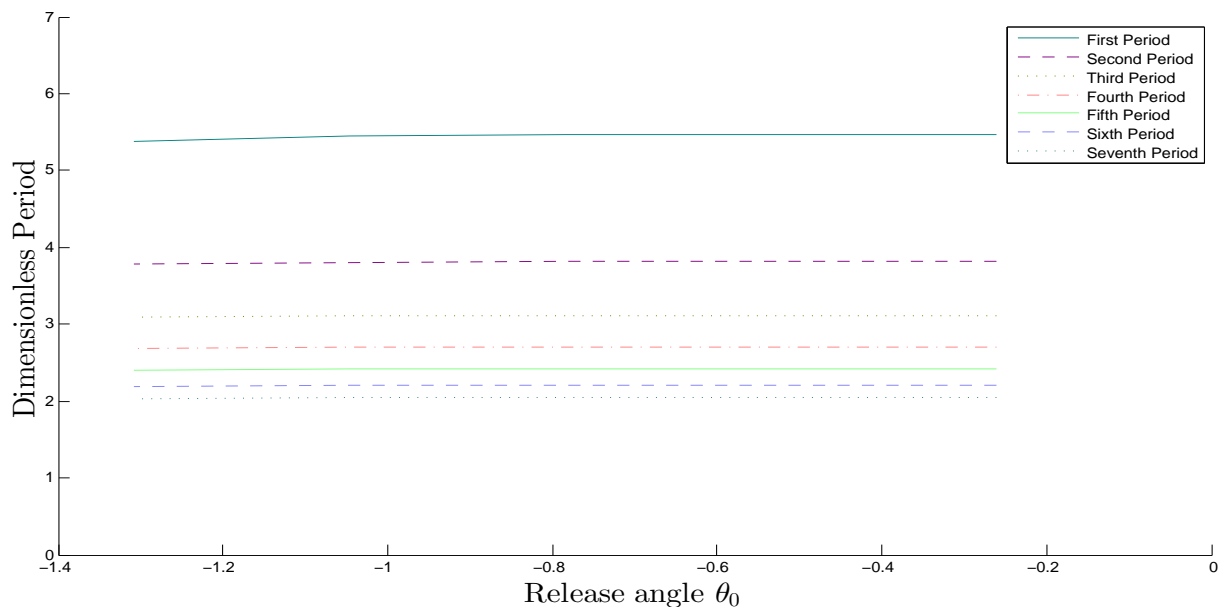


Figure 6.12: Dimensionless periods for  $\theta$  change with release angle

Fig. 6.8 also shows that different release angles have different peak oscillation amplitudes. Peak amplitude changing with release angle is illustrated in Fig. 6.10. It increases with the magnitude of  $\theta$  and the largest peak amplitude happens between  $\theta_0 = -1.3228$  and  $\theta_0 = -1.4054$ ; after that it starts to decrease.

Not only the horizontal displacement of SB but also its angular displacement  $\theta$  oscillates. Fig. 6.11 shows the histories of  $\theta$  for different release angles and Fig. 6.12 shows its oscillation periods. Comparing Figs. 6.9 and 6.12, it is noted that lengths of periods for  $\bar{x}$  and  $\theta$  are different.

## 6.6 OSCILLATION PERIOD CHANGES WITH INITIAL VELOCITY

### Simulation 4

In this simulation, model has the same parameters as previous simulations (Simulation 2&3). Release angle  $\theta_0$  is fixed to be  $-\pi/4$ , and the dimensionless initial velocity  $\bar{u}$  along major axis is taken as a variable between 0 and 0.4. Fig. 6.13 shows the historical responses of  $\bar{x}$  for all cases. It is noted that in case the initial velocity is not zero, horizontal displacement keeps increasing with oscillating speed.

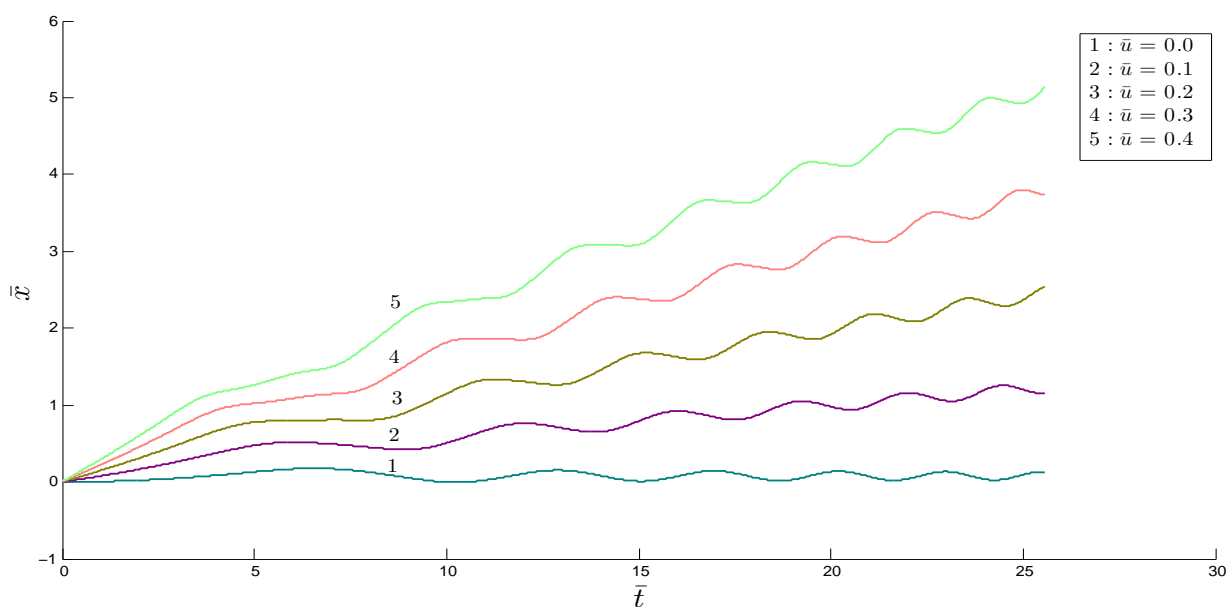


Figure 6.13: Histories of  $\bar{x}$  when the release angle  $= -\frac{\pi}{4}$  and initial speed is changed

Fig. 6.14 shows the historical responses of angle  $\theta$  for all cases and Fig. 6.15 shows how its oscillation period changes with the initial speed when the release angle is fixed. It is noted that, when the release angle is fixed, a small initial velocity has little influence on the period of  $\theta$ 's oscillation. Combining Figs. 6.12 and 6.15 indicates that changing release angle or initial speed has little influence on the oscillation period of angular displacement  $\theta$ .

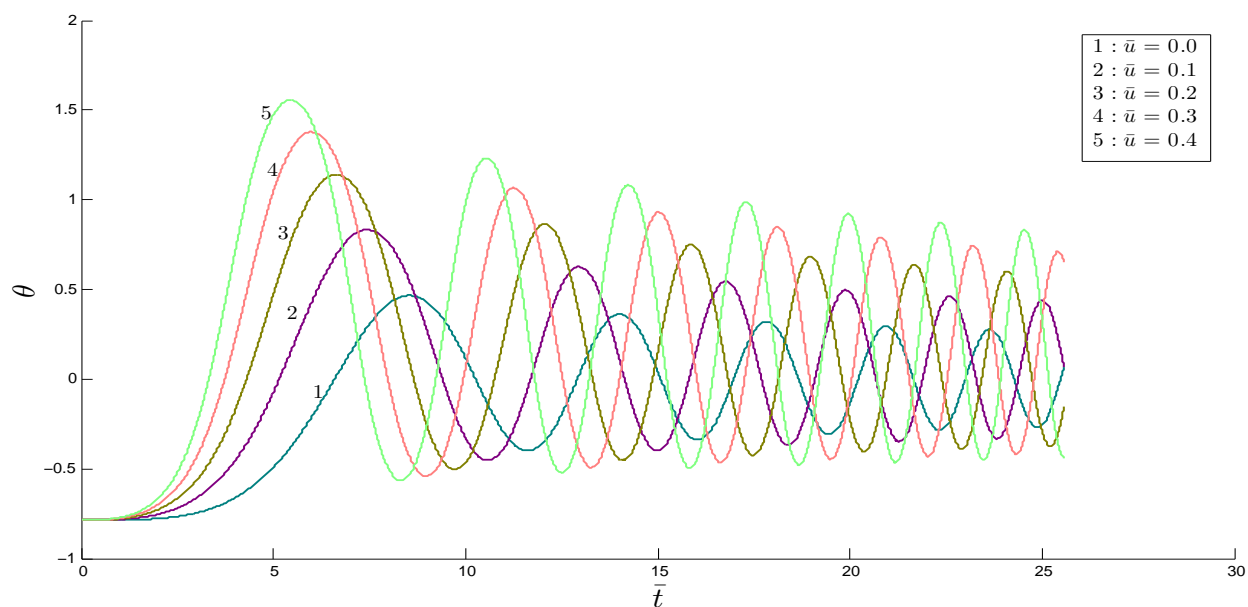


Figure 6.14: Histories of  $\theta$  when fix the release angle and change initial speed

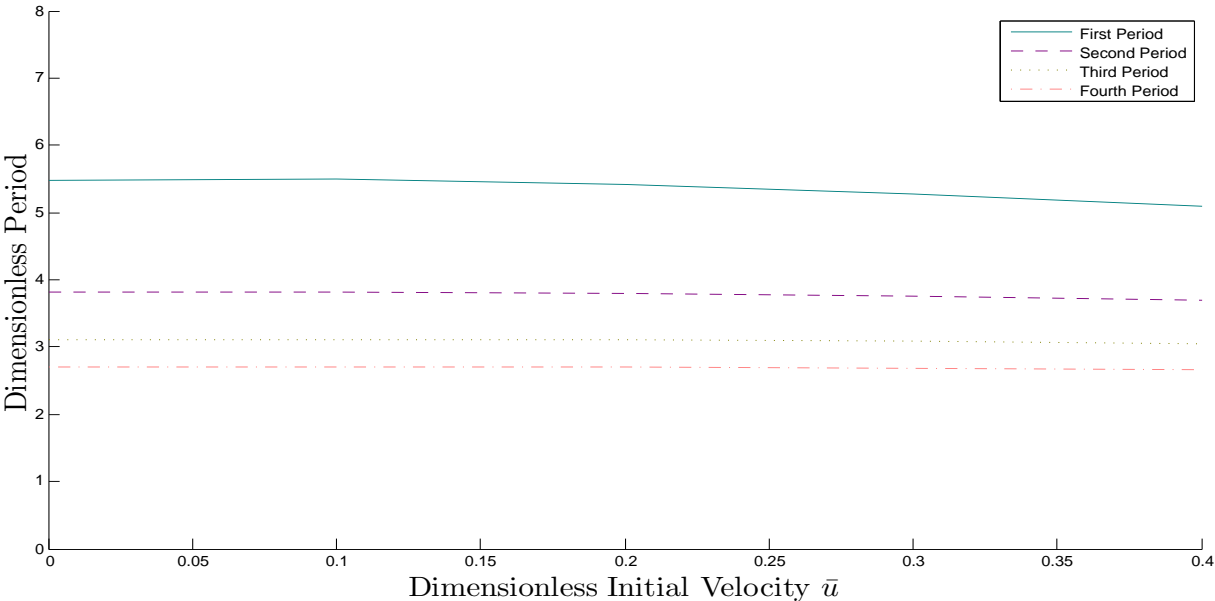


Figure 6.15: Periods for  $\theta$  vs initial Speed

## CHAPTER 7

### CONCLUSIONS

#### 7.1 SUMMARY AND CONCLUSIONS

This report first defines two coordinate systems, EFF and BFF, and then the transformation between the two was developed. Gravitational force, buoyancy, and hydrodynamic force were discussed and their expressions were derived in BFF; among them hydrodynamic force is the most complicated and its derivation is based on added-mass theory [19]. Equations of motion were developed based on Newton's Second Law and Euler equations. The crux of this study is applying these two laws in BFF, which is not an inertia coordinate system. Connections between the acceleration and angular acceleration in BFF and in EFF were built to solve this problem. Because the system is allowed to have six degrees of freedom, Euler angles were introduced, thus making the coordinate transformation complex. As a result, the system is high-order, time-dependant, nonlinear, and fully coupled after nondimensionalization. No analytical solution can be found for such a system; A 4<sup>th</sup>-order Runge-Kutta integration method was adopted to obtain instantaneous twelve state variables Eqs. 5.23 and 5.24 including position, attitude, velocity, and angular velocity.

A free-falling prolate-spheroidal rigid body under gravitational force is simulated as a numerical application. Analysis of the dynamic equations shows the coupled term, known as Munk moment, is an important cause of oscillation. When weight equals to buoyancy and center of mass is below center of buoyancy, buoyancy and gravitational force act on different points resulting in an attitude-dependent moment. This moment together with Munk moment lead to an oscillating moving pattern. When weight is higher than buoyancy and the body is released from static, instead of gliding down, oscillation is observed during its falling. Changing the release angle has little influence on the *period* of horizontal oscillation; however, the oscillating amplitude greatly depends on the release angle. If initial velocity of the body is not zero, oscillation period of angular displacement will not change much, but the horizontal displacement will lose the oscillating property. Compared with pendulum's oscillation, the oscillation of falling prolate-spheroidal rigid body is much more complicated because of the nonlinear coupled hydrodynamic force.

#### 7.2 FUTURE WORK

This report studied numerically the oscillation of a descending prolate spheroid under gravitational and the factors influencing the oscillation, such as release angle and initial velocity. However, the simulation did not consider viscous effects. Thus, it is interesting to conduct model tests and validate the simulation and investigate the effects of viscosity.

In addition, adding fins to the body to control its falling is of great interests. No power input or control force was included in the present study. Adding fins will introduce a new force that can be applied to control the descending history of the body.

## REFERENCES

- [1] R.H. Davis (1995). *Deep Diving and Submarine Operation Part 1 and 2*, 9th edition. Gwent: Siebe Gorman and Co Ltd.
- [2] D.R. Blidberg (2000). “The Development of Autonomous Underwater Vehicles (AUV)”. A Brief Summary. Autonomous Undersea Systems Institute.
- [3] “Submarine Technology Through the Years”, Chief of Naval Operations, Submarine Warfare Division. Retrieved January 19, 2015.  
<http://www.navy.mil/navydata/cno/n87/history/subhistory.html>
- [4] Wikimedia Commons, “Ohio-class submarine launches Tomahawk Cruise missiles”. Retrieved January 19, 2015.  
[http://commons.wikimedia.org/wiki/File:Ohio-class\\_submarine\\_launches\\_Tomahawk\\_Cruise\\_missiles\\_\(artist\\_concept\).jpg](http://commons.wikimedia.org/wiki/File:Ohio-class_submarine_launches_Tomahawk_Cruise_missiles_(artist_concept).jpg)
- [5] “Russian Submarine classes”. Retrieved January 20, 2015. <http://i.imgur.com/SktkYGC.jpg>
- [6] Global Fire Power Strength in Numbers. Retrieved January 20, 2015. [www.globalfirepower.com](http://www.globalfirepower.com)
- [7] Office of Naval Research, Science & Technology Focus. Retrieved January 21, 2015.  
<http://www.onr.navy.mil/focus/ocean/vessels/submersibles1.htm>
- [8] Marine Technology News. “Chinese Submarine Dives into Indian Ocean”. Retrieved January 21, 2015. <http://www.marinetechologynews.com/news/chinese-submarine-dives-indian-506350>
- [9] J.H.A.M. Vervoort (2009). “Modeling and Control of an Unmanned Underwater Vehicle”. Master traineeship report, University of Canterbury, New Zealand.
- [10] T.Q. Donaldson (2001). *Review of Autonomous Underwater Vehicle (AUV) Developments*. U.S. Naval Meteorology and Oceanography Command; Naval Research Laboratory.
- [11] MIT Sea Grant. Retrieved January 21, 2015.  
[http://seagrant.mit.edu/press\\_releases.php?nwsID=475](http://seagrant.mit.edu/press_releases.php?nwsID=475)
- [12] M. Gertler and G.R. Hagen (1967). “Standard Equations of motion for submarine simulation”. Naval Ship Research and Development Center Report. No. NSRDC-2510
- [13] J. Feldman (1979). “Revised Standard Submarine Equation of Motion”. David W. Taylor Naval Ship Research And Development Center. No. DTNSRDC/SPD-0393-09
- [14] T.I. Fossen (1994). *Guidance and Control of Ocean Vehicles*. John Wiley and Sons, New York.
- [15] M. Nahon (1996). “A Simplified Dynamics Model for Autonomous Underwater Vehicles”. *Autonomous Underwater Vehicle Technology AUV’96, Proceedings of the 1996 Symposium on. IEEE, 1996.*
- [16] M.F. Hajosy (1994). “Six Degree of Freedom Vehicle Controller Design for the Operation of an Unmanned Underwater Vehicle in a Shallow Water Environment”. Master of Science thesis, Massachusetts Institute of Technology, USA.

- [17] T. Prestero (2001). “Verification of a Six-Degree of Freedom Simulation Model for the REMUS Autonomous Underwater Vehicle”. Master of Science thesis, Massachusetts Institute of Technology, USA.
- [18] SNAME (1950). “Nomenclature for treating the motion of a submerged body through a fluid”. Technical Report Bulletin 1-5. Society of Naval Architects and Marine Engineers, New York.
- [19] R.W. Yeung (2014). *Hydrodynamics of Ships and Ocean Systems*, Lecture Notes for course ME241A. University of California at Berkeley.
- [20] H. Lamb (1932). *Hydrodynamics*, Cambridge University Press, London.
- [21] F.H. Imlay (1961). The complete expressions for “added mass” of a rigid body moving in an ideal fluid. Hydro. Lab. R&D Report 1528, David Taylor Model Basin, Carderock, MD, USA.
- [22] W. Wang (2001). “Modeling and Simulation of the VideoRay Pro III Underwater Vehicle”. OCEANS 2006-Asia Pacific. IEEE.

## APPENDIX A

### $\mathbf{J}_2$

Time derivative of the Euler angles  $\dot{\boldsymbol{\alpha}} = [\dot{\phi}, \dot{\theta}, \dot{\psi}]^T$  and angular velocities  $\boldsymbol{\omega} = [p, q, r]^T$  are connected by a 3 by 3 transformation matrix  $\mathbf{J}_2$ , as shown in Eq. (A.1)

$$\dot{\boldsymbol{\alpha}} = \mathbf{J}_2 \cdot \boldsymbol{\omega} \quad (\text{A.1})$$

where  $\mathbf{J}_2$  has the following expression

$$\mathbf{J}_2 = \begin{bmatrix} 1 & \sin(\phi) \tan(\theta) & \cos(\phi) \tan(\theta) \\ 0 & \cos(\phi) & -\sin(\phi) \\ 0 & \frac{\sin(\phi)}{\cos\theta} & \frac{\cos(\phi)}{\cos(\theta)} \end{bmatrix} \quad (\text{A.2})$$

To derive  $\mathbf{J}_2$ , we assume at time  $t = t_1$ , the orientation of BFF is described as  $\boldsymbol{\alpha}_1 = [\phi_1; \theta_1; \psi_1]$ , and we name it *orientation*<sub>1</sub>. Then after a tiny time step  $dt$ , it arrives at attitude  $\boldsymbol{\alpha}_2 = [\phi_2; \theta_2; \psi_2]$ , which is *orientation*<sub>2</sub>. Rotation from *orientation*<sub>1</sub> to *orientation*<sub>2</sub> is described as  $\boldsymbol{\alpha}_b = [\phi_b; \theta_b; \psi_b]$ . All of these angles are Euler angles in rotational sequence  $\psi \rightarrow \theta \rightarrow \phi$ . Based on above definition, relationships between  $\boldsymbol{\alpha}_1$ ,  $\boldsymbol{\alpha}_2$ , and  $\boldsymbol{\alpha}_b$  could be connected through Eq. (A.3)

$$\mathbf{T}_2 = \mathbf{T}_b \cdot \mathbf{T}_1 \quad (\text{A.3})$$

where

$$\mathbf{T}_1 = \begin{bmatrix} c(\theta_1)c(\psi_1) & c(\theta_1)s(\psi_1) & -s(\theta_1) \\ c(\psi_1)s(\phi_1)s(\theta_1) - c(\phi_1)s(\psi_1) & c(\phi_1)c(\psi_1) + s(\phi_1)s(\theta_1)s(\psi_1) & c(\theta_1)s(\phi_1) \\ s(\phi_1)s(\psi_1) + c(\phi_1)c(\psi_1)s(\theta_1) & c(\phi_1)s(\theta_1)s(\psi_1) - c(\psi_1)s(\phi_1) & c(\phi_1)c(\theta_1) \end{bmatrix} \quad (\text{A.4a})$$

$$\mathbf{T}_2 = \begin{bmatrix} c(\theta_2)c(\psi_2) & c(\theta_2)s(\psi_2) & -s(\theta_2) \\ c(\psi_2)s(\phi_2)s(\theta_2) - c(\phi_2)s(\psi_2) & c(\phi_2)c(\psi_2) + s(\phi_2)s(\theta_2)s(\psi_2) & c(\theta_2)s(\phi_2) \\ s(\phi_2)s(\psi_2) + c(\phi_2)c(\psi_2)s(\theta_2) & c(\phi_2)s(\theta_2)s(\psi_2) - c(\psi_2)s(\phi_2) & c(\phi_2)c(\theta_2) \end{bmatrix} \quad (\text{A.4b})$$

$$\mathbf{T}_b = \begin{bmatrix} c(\theta_b)c(\psi_b) & c(\theta_b)s(\psi_b) & -s(\theta_b) \\ c(\psi_b)s(\phi_b)s(\theta_b) - c(\phi_b)s(\psi_b) & c(\phi_b)c(\psi_b) + s(\phi_b)s(\theta_b)s(\psi_b) & c(\theta_b)s(\phi_b) \\ s(\phi_b)s(\psi_b) + c(\phi_b)c(\psi_b)s(\theta_b) & c(\phi_b)s(\theta_b)s(\psi_b) - c(\psi_b)s(\phi_b) & c(\phi_b)c(\theta_b) \end{bmatrix} \quad (\text{A.4c})$$

After some basic matrix operations,  $\mathbf{T}_b$  could be expressed in terms of  $\mathbf{T}_1$  and  $\mathbf{T}_2$ , shown in Eq. (A.5)

$$\mathbf{T}_b = ((\mathbf{T}_1^T)^{-1} \cdot \mathbf{T}_2^T)^T \quad (\text{A.5})$$

Let  $dt \rightarrow 0$ , above equation is still sound:

$$\lim_{dt \rightarrow 0} \mathbf{T}_b = \lim_{dt \rightarrow 0} ((\mathbf{T}_1^T)^{-1} \cdot \mathbf{T}_2^T)^T \quad (\text{A.6})$$

As time step  $dt$  approaches zero,  $\psi_b, \theta_b, \phi_b$  will converges to zero. In this case, changing the sequence of rotation, the arrived orientation of BFF will be the same, which means rotations around three axes with Euler angles could be believed to happen simultaneously. Thus, relationship between Euler angles describing rotation from *orientation*<sub>1</sub> to *orientation*<sub>2</sub> could be expressed in terms of angular velocities as:

$$\lim_{dt \rightarrow 0} \phi_b = p \cdot dt; \quad \lim_{dt \rightarrow 0} \theta_b = q \cdot dt; \quad \lim_{dt \rightarrow 0} \psi_b = r \cdot dt \quad (\text{A.7})$$

Further, with  $\phi_b, \theta_b, \psi_b$  approaching zero, their trigonometric function limits could be expressed as

$$\lim_{dt \rightarrow 0} \sin(\phi_b) = \phi_b = p \cdot dt \quad (\text{A.7a})$$

$$\lim_{dt \rightarrow 0} \sin(\theta_b) = \theta_b = q \cdot dt \quad (\text{A.7b})$$

$$\lim_{dt \rightarrow 0} \sin(\psi_b) = \psi_b = r \cdot dt \quad (\text{A.7c})$$

$$\lim_{dt \rightarrow 0} \cos(\phi_b) = \lim_{dt \rightarrow 0} \cos(\theta_b) = \lim_{dt \rightarrow 0} \cos(\psi_b) = 1 \quad (\text{A.7d})$$

Putting these sine and cosine values into Eq. (A.4c) and ignoring higher-order terms for small  $dt$ ,  $\lim_{dt \rightarrow 0} \mathbf{T}_b$  could be rewritten as

$$\lim_{dt \rightarrow 0} \mathbf{T}_b = \begin{bmatrix} 1 & r \cdot dt & -q \cdot dt \\ -r \cdot dt & 1 & p \cdot dt \\ q \cdot dt & -p \cdot dt & 1 \end{bmatrix} \quad (\text{A.8})$$

This is the detailed expression of left side of Eq. (A.4c), which is a skew-symmetric matrix and just about  $p, q,$  and  $r$ . Besides, the diagonal elements are all equal to 1, thus there are just three independent elements. The right-hand side of Eq. (A.6), denoted as  $R$ , has a very complicated expression.

$$R = \lim_{dt \rightarrow 0} ((T_1^T)^{-1} \cdot T_2^T)^T \quad (\text{A.9})$$

which could be calculated analytically and expressed in terms of  $\phi_1, \phi_2, \theta_1, \theta_2, \psi_1,$  and  $\psi_2$ . Here we just provide expressions of  $R(2, 3), R(2, 3),$  and  $R(2, 3)$ .

$$\begin{aligned} R(2, 3) = & c(\phi_1)c(\theta_1)c(\theta_2)s(\phi_2) - c(\phi_2)c(\psi_1)c(\psi_2)s(\phi_1) - c(\phi_2)s(\phi_1)s(\psi_1)s(\psi_2) \\ & + c(\phi_1)c(\psi_1)c(\psi_2)s(\phi_2)s(\theta_1)s(\theta_2) + c(\phi_1)s(\phi_2)s(\theta_1)s(\theta_2)s(\psi_1)s(\psi_2) \\ & - c(\psi_1)s(\phi_1)s(\phi_2)s(\theta_2)s(\psi_2) + c(\psi_2)s(\phi_1)s(\phi_2)s(\theta_2)s(\psi_1) \\ & - c(\phi_1)c(\phi_2)c(\psi_1)s(\theta_1)s(\psi_2) + c(\phi_1)c(\phi_2)c(\psi_2)s(\theta_1)s(\psi_1) \end{aligned} \quad (\text{A.10a})$$

$$\begin{aligned} R(3, 1) = & c(\theta_1)c(\psi_1)s(\phi_2)s(\psi_2) - c(\phi_2)c(\theta_2)s(\theta_1) - c(\theta_1)c(\psi_2)s(\phi_2)s(\psi_1) \\ & + c(\phi_2)c(\theta_1)c(\psi_1)c(\psi_2)s(\theta_2) + c(\phi_2)c(\theta_1)s(\theta_2)s(\psi_1)s(\psi_2) \end{aligned} \quad (\text{A.10b})$$

$$\begin{aligned} R(1, 2) = & c(\phi_1)c(\theta_2)c(\psi_1)s(\psi_2) - c(\theta_1)s(\phi_1)s(\theta_2) - c(\phi_1)c(\theta_2)c(\psi_2)s(\psi_1) \\ & + c(\theta_2)c(\psi_1)c(\psi_2)s(\phi_1)s(\theta_1) + c(\theta_2)s(\phi_1)s(\theta_1)s(\psi_1)s(\psi_2) \end{aligned} \quad (\text{A.10c})$$

By using Sum and Difference identities of trigonometric functions, some combinations could be

made,  $R(2, 3)$ ,  $R(2, 3)$ , and  $R(2, 3)$  are simplified into

$$\begin{aligned}
 R(2, 3) &= c(\phi_1)c(\theta_1)c(\theta_2)s(\phi_2) - c(\phi_2)s(\phi_1)c(\psi_2 - \psi_1) \\
 &\quad + c(\phi_1)s(\phi_2)s(\theta_1)s(\theta_2)c(\psi_2 - \psi_1) \\
 &\quad - s(\phi_1)s(\phi_2)s(\theta_2)s(\psi_2 - \psi_1) \\
 &\quad - c(\phi_1)c(\phi_2)s(\theta_1)s(\psi_2 - \psi_1)
 \end{aligned} \tag{A.11a}$$

$$\begin{aligned}
 R(3, 1) &= c(\theta_1)s(\phi_2)s(\psi_2 - \psi_1) - c(\phi_2)c(\theta_2)s(\theta_1) \\
 &\quad + c(\phi_2)c(\theta_1)s(\theta_2)c(\psi_2 - \psi_1)
 \end{aligned} \tag{A.11b}$$

$$\begin{aligned}
 R(1, 2) &= c(\phi_1)c(\theta_2)s(\psi_2 - \psi_1) - c(\theta_1)s(\phi_1)s(\theta_2) \\
 &\quad + c(\theta_2)s(\phi_1)s(\theta_1)c(\psi_2 - \psi_1)
 \end{aligned} \tag{A.11c}$$

Also, when  $dt$  approaches zero,  $\psi_2 - \psi_1$ ,  $\theta_2 - \theta_1$ , and  $\phi_2 - \phi_1$  all go to zero. Their sine and cosine function values are obtained

$$\lim_{dt \rightarrow 0} \sin(\phi_1) = \sin(\phi_2); \quad \lim_{dt \rightarrow 0} \sin(\theta_1) = \sin(\theta_2) \tag{A.12a}$$

$$\lim_{dt \rightarrow 0} \cos(\psi_2 - \psi_1) = \lim_{dt \rightarrow 0} \cos(\theta_2 - \theta_1) = \lim_{dt \rightarrow 0} \cos(\phi_2 - \phi_1) = 1 \tag{A.12b}$$

$$\lim_{dt \rightarrow 0} \sin(\phi_2 - \phi_1) = \phi_2 - \phi_1 \tag{A.12c}$$

$$\lim_{dt \rightarrow 0} \sin(\theta_2 - \theta_1) = \theta_2 - \theta_1 \tag{A.12d}$$

$$\lim_{dt \rightarrow 0} \sin(\psi_2 - \psi_1) = \psi_2 - \psi_1 \tag{A.12e}$$

With these limits,  $R(2, 3)$ ,  $R(2, 3)$ , and  $R(2, 3)$  could be further simplified into

$$R(2, 3) = -\sin(\theta_1)(\psi_2 - \psi_1) + (\phi_2 - \phi_1) \tag{A.13a}$$

$$R(3, 1) = \cos(\phi_1)(\theta_2 - \theta_1) + \cos(\theta_1)\sin(\phi_1)(\psi_2 - \psi_1) \tag{A.13b}$$

$$R(1, 2) = -\sin(\phi_1)(\theta_2 - \theta_1) + \cos(\phi_1)\cos(\theta_1)(\psi_2 - \psi_1) \tag{A.13c}$$

The equality between left-hand side and right-hand side of Eq. (A.5) will lead to

$$\lim_{dt \rightarrow 0} p \cdot dt = R(2, 3); \quad \lim_{dt \rightarrow 0} q \cdot dt = R(3, 1); \quad \lim_{dt \rightarrow 0} r \cdot dt = R(1, 2) \tag{A.14}$$

Then  $p$ ,  $q$ , and  $r$  could be expressed in terms of  $\phi_1$ ,  $\phi_2$ ,  $\theta_1$ ,  $\theta_2$ ,  $\psi_1$ , and  $\psi_2$  as

$$p = \lim_{dt \rightarrow 0} \frac{\phi_2 - \phi_1}{dt} - \sin(\theta_1) \lim_{dt \rightarrow 0} \frac{\psi_2 - \psi_1}{dt} \tag{A.15a}$$

$$q = \cos(\phi_1) \lim_{dt \rightarrow 0} \frac{\theta_2 - \theta_1}{dt} + \cos(\theta_1)\sin(\phi_1) \lim_{dt \rightarrow 0} \frac{\psi_2 - \psi_1}{dt} \tag{A.15b}$$

$$r = \cos(\phi_1)\cos(\theta_1) \lim_{dt \rightarrow 0} \frac{\psi_2 - \psi_1}{dt} - \sin(\phi_1) \lim_{dt \rightarrow 0} \frac{\theta_2 - \theta_1}{dt} \tag{A.15c}$$

According to the definition of time derivatives of  $\phi$ ,  $\theta$ , and  $\psi$

$$\dot{\phi} = \lim_{dt \rightarrow 0} \frac{\phi_2 - \phi_1}{dt}; \quad \dot{\theta} = \lim_{dt \rightarrow 0} \frac{\theta_2 - \theta_1}{dt}; \quad \dot{\psi} = \lim_{dt \rightarrow 0} \frac{\psi_2 - \psi_1}{dt}; \quad (\text{A.16})$$

Finally, relationship between  $\boldsymbol{\omega}$  and  $\dot{\boldsymbol{\phi}}$  is obtained in matrix form as

$$\begin{bmatrix} p \\ q \\ r \end{bmatrix} = \begin{bmatrix} 1 & 0 & \sin(\theta) \\ 0 & \cos(\phi) & \cos(\theta) \sin(\phi) \\ 0 & -\sin(\phi) & \cos(\phi) \cos(\theta) \end{bmatrix} \cdot \begin{bmatrix} \dot{\phi} \\ \dot{\theta} \\ \dot{\psi} \end{bmatrix} \quad (\text{A.17})$$

Thus,  $\mathbf{J}_2$  in Eq. (A.1) has the following expression

$$\mathbf{J}_2 = \begin{bmatrix} 1 & 0 & \sin(\theta) \\ 0 & \cos(\phi) & \cos(\theta) \sin(\phi) \\ 0 & -\sin(\phi) & \cos(\phi) \cos(\theta) \end{bmatrix}^{-1} = \begin{bmatrix} 1 & \sin(\phi) \tan(\theta) & \cos(\phi) \tan(\theta) \\ 0 & \cos(\phi) & -\sin(\phi) \\ 0 & \frac{\sin(\phi)}{\cos \theta} & \frac{\cos(\phi)}{\cos(\theta)} \end{bmatrix} \quad (\text{A.18})$$

## APPENDIX B

### TRANSLATIONAL MOTION AND ROTATIONAL MOTION

Eqs. (5.1), (5.2), and (5.3) are provided in Chap. 5 as SB's equations of motion. Its derivation could be found in [14] and is developed below again.

#### B.1 TRANSLATIONAL MOTION

For an arbitrary vector  $\mathbf{C}$  in space, its time derivative with respect to EFF ( $\dot{\mathbf{C}}$ ) and BFF ( $\dot{\mathbf{C}}$ ) have the following relationship

$$\dot{\mathbf{C}} = \dot{\mathbf{C}} + \boldsymbol{\omega} \times \mathbf{C} \quad (\text{B.1})$$

where  $\boldsymbol{\omega}$  is the angular velocity of the rotating coordinate system. It is noted that

$$\dot{\boldsymbol{\omega}} = \dot{\boldsymbol{\omega}} + \boldsymbol{\omega} \times \boldsymbol{\omega} = \dot{\boldsymbol{\omega}} \quad (\text{B.2})$$

which means angular acceleration of the rotating coordinate system described in EFF is same as that in BFF. Position vector of center of mass in EFF ( $\mathbf{R}_G$ ) can be expressed as the summation of position vector of the BFF's origin in EFF ( $\mathbf{r}_{O'}$ ) and position vector of center of mass ( $\mathbf{r}_G$ ) with respect to  $O'$ .

$$\mathbf{R}_G = \mathbf{R}_{O'} + \mathbf{r}_G \quad (\text{B.3})$$

Time derivative with respect to EFF gives

$$\dot{\mathbf{R}}_G = \dot{\mathbf{R}}_{O'} + \dot{\mathbf{r}}_G \quad (\text{B.4})$$

where

$$\dot{\mathbf{r}}_G = \dot{\mathbf{r}}_G + \boldsymbol{\omega} \times \mathbf{r}_G = \boldsymbol{\omega} \times \mathbf{r}_G \quad (\text{B.5})$$

in which,  $\dot{\mathbf{r}}_G$  equals to zero because SB is assumed to be a rigid body and BFF is fixed on SB. Substitution leads to

$$\dot{\mathbf{R}}_G = \dot{\mathbf{R}}_{O'} + \boldsymbol{\omega} \times \mathbf{r}_G \quad (\text{B.6})$$

which can also be written as:

$$\mathbf{v}_G = \mathbf{v}_{O'} + \boldsymbol{\omega} \times \mathbf{r}_G \quad (\text{B.7})$$

Time derivative of  $\mathbf{v}_G$  with respect to EFF is  $\mathbf{a}_G$  in Eq. (5.2)

$$\begin{aligned} \mathbf{a}_G &= \dot{\mathbf{v}}_G = \dot{\mathbf{v}}_{O'} + \dot{\boldsymbol{\omega}} \times \mathbf{r}_G + \boldsymbol{\omega} \times \dot{\mathbf{r}}_G \\ &= \dot{\mathbf{v}}_{O'} + \boldsymbol{\omega} \times \mathbf{v}_{O'} + \dot{\boldsymbol{\omega}} \times \mathbf{r}_G + \boldsymbol{\omega} \times (\boldsymbol{\omega} \times \mathbf{r}_G) \end{aligned} \quad (\text{B.8})$$

where  $\mathbf{v}_{O'}$  is velocity of BFF's origin measured in EFF, and  $\dot{\mathbf{v}}_{O'}$  is its time derivative with respect to BFF.

## B.2 ROTATIONAL MOTION

According to the definition of angular momentum, SB's absolute angular momentum about  $O'$  is

$$\mathbf{L}_{O'} \equiv \int_V \mathbf{r} \times \mathbf{v} \rho \, dV \quad (\text{B.9})$$

where  $\mathbf{r}$  is position vector pointing at an arbitrary point on SB from  $O'$ ,  $\mathbf{v}$  is that point's absolute velocity viewed in EFF.

Time derivative of  $\mathbf{L}_{O'}$  has two components

$$\dot{\mathbf{L}}_{O'} = \int_V \mathbf{r} \times \dot{\mathbf{v}} \rho \, dV + \int_V \dot{\mathbf{r}} \times \mathbf{v} \rho \, dV \quad (\text{B.10})$$

in which, the first term is defined as moment around  $O'$

$$\mathbf{M}_{r_{O'}} \equiv \int_V \mathbf{r} \times \dot{\mathbf{v}} \rho \, dV \quad (\text{B.11})$$

Considering

$$\dot{\mathbf{r}} = \dot{\mathbf{R}} - \dot{\mathbf{R}}_{O'} = \mathbf{v} - \mathbf{v}_{O'} \quad (\text{B.12})$$

Substitution of Eqs. (B.12) and (B.11) into (B.10) gives

$$\begin{aligned} \dot{\mathbf{L}}_{O'} &= \mathbf{M}_{r_{O'}} - \mathbf{v}_{O'} \times \int_V \mathbf{v} \rho \, dV \\ &= \mathbf{M}_{r_{O'}} - \mathbf{v}_{O'} \times \int_V \dot{\mathbf{R}} \rho \, dV \\ &= \mathbf{M}_{r_{O'}} - \mathbf{v}_{O'} \times m \dot{\mathbf{R}}_G \\ &= \mathbf{M}_{r_{O'}} - \mathbf{v}_{O'} \times m (\dot{\mathbf{R}}_{O'} + \boldsymbol{\omega} \times \mathbf{r}_G) \\ &= \boxed{\mathbf{M}_{r_{O'}} - m \mathbf{v}_{O'} \times (\boldsymbol{\omega} \times \mathbf{r}_G)} \end{aligned} \quad (\text{B.13})$$

Eq. (B.9) could also be written as

$$\begin{aligned} \mathbf{L}_{O'} &= \int_V \mathbf{r} \times \mathbf{v} \rho \, dV \\ &= \int_V \mathbf{r} \times \mathbf{v}_{O'} \rho \, dV + \int_V \mathbf{r} \times (\boldsymbol{\omega} \times \mathbf{r}) \rho \, dV \\ &= m \mathbf{r}_G \times \mathbf{v}_{O'} + \int_V \mathbf{r} \times (\boldsymbol{\omega} \times \mathbf{r}) \rho \, dV \end{aligned} \quad (\text{B.14})$$

Introducing the definition of inertia tensor

$$\mathbf{I}_{O'} \boldsymbol{\omega} = \int_V \mathbf{r} \times (\boldsymbol{\omega} \times \mathbf{r}) \rho \, dV \quad (\text{B.15})$$

Expression of  $\mathbf{L}_{O'}$  is simplified as

$$\mathbf{L}_{O'} = \mathbf{I}_{O'} \boldsymbol{\omega} + m \mathbf{r}_G \times \mathbf{v}_{O'} \quad (\text{B.16})$$

Time derivative of Eq. (B.16) results in

$$\begin{aligned}
 \dot{\mathbf{L}}_{O'} &= \mathbf{I}_{O'} \dot{\boldsymbol{\omega}} + \boldsymbol{\omega} \times (\mathbf{I}_{O'} \boldsymbol{\omega}) + m \dot{\mathbf{r}}_G \times \mathbf{v}_{O'} + m \mathbf{r}_G \times \dot{\mathbf{v}}_{O'} \\
 &= \mathbf{I}_{O'} \dot{\boldsymbol{\omega}} + \boldsymbol{\omega} \times (\mathbf{I}_{O'} \boldsymbol{\omega}) + m (\boldsymbol{\omega} \times \mathbf{r}_G) \times \mathbf{v}_{O'} + m \mathbf{r}_G \times (\dot{\mathbf{v}}_{O'} + \boldsymbol{\omega} \times \mathbf{v}_{O'}) \\
 &= \boxed{\mathbf{I}_{O'} \dot{\boldsymbol{\omega}} + \boldsymbol{\omega} \times (\mathbf{I}_{O'} \boldsymbol{\omega}) + m \mathbf{r}_G \times (\dot{\mathbf{v}}_{O'} + \boldsymbol{\omega} \times \mathbf{v}_{O'}) - m \mathbf{v}_{O'} \times (\boldsymbol{\omega} \times \mathbf{r}_G)} \quad (\text{B.17})
 \end{aligned}$$

Comparing Eqs. (B.13) and (B.16), we could obtain Eq. (5.3)

$$\mathbf{M}_{r_{O'}} = \mathbf{I}_{O'} \dot{\boldsymbol{\omega}} + \boldsymbol{\omega} \times (\mathbf{I}_{O'} \boldsymbol{\omega}) + m \mathbf{r}_G \times (\dot{\mathbf{v}}_{O'} + \boldsymbol{\omega} \times \mathbf{v}_{O'}) \quad (\text{B.18})$$

## APPENDIX C

### A CASE OF NON-UNIFORM MASS DISTRIBUTION

Fig. C.1 below shows a distribution of density for prolate spheroid, in which, there are four densities  $\rho_1$ ,  $\rho_2$ ,  $\rho_3$ , and  $\rho_4$ , its overall distribution is symmetric about plane  $O'\hat{x}\hat{z}$ .

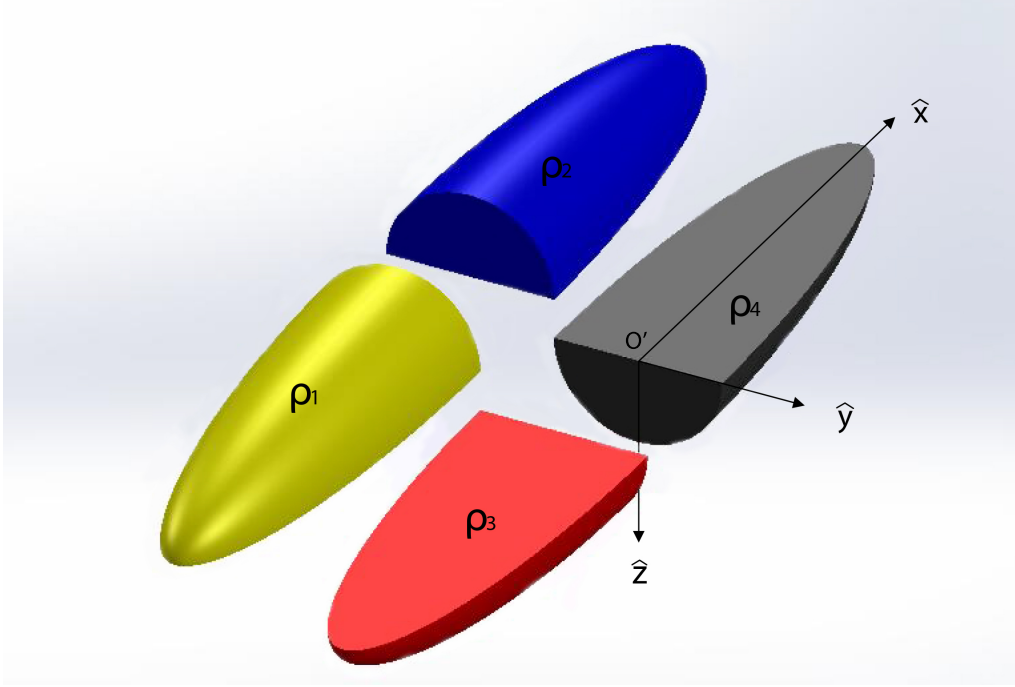


Figure C.1: Distribution of density

Mass and center of mass for this case could be developed as

$$\begin{aligned} m &= \int_{-a}^a \int_0^b \sqrt{1 - \frac{\hat{x}^2}{a^2}} \int_0^{2\pi} \rho(\theta, r, \hat{x}) r d\theta dr d\hat{x} \\ &= \frac{\pi}{3} ab^2 (\rho_1 + \rho_2 + \rho_3 + \rho_4) \end{aligned} \quad (\text{C.1a})$$

$$\begin{aligned} x_G &= \frac{\int_{-a}^a \int_0^b \sqrt{1 - \frac{\hat{x}^2}{a^2}} \int_0^{2\pi} \rho(\theta, r, \hat{x}) \hat{x} r d\theta dr d\hat{x}}{m} \\ &= \frac{3a(\rho_2 + \rho_4 - \rho_1 - \rho_3)}{8(\rho_1 + \rho_2 + \rho_3 + \rho_4)} \end{aligned} \quad (\text{C.1b})$$

$$y_G = \frac{\int_{-a}^a \int_0^b \sqrt{1 - \frac{\hat{x}^2}{a^2}} \int_0^{2\pi} \rho(\theta, r, \hat{x}) r^2 \cos \theta d\theta dr d\hat{x}}{m} = 0 \quad (\text{C.1c})$$

$$\begin{aligned} z_G &= -\frac{\int_{-a}^a \int_0^b \sqrt{1 - \frac{\hat{x}^2}{a^2}} \int_0^{2\pi} \rho(\theta, r, \hat{x}) r^2 \sin \theta d\theta dr d\hat{x}}{m} \\ &= \frac{3b(\rho_3 + \rho_4 - \rho_1 - \rho_2)}{8(\rho_1 + \rho_2 + \rho_3 + \rho_4)} \end{aligned} \quad (\text{C.1d})$$

Its vector form can be shown as

$$\mathbf{r}_G = \begin{bmatrix} \frac{3a(\rho_2 + \rho_4 - \rho_1 - \rho_3)}{8(\rho_1 + \rho_2 + \rho_3 + \rho_4)} \\ 0 \\ \frac{3b(\rho_3 + \rho_4 - \rho_1 - \rho_2)}{8(\rho_1 + \rho_2 + \rho_3 + \rho_4)} \end{bmatrix} \quad (\text{C.2})$$

Based on the definition of inertia tensor in Eqs. (5.4) and (5.5), the integration results are shown below

$$\mathbf{I}_{O'} = \begin{bmatrix} I_x & -I_{xy} & -I_{xz} \\ -I_{yx} & I_y & -I_{yz} \\ -I_{zx} & -I_{xy} & I_z \end{bmatrix} \quad (\text{C.3})$$

where

$$\begin{aligned} I_x &= \int_{-a}^a \int_0^b \int_0^{2\pi} \rho(\theta, r, \hat{x}) r^3 d\theta dr d\hat{x} \\ &= \frac{2\pi}{15} ab^4 [\rho_1 + \rho_2 + \rho_3 + \rho_4] \end{aligned} \quad (\text{C.4a})$$

$$\begin{aligned} I_y &= \int_{-a}^a \int_0^b \int_0^{2\pi} \rho(\theta, r, \hat{x}) (\hat{x}^2 + r^2 \sin^2(\theta)) r d\theta dr d\hat{x} \\ &= \frac{\pi}{15} ab^2 (b^2 + a^2) [\rho_1 + \rho_2 + \rho_3 + \rho_4] \end{aligned} \quad (\text{C.4b})$$

$$\begin{aligned} I_z &= \int_{-a}^a \int_0^b \int_0^{2\pi} \rho(\theta, r, \hat{x}) (\hat{x}^2 + r^2 \cos^2(\theta)) r d\theta dr d\hat{x} \\ &= \frac{\pi}{15} ab^2 (b^2 + a^2) [\rho_1 + \rho_2 + \rho_3 + \rho_4] \end{aligned} \quad (\text{C.4c})$$

$$I_{xy} = I_{yx} = \int_{-a}^a \int_0^b \int_0^{2\pi} \rho(\theta, r, \hat{x}) \hat{x} r^2 \cos(\theta) d\theta dr d\hat{x} = 0 \quad (\text{C.4d})$$

$$\begin{aligned} I_{xz} = I_{zx} &= - \int_{-a}^a \int_0^b \int_0^{2\pi} \rho(\theta, r, \hat{x}) \hat{x} r^2 \sin(\theta) d\theta dr d\hat{x} \\ &= \frac{2}{15} a^2 b^3 [\rho_1 - \rho_2 + \rho_4 - \rho_3] \end{aligned} \quad (\text{C.4e})$$

$$I_{yz} = I_{zy} = \int_{-a}^a \int_0^b \int_0^{2\pi} \rho(\theta, r, \hat{x}) r^3 s(\theta) c(\theta) d\theta dr d\hat{x} = 0 \quad (\text{C.4f})$$

in which, as shown in Fig. 4.1,  $a$  is the length of semi-major axis and  $b$  is the length of semi-minor axis.

In the case that prolate spheroid with uniform distribution of density

$$\rho_1 = \rho_2 = \rho_3 = \rho_4 = \rho$$

$I_{xy} = I_{yx} = I_{xz} = I_{zx} = I_{yz} = I_{zy} = 0$  due to prolate spheroid's symmetry, thus  $\mathbf{I}_{O'}$  is simplified

into a diagonal matrix

$$\mathbf{I}_{O'} = \begin{bmatrix} \frac{8}{15}\rho\pi ab^4 & 0 & 0 \\ 0 & \frac{4}{15}\rho\pi ab^2(a^2 + b^2) & 0 \\ 0 & 0 & \frac{4}{15}\rho\pi ab^2(a^2 + b^2) \end{bmatrix} \quad (\text{C.5})$$

Non-dimensionalizing expressions of mass, center of mass, and inertia tensor by using major axis  $2a$ , displacement mass  $m_d$  as dimension bases results in

$$\bar{m} = \frac{\rho_1 + \rho_2 + \rho_3 + \rho_4}{4\rho_w} \quad (\text{C.6})$$

$$\bar{\mathbf{r}}_G = \begin{bmatrix} \bar{x}_G \\ \bar{y}_G \\ \bar{z}_G \end{bmatrix} = \begin{bmatrix} \frac{3(\rho_2 + \rho_4 - \rho_1 - \rho_3)}{16(\rho_1 + \rho_2 + \rho_3 + \rho_4)} \\ 0 \\ \frac{3(\rho_3 + \rho_4 - \rho_1 - \rho_2)}{16(\rho_1 + \rho_2 + \rho_3 + \rho_4)} \bar{b} \end{bmatrix} \quad (\text{C.7})$$

$$\bar{I}_x = \frac{1}{40} \bar{b}^2 \frac{\rho_1 + \rho_2 + \rho_3 + \rho_4}{\rho_w} \quad (\text{C.8a})$$

$$\bar{I}_y = \bar{I}_z = \frac{1}{80} (\bar{b}^2 + 1) \frac{\rho_1 + \rho_2 + \rho_3 + \rho_4}{\rho_w} \quad (\text{C.8b})$$

$$\bar{I}_{xz} = \bar{I}_{zx} = \frac{1}{40\pi} \bar{b}^2 \frac{\rho_1 - \rho_2 + \rho_4 - \rho_3}{\rho_w} \quad (\text{C.8c})$$

$$\bar{I}_{yz} = \bar{I}_{zy} = \bar{I}_{xy} = \bar{I}_{yx} = 0 \quad (\text{C.8d})$$

where,  $\rho_w$  is the density of water.

For prolate spheroid with uniform density distribution  $\rho$

$$\bar{m} = \frac{\rho}{\rho_w} \quad (\text{C.9})$$

$$\bar{\mathbf{r}}_G = \mathbf{0} \quad (\text{C.10})$$

$$\bar{\mathbf{I}}_{O'} = \begin{bmatrix} \frac{\bar{b}^2}{10} & 0 & 0 \\ 0 & \frac{\bar{b}^2 + 1}{20} & 0 \\ 0 & 0 & \frac{\bar{b}^2 + 1}{20} \end{bmatrix} \quad (\text{C.11})$$

# APPENDIX D

## 3-D CHECK

This numerical experiment briefly tests if the code works for 3 dimensions. There are four sub-cases defined in Tabs. D.1 and D.2. The prolate spheroid is released with zero initial velocities, and the differences between them are releasing angle.

Case	1	2	3	4
$\phi$	0	0	0	0
$\theta$	$-\frac{\pi}{4}$	$-\frac{\pi}{4}$	$-\frac{\pi}{4}$	$\frac{\pi}{4}$
$\psi$	0	$\frac{\pi}{2}$	$\frac{\pi}{4}$	0

Table D.1: Release attitudes of Four Cases

Variables	Values
Major Axis	0.12 m
Minor Axis	0.012m
Density of Prolate Spheroid	$1050 \text{ kg/m}^3$
Density of Water	$998.6 \text{ kg/m}^3$

Table D.2: Parameters of the model

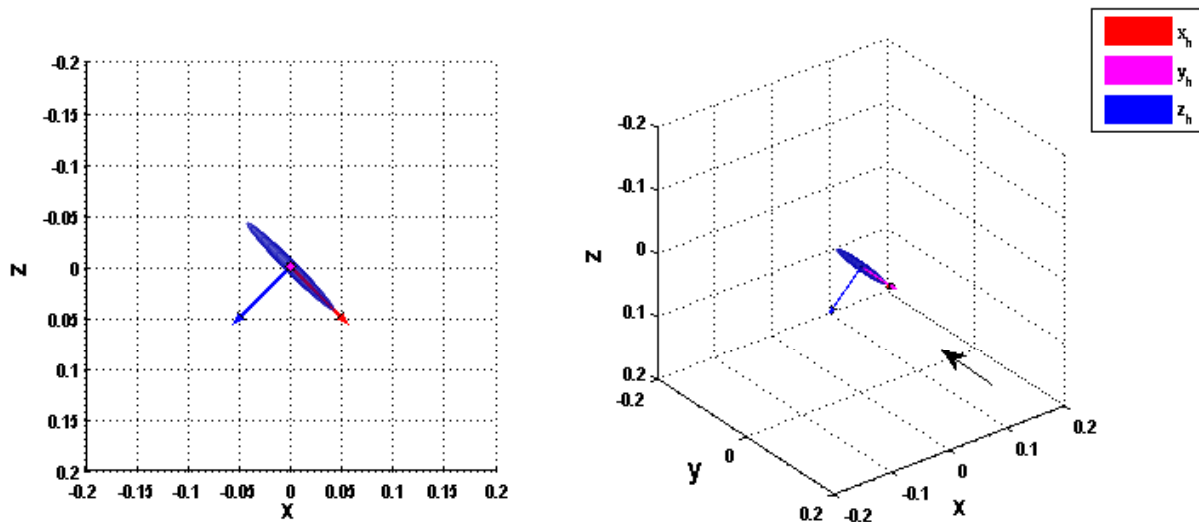


Figure D.1: Case 1

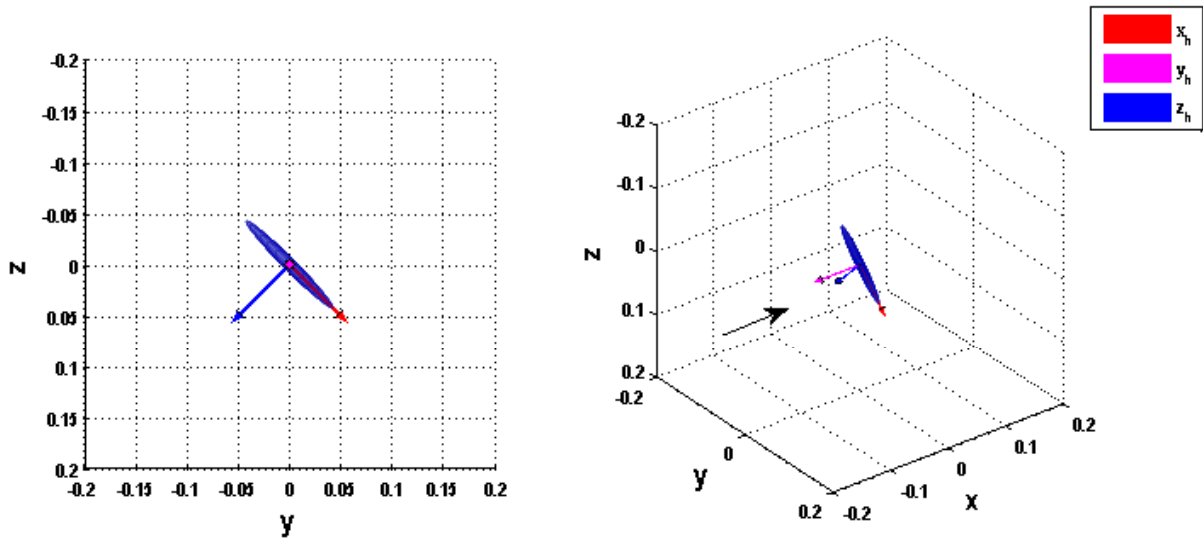


Figure D.2: Case 2

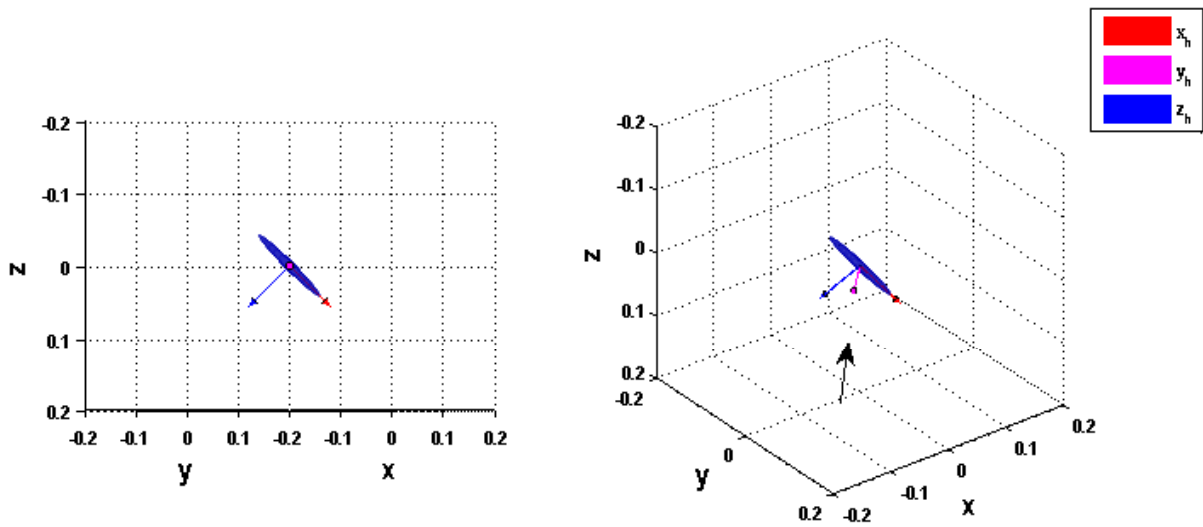


Figure D.3: Case 3

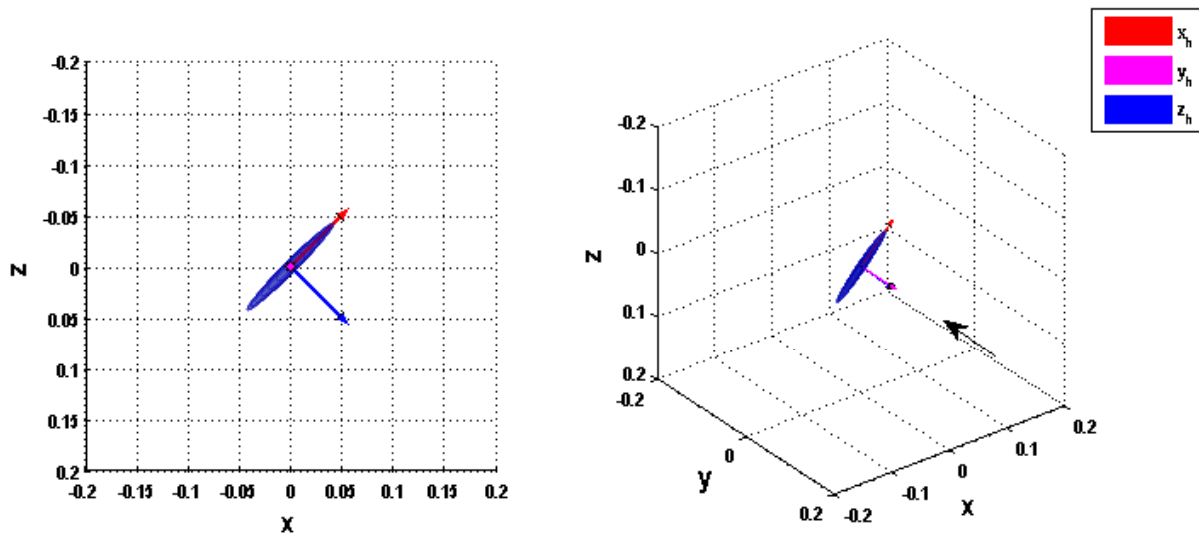


Figure D.4: Case 4

Intuition tells us four cases should have the same the histories of  $z$  coordinate, because the angle between their major axes and  $OZ$  axis is same. It is shown in Fig. D.5.

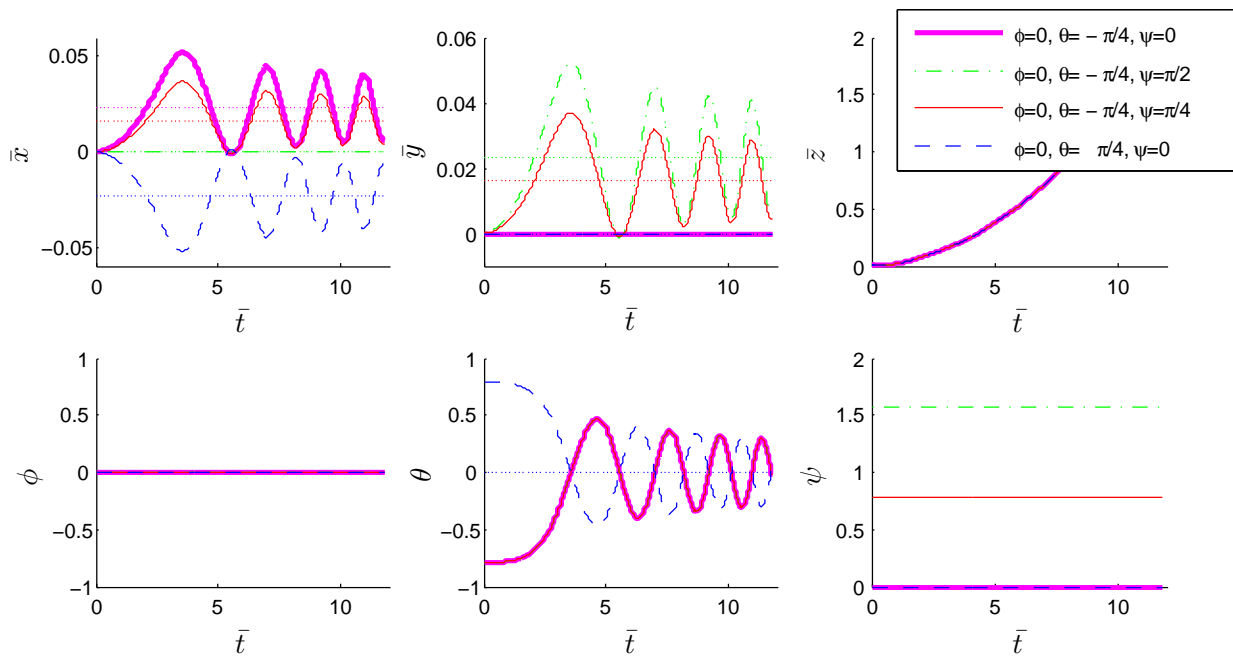


Figure D.5: Dimensionless position in EFF and attitude

Case.1 and Case.4 have  $x$  coordinate histories of same magnitude but opposite signs. It also shows all four cases have same oscillation period as expected. Fig. D.6 illustrates the histories of dimensionless velocities in body-fixed coordinate system. It can be seen degrees of freedom are

reduced to three because zero initial velocities. Case.4 has opposite sign in  $\bar{u}$  and  $\bar{q}$  compared with Case.1,2,3, as expected.

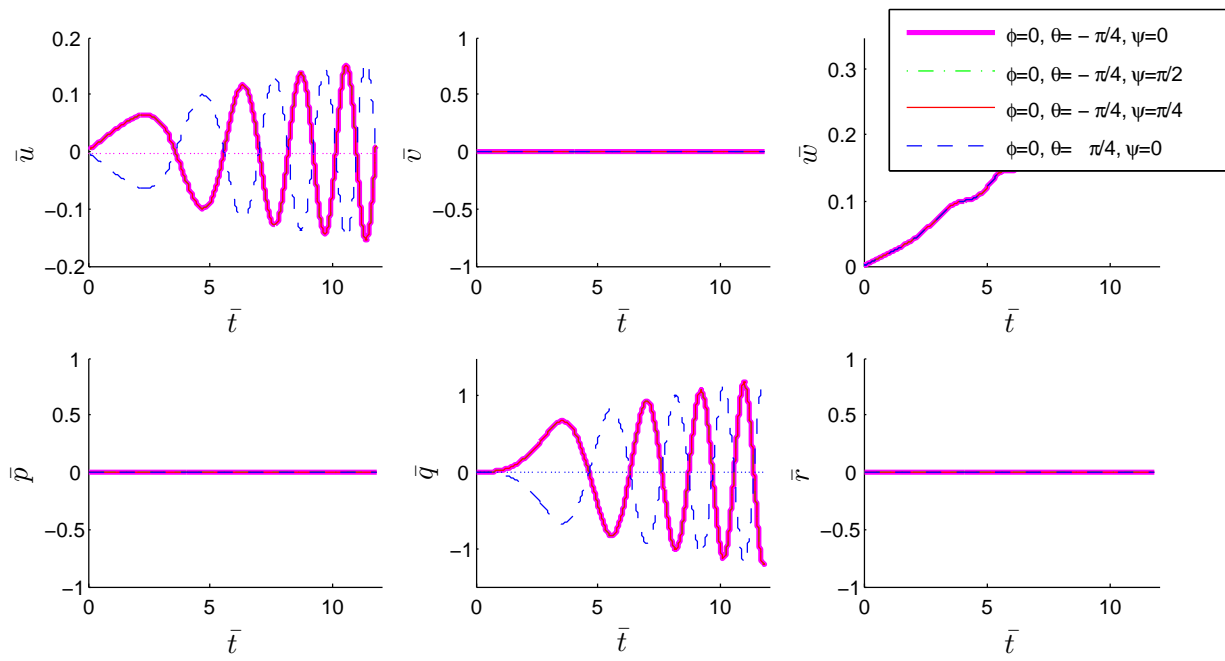


Figure D.6: Dimensionless velocity in BFF

## APPENDIX E

### MATLAB CODE

MatLab code for **Simulation 2**

#### E.1 MODEL DEFINE

```
1 %% Define variables
2 aa = 0.24; % Major axis in (m)
3 bb = 0.024; % Minor axis in (m)
4 X0 = [0;0;0;0;-pi/4;0]; % Initial Position vector in EFF (m,rad)
5 U0 = [0;0;0;0;0;0];
6 % Initial Translation velocity and angular velocity (m/s , rad/s)
7 ro = [1050,1050,1050,1050]; % Desity distribution kg/m^3
8 t = 3+0.002; % computation time from 0 - time(s)
9 tstep = 1e-5; % Time step
10 %% Computation
11 [T,Td,X,Xd,Vb,Vbd,Ve,Ved,omega,omegad,energy,K,P]=prolate_s(aa,bb,X0,U0,ro,t,tstep);
12 % output arguement
13 % T Dimensionless time series (1 by n)
14 % Td Dimensional time series (1 by n)
15 % X Dimensionless position vector in EFF (6 by n)
16 % Xd Dimensional position vector in EFF (6 by n)
17 % Vb Dimensionless velocity vector in BFF (3 by n)
18 % Vbd Dimensional Vecocity vector in BFF (3 by n)
19 % Ve Dimensionless translational velocity in EFF (3 by n)
20 % Ved Dimensional translational velocity in EFF (3 by n)
21 % omega Dimensionless angular velocity in BFF (3 by n)
22 % omegad Dimensional angular velocity in BFF (3 by n)
23 % K Kinetic energy (1 by n)
24 % P Gravitational potential energy (1 by n)
25 name = 2;
26 name = ['simulation',num2str(name)];
27 save(num2str(name)) %save data
28 %% Postprocessing
29 % plot state variables
30 plotfigure([T,Td],[X;Xd;Vb;omega;Vbd;omegad;Ve;Ved],name)
31 % animation
32 close
33 plotmoving ( Td, Xd,aa/2,bb/2,tstep,[name,'.mp4'] ) ;
34 % plot energy
35 fg1 = figure();
36 set(fg1,'Position',[50 30 1270 630]);
37 plot(T,energy,T,K,T,P)
38 legend('Total Energy','Kinetic Energy','Gravitational Potential Energy')
39 xlabel('$\bar{t}$','Interpreter','latex','FontSize',20);
40 ylabel('Energy','Interpreter','latex','FontSize',20);
41 title('Dimensionless energy vs time','FontSize',20)
42 ylim([-0.5,0.5])
```

## E.2 PROCESSING

4<sup>th</sup> Order Runge-Kutta integration

```

1 function [T,Td,X,Xd,Vb,Vbd,Ve,Ved,omega,omegad,E,K,P]=prolate_s(aa,bb,X,U,ro,t,tstep)
2 % Input arguments
3 % aa      Major axis in (m)
4 % bb      Minor axis in (m)
5 % X       Position vector in EFF (m,rad)
6 % U       Initial Translation velocity and angular velocity
7 % ro      Desity distribution kg/m^3
8 % t       Computation time from 0 - time(s)
9 % tstep   Time step
10 % rs     density of steel - density of ABS
11 % rr     radius of steel ball
12 % Output arguments
13 % T       Dimensionless time series
14 % Td     Dimensional time series
15 % X       Dimensionless position vector in EFF
16 % Xd     Dimensional position vector in EFF and velocity vector in BFF
17 % Vb     Dimensionless translational velocity vector in BFF
18 % Vbd    Dimensional translational vecocity vector in BFF
19 % Ve     Dimensionless translational velocity in EFF
20 % Ved    Dimensional translational velocity in EFF
21 % omega  Dimensionless angular velocity in BFF
22 % omegad Dimensional angular velocity in BFF
23 % E       Total energy
24 % K       Kinetic energy
25 % P       Gravitation potential energy
26 g = 9.81; % gravitational acceleration
27 row = 998.6; % water density kg/m^3
28 %% non-dimensionalization
29 t = t /sqrt(aa/g); % dimensionless time period
30 dt = tstep/sqrt(aa/g); % dimensionless time step
31 X(1:3)= X(1:3)/aa; % dimensionless position vector expressed in EFF
32 U(1:3) = U(1:3)/sqrt(g*aa); % dimensionless translational velocity in BFF
33 U(4:6) = U(4:6)/sqrt(g/aa); % dimensionless angular velocity in BFF
34 ro = ro/row; % dimensionless density
35 %rs = rs/row; % dimensionless density of additional ball
36 b = bb/aa; % dimensionless minor axis
37 [m,rg,I]= Property(ro,b);
38 % m: dimensionless mass
39 % rg: dimensionless center of mass
40 % I: dimensionless inertia tensor
41 %% Addedmass
42 mu = addedmass ( b ); % dimensionless added mass [mu11;mu22;mu55]
43 M = massm ( m, mu, rg, I ); % dimensionless mass matrix
44 %det(M)
45 %% 4th order Runge-kutta
46 T = 0 : dt : t ; % time series
47 T = T'; % Make it a column vecotor
48 all = zeros( 12 , length(T) ); % initialization all state variables
49 all (:,1) = [ X ; U ] ;
50 Ve = zeros (3, length(T));
51 J1 = transform(X(4:6));
52 Ve(1:3,1) = J1*U(1:3);
53 for i = 1 : length(T)-1

```

```

54 [ac1,vo1] = accelerate ( U, X, m, rg, mu, M ,I) ;
55 K1 = dt * ac1 ;
56 L1 = dt * vo1 ;
57 [ac2,vo2] = accelerate ( U+0.5*K1, X+0.5*L1, m, rg, mu, M , I ) ;
58 K2 = dt * ac2 ;
59 L2 = dt * vo2 ;
60 [ac3,vo3] = accelerate ( U+0.5*K2, X+0.5*L2, m, rg, mu, M , I ) ;
61 K3 = dt * ac3 ;
62 L3 = dt * vo3 ;
63 [ac4,vo4] = accelerate ( U+K3, X+L3, m, rg, mu, M , I ) ;
64 K4 = dt * ac4 ;
65 L4 = dt * vo4 ;
66 U = U + 1/6 * ( K1 + 2 * K2 + 2 * K3 + K4 ) ;
67 X = X + 1/6 * ( L1 + 2 * L2 + 2 * L3+ L4 ) ;
68 all ( : , i+1 ) = [ X; U ] ;
69 J1 = transform(X(4:6));
70 Ve(1:3,i+1) = J1*U(1:3);    % Dimensionless translation velocity in EFF
71 end
72 %% dimensionalize
73 Td = T*sqrt(aa/g); % dimensional time series
74 X = all(1:6,:);    % dimensionless position vector in EFF
75 Vb = all(7:9,:); % dimensionless translational velocity in BFF
76 omega = all(10:12,:); % dimensionless angular velocity in BFF
77 Xd([1,2,3],:) = X([1,2,3],:)*aa;
78 Xd([4,5,6],:) = X([4,5,6],:); % dimensional position vector in EFF
79 Vbd = Vb*sqrt(g*aa); % dimensional translational velocity in BFF
80 omegad = omega*sqrt(g/aa); % dimensional angular velocity in BFF
81 Ved = Ve*sqrt(g*aa); % dimensional velocity in EFF
82 K =0.5*(m+mu(1))*Vb(1,:).^2+0.5*(m+mu(2))*Vb(2,:).^2 ...
83     +0.5*(m+mu(2))*Vb(3,:).^2+0.5*I(1,1)*omega(1,:).^2 ...
84     +0.5*(I(2,2)+mu(3))*omega(2,:).^2+0.5*(I(3,3)+mu(3))*omega(3,:).^2 ...
85     -I(1,2)*omega(1,:).*omega(2,:)-I(2,3)*omega(2,:).*omega(3,:)...
86     -I(3,1)*omega(3,:).*omega(1,:);
87 P = -(m-1)*X(3,:);
88 E = K+P;
89 end
90 function [m,rg,I] = Property(ro,b)
91 % input arguments
92 % ro: density vector / density of water
93 % b: minor axis / mijor axis
94 % output arguments
95 % rg dimensionless center of mass in BFF
96 rg = [ 3/16*(ro(2)+ro(4)-ro(1)-ro(3))/(ro(1)+ro(2)+ro(3)+ro(4))
97       0
98       3/16*(ro(3)+ro(4)-ro(1)-ro(2))/(ro(1)+ro(2)+ro(3)+ro(4))*b];
99 % dimensionless inertia tensor
100 I11 = 1/40*b^2*(sum(ro));
101 I22 = 1/80*(b^2+1)*(sum(ro));
102 I33 = I22;
103 I13 = 1/40/pi*b^2*(ro(1)+ro(4)-ro(2)-ro(3));
104 I31 = I13;
105 I = [I11 , 0 , -I13
106     0 , I22 , 0
107     -I31 , 0 , I33];
108 % dimensionless mass
109 m = sum(ro)/4;
110 end
111 % Added mass
112 function mu= addedmass(b)

```

```

113 if b == 1
114     mu11 = 0.5;
115     mu22 = 0.5;
116     mu55 = 0;
117 else
118     % Eccentricity
119     e = sqrt(1-b^2);
120     % dimensionless factor l
121     k1 = 2*(1-e^2)/e^3*((0.5*log((1+e)/(1-e))-e));
122     % dimensionless factor n
123     k2 = 1/e^2-(1-e^2)/2/e^3*log((1+e)/(1-e));
124     % added mass for prolate spheroid
125     mu11 = k1/(2-k2);
126     mu22 = k2/(2-k2);
127     mu55 = -1/20*e^4*(k2-k1)/(-2*e^2+(b^2+1)*(k2-k1));
128 end
129 mu = [mu11;mu22;mu55];
130 end
131 % Mass matrix
132 function M = massm(m,mu,rg,I)
133 % Mass matrix
134 M1 = [m+mu(1),0,0,0,m*rg(3),-m*rg(2)];
135 M2 = [0,m+mu(2),0,-m*rg(3),0,m*rg(1)];
136 M3 = [0,0,m+mu(2),m*rg(2),-m*rg(1),0];
137 M4 = [0,-m*rg(3),m*rg(2),I(1,1),I(1,2),I(1,3)];
138 M5 = [m*rg(3),0,-m*rg(1),I(2,1),I(2,2)+mu(3),I(2,3)];
139 M6 = [-m*rg(2),m*rg(1),0,I(3,1),I(3,2),I(3,3)+mu(3)];
140 M = [M1;M2;M3;M4;M5;M6];
141 end
142 % Transformation matrix
143 function J1=transform(alpha)
144 J1 = [cos(alpha(2))*cos(alpha(3)),sin(alpha(1))*sin(alpha(2))*cos(alpha(3))-...
145       cos(alpha(1))*sin(alpha(3)),sin(alpha(1))*sin(alpha(3))+cos(alpha(1))*...
146       sin(alpha(2))*cos(alpha(3))
147       cos(alpha(2))*sin(alpha(3)),cos(alpha(1))*cos(alpha(3))+sin(alpha(1))*...
148       sin(alpha(2))*sin(alpha(3)),cos(alpha(1))*sin(alpha(2))*sin(alpha(3))-...
149       sin(alpha(1))*cos(alpha(3))
150       -sin(alpha(2)),sin(alpha(1))*cos(alpha(2)),cos(alpha(1))*cos(alpha(2))];
151 end

```

## Integrated function

```

1 function [ac,vo]=accelerate(U,X,m,rg,mu,M,I)
2 % input arguments :
3 % U: Dimensionless Velocity Vector in BFF
4 % X: Dimensionless Position Vector [x y z phi theta psi] in EFF
5 % m: Dimensionless Mass
6 % rg: Dimensionless Center of mass expressed in BFF
7 % mu: Dimensionless Added mass
8 % M: Dimensionless Mass matrix
9 % I: Dimensionless inertia tensor
10 v = U(1:3); % Dimensionless Translational velocity expressed in BFF
11 omega = U(4:6); % Dimensionless Angular velocity in BFF
12 alpha = X(4:6); % Euler Angles
13 [T,J,-,-] = transform(alpha);
14 % T transform a vector's expression from EFF to BFF
15 % J transform velocity vector in BFF to time derivative of position vector

```

```

16 %% Gravitational force and Buoyance
17 F = T*[0;0;(m-1)]; % Dimensionless Combination of Gravitational Force and Buoyance
18 % expressed in BFF
19 G = T*[0;0;m]; % Dimensionless Gravitational force expressed in BFF
20 m1 = cross(rg,G); % Dimensionless Moment produced by Gravitational expressed in BFF
21 %Force Moment produced by Buoyance equals to zero
22 GF = [F;m1]; % Dimensionless Generalized Froce expressed in BFF
23 %% Non-dimensional dynamic force
24 D = dyna(mu,v,omega);
25 %% Hydrodynamic damping
26 %%%
27 %%%
28 %% Non-dimensional force of coupling velocity, angular velocity, and rg
29 C = [m*cross(omega,v)+m*cross(omega,cross(omega,rg))
30      cross(omega,I*omega)+ m*cross(rg,cross(omega,v))];
31 %% Acceleration
32 ac = M\(D-C+GF); % Dimensionless Acceleration in BFF
33 vo = J*U; % Dimensionless Time derivative of position vector
34 end
35 % Transformation matrix
36 function [T,J,J1,J2]=transform(alpha)
37 % Transformation from EFF to BFF
38 % Effect of phi
39 Ta21 = cos(alpha(1));
40 Ta23 = sin(alpha(1));
41 Ta32 = -sin(alpha(1));
42 Ta33 = cos(alpha(1));
43 if alpha(1) == pi/2
44     Ta21 = 0;
45     Ta33 =0;
46 end
47 if alpha(1) == pi
48     Ta23 = 0;
49     Ta32 = 0;
50 end
51 Tphi = [1,      0,      0;
52         0, Ta21,      Ta23;
53         0, Ta32,      Ta33];
54 % Effect of theta
55 Tb11 = cos(alpha(2));
56 Tb13 = -sin(alpha(2));
57 Tb31 = sin(alpha(2));
58 Tb33 = cos(alpha(2));
59 if alpha(2) == pi/2
60     Tb11 = 0;
61     Tb33 =0;
62 end
63 if alpha(2) == pi
64     Tb13 = 0;
65     Tb31 = 0;
66 end
67 Ttheta = [Tb11, 0, Tb13;
68           0,      1,      0;
69           Tb31, 0, Tb33];
70 % Effect of psi
71 Tg11 = cos(alpha(3));
72 Tg12 = sin(alpha(3));
73 Tg21 = -sin(alpha(3));
74 Tg22 = cos(alpha(3));

```

```

75 if alpha(3) == pi/2
76     Tg11 = 0;
77     Tg22 = 0;
78 end
79 if alpha(2) == pi
80     Tg12 = 0;
81     Tg21 = 0;
82 end
83 Tpsi = [Tg11,Tg12,0;
84         Tg21,Tg22,0;
85         0, 0, 1];
86 % Transform vector's expression from EFF to BFF
87 T = Tphi*Ttheta*Tpsi;
88 T1 = Tphi*Ttheta;
89 Tt = [Tphi(:,1),T1(:,2),T(:,3)];
90 J1 = inv(T);
91 %J1 = [cos(alpha(2))*cos(alpha(3)) sin(alpha(1))*sin(alpha(2))*cos(alpha(3))...
92 %      -cos(alpha(1))*sin(alpha(3)) sin(alpha(1))*sin(alpha(3))+cos(alpha(1))*...
93 %      sin(alpha(2))*cos(alpha(3))
94 %      cos(alpha(2))*sin(alpha(3)) cos(alpha(1))*cos(alpha(3))+sin(alpha(1))*...
95 %      sin(alpha(2))*sin(alpha(3)) cos(alpha(1))*sin(alpha(2))*sin(alpha(3))-...
96 %      sin(alpha(1))*cos(alpha(3))
97 %      -sin(alpha(2)) sin(alpha(1))*cos(alpha(2)) cos(alpha(1))*cos(alpha(2))];
98 J2 = inv(Tt);
99 O = [0 0 0; 0 0 0; 0 0 0];
100 J = [J1, O; O, J2];
101 %J2 = [1 sin(alpha(1))*tan(alpha(2)) cos(alpha(1))*tan(alpha(2))
102 %      0 cos(alpha(1)) -sin(alpha(1))
103 %      0 sin(alpha(1))/cos(alpha(2)) cos(alpha(1))/cos(alpha(2))]
104 % J1 transform a vector's expression from BFF to EFF
105 % J2 transform angular velocity to time derivative of Euler angles
106 end
107 % Dynamic force
108 function D=dyna(mu,v,omega)
109 % Dynamic force
110 D1 = mu(2)*(v(2)*omega(3)-v(3)*omega(2));
111 D2 = mu(2)*v(3)*omega(1)-v(1)*omega(3)*mu(1);
112 D3 = v(1)*omega(2)*mu(1)-v(2)*omega(1)*mu(2);
113 D4 = 0;
114 D5 = mu(3)*omega(1)*omega(3)+v(1)*v(3)*(mu(2)-mu(1));
115 D6 = -mu(3)*omega(1)*omega(2)+v(1)*v(2)*(mu(1)-mu(2));
116 D = [D1;D2;D3;D4;D5;D6];
117 end

```

## E.3 POST-PROCESSING

### Plot histories of state variables

```

1 function plotfigure(T,all,model)
2 %% Dimensionless position and attitude in EFF
3 fg1 = figure(1);
4 set(fg1,'Position',[50 30 1270 630]);
5 subplot(2,3,1), plot(T(:,1),all(1,:));
6 xlabel('$\bar{t}$','Interpreter','latex','FontSize',20);

```

```

7 ylabel('$\bar{x}$', 'Interpreter', 'latex', 'FontSize', 20);
8
9 subplot(2,3,2), plot(T(:,1),all(2,:));
10 xlabel('$\bar{t}$', 'Interpreter', 'latex', 'FontSize', 20);
11 ylabel('$\bar{y}$', 'Interpreter', 'latex', 'FontSize', 20);
12
13 subplot(2,3,3), plot(T(:,1),all(3,:));
14 xlabel('$\bar{t}$', 'Interpreter', 'latex', 'FontSize', 20);
15 ylabel('$\bar{z}$', 'Interpreter', 'latex', 'FontSize', 20);
16
17
18 subplot(2,3,4), plot(T(:,1),all(4,:));
19 xlabel('$\bar{t}$', 'Interpreter', 'latex', 'FontSize', 20);
20 ylabel('$\phi$', 'Interpreter', 'latex', 'FontSize', 20, 'FontWeight', 'bold')
21
22 subplot(2,3,5), plot(T(:,1),all(5,:));
23 xlabel('$\bar{t}$', 'Interpreter', 'latex', 'FontSize', 20);
24 ylabel('$\theta$', 'Interpreter', 'latex', 'FontSize', 20, 'FontWeight', 'bold')
25
26 subplot(2,3,6), plot(T(:,1),all(6,:));
27 xlabel('$\bar{t}$', 'Interpreter', 'latex', 'FontSize', 20);
28 ylabel('$\psi$', 'Interpreter', 'latex', 'FontSize', 20, 'FontWeight', 'bold')
29 ti = suptitle('Dimensionless Position in EFF and Attitude');
30 set(ti, 'FontSize', 20);
31 saveas(fg1, [model, 'Dimensionless.Position.fig'])
32 %% Dimensional position and attitude in EFF
33 fg2 = figure(2);
34 set(fg2, 'Position', [50 30 1270 630]);
35 subplot(2,3,1), plot(T(:,2),all(7,:));
36 xlabel('$t$', 'Interpreter', 'latex', 'FontSize', 20);
37 ylabel('$x$', 'Interpreter', 'latex', 'FontSize', 20);
38
39 subplot(2,3,2), plot(T(:,2),all(8,:));
40 xlabel('$t$', 'Interpreter', 'latex', 'FontSize', 20);
41 ylabel('$y$', 'Interpreter', 'latex', 'FontSize', 20);
42
43 subplot(2,3,3), plot(T(:,2),all(9,:));
44 xlabel('$t$', 'Interpreter', 'latex', 'FontSize', 20);
45 ylabel('$z$', 'Interpreter', 'latex', 'FontSize', 20);
46
47 subplot(2,3,4), plot(T(:,2),all(10,:));
48 xlabel('$t$', 'Interpreter', 'latex', 'FontSize', 20);
49 ylabel('$\phi$', 'Interpreter', 'latex', 'FontSize', 20, 'FontWeight', 'bold')
50
51 subplot(2,3,5), plot(T(:,2),all(11,:));
52 xlabel('$t$', 'Interpreter', 'latex', 'FontSize', 20);
53 ylabel('$\theta$', 'Interpreter', 'latex', 'FontSize', 20, 'FontWeight', 'bold')
54
55 subplot(2,3,6), plot(T(:,2),all(12,:));
56 xlabel('$t$', 'Interpreter', 'latex', 'FontSize', 20);
57 ylabel('$\psi$', 'Interpreter', 'latex', 'FontSize', 20, 'FontWeight', 'bold')
58 ti = suptitle('Position and Attitude in EFF');
59 set(ti, 'FontSize', 20);
60 saveas(fg2, [model, 'Dimensional.Position.fig'])
61 %% Dimensionless velocity and angular velocity in BFF
62 fg3 = figure(3);
63 set(fg3, 'Position', [50 30 1270 630]);
64 subplot(2,3,1), plot(T(:,1),all(13,:));
65 xlabel('$\bar{t}$', 'Interpreter', 'latex', 'FontSize', 20);

```

```

66 ylabel('$\bar{u}$', 'Interpreter', 'latex', 'FontSize', 20);
67
68 subplot(2,3,2), plot(T(:,1),all(14,:));
69 xlabel('$\bar{t}$', 'Interpreter', 'latex', 'FontSize', 20);
70 ylabel('$\bar{v}$', 'Interpreter', 'latex', 'FontSize', 20);
71
72 subplot(2,3,3), plot(T(:,1),all(15,:));
73 xlabel('$\bar{t}$', 'Interpreter', 'latex', 'FontSize', 20);
74 ylabel('$\bar{w}$', 'Interpreter', 'latex', 'FontSize', 20);
75
76 subplot(2,3,4), plot(T(:,1),all(16,:));
77 xlabel('$\bar{t}$', 'Interpreter', 'latex', 'FontSize', 20);
78 ylabel('$\bar{p}$', 'Interpreter', 'latex', 'FontSize', 20);
79
80 subplot(2,3,5), plot(T(:,1),all(17,:));
81 xlabel('$\bar{t}$', 'Interpreter', 'latex', 'FontSize', 20);
82 ylabel('$\bar{q}$', 'Interpreter', 'latex', 'FontSize', 20);
83
84 subplot(2,3,6), plot(T(:,1),all(18,:));
85 xlabel('$\bar{t}$', 'Interpreter', 'latex', 'FontSize', 20);
86 ylabel('$\bar{r}$', 'Interpreter', 'latex', 'FontSize', 20);
87 c=suptitle('Dimensionless Translational Velocity and Angular Velocity in BFF');
88 set(c, 'FontSize', 20);
89 saveas(fig3, [model, 'Dimensionless.BFF.Velocity.fig'])
90 %% Dimensional velocity and angular velocity in BFF
91 fg4 = figure(4);
92 set(fig4, 'Position', [50 30 1270 630]);
93 subplot(2,3,1), plot(T(:,2),all(19,:));
94 xlabel('${t}$', 'Interpreter', 'latex', 'FontSize', 20);
95 ylabel('${u}$', 'Interpreter', 'latex', 'FontSize', 20);
96
97 subplot(2,3,2), plot(T(:,2),all(20,:));
98 xlabel('${t}$', 'Interpreter', 'latex', 'FontSize', 20);
99 ylabel('${v}$', 'Interpreter', 'latex', 'FontSize', 20);
100
101 subplot(2,3,3), plot(T(:,2),all(21,:));
102 xlabel('${t}$', 'Interpreter', 'latex', 'FontSize', 20);
103 ylabel('${w}$', 'Interpreter', 'latex', 'FontSize', 20);
104
105 subplot(2,3,4), plot(T(:,2),all(22,:));
106 xlabel('${t}$', 'Interpreter', 'latex', 'FontSize', 20);
107 ylabel('${p}$', 'Interpreter', 'latex', 'FontSize', 20);
108
109 subplot(2,3,5), plot(T(:,2),all(23,:));
110 xlabel('${t}$', 'Interpreter', 'latex', 'FontSize', 20);
111 ylabel('${q}$', 'Interpreter', 'latex', 'FontSize', 20);
112
113 subplot(2,3,6), plot(T(:,2),all(24,:));
114 xlabel('${t}$', 'Interpreter', 'latex', 'FontSize', 20);
115 ylabel('${r}$', 'Interpreter', 'latex', 'FontSize', 20);
116 ti = suptitle('Translational Velocity in EFF and Angular Velocity in BFF');
117 set(ti, 'FontSize', 20);
118 saveas(fig4, [model, 'Dimensional.BFF.Velocity.fig'])
119 %% Dimensionless velocity in EFF and angular velocity in BFF
120 fg5 = figure(5);
121 set(fig5, 'Position', [50 30 1270 630]);
122 subplot(2,3,1), plot(T(:,1),all(25,:));
123 xlabel('$\bar{t}$', 'Interpreter', 'latex', 'FontSize', 20);
124 ylabel('$\bar{u}_x$', 'Interpreter', 'latex', 'FontSize', 20);

```

```

125
126 subplot(2,3,2), plot(T(:,1),all(26,:));
127 xlabel('$\bar{t}$','Interpreter','latex','FontSize',20);
128 ylabel('$\bar{u}_y$','Interpreter','latex','FontSize',20);
129
130 subplot(2,3,3), plot(T(:,1),all(27,:));
131 xlabel('$\bar{t}$','Interpreter','latex','FontSize',20);
132 ylabel('$\bar{u}_z$','Interpreter','latex','FontSize',20);
133
134 subplot(2,3,4), plot(T(:,1),all(16,:));
135 xlabel('$\bar{t}$','Interpreter','latex','FontSize',20);
136 ylabel('$\bar{p}$','Interpreter','latex','FontSize',20);
137
138 subplot(2,3,5), plot(T(:,1),all(17,:));
139 xlabel('$\bar{t}$','Interpreter','latex','FontSize',20);
140 ylabel('$\bar{q}$','Interpreter','latex','FontSize',20);
141
142 subplot(2,3,6), plot(T(:,1),all(18,:));
143 xlabel('$\bar{t}$','Interpreter','latex','FontSize',20);
144 ylabel('$\bar{r}$','Interpreter','latex','FontSize',20);
145 ti = supitle('Dimensionless Translational Velocity in EFF and Angular Velocity in BFF');
146 set(ti,'FontSize',20);
147 saveas(fig5,[model,'Dimensionless.EFF_Velocity.fig'])
148 %% Dimensional velocity in EFF and angular velocity in BFF
149 fig6 = figure(6);
150 set(fig6,'Position',[50 30 1270 630]);
151 subplot(2,3,1), plot(T(:,2),all(28,:));
152 xlabel('${t}$','Interpreter','latex','FontSize',20);
153 ylabel('${u}_x$','Interpreter','latex','FontSize',20);
154
155 subplot(2,3,2), plot(T(:,2),all(29,:));
156 xlabel('${t}$','Interpreter','latex','FontSize',20);
157 ylabel('${u}_y$','Interpreter','latex','FontSize',20);
158
159 subplot(2,3,3), plot(T(:,2),all(30,:));
160 xlabel('${t}$','Interpreter','latex','FontSize',20);
161 ylabel('${u}_z$','Interpreter','latex','FontSize',20);
162
163 subplot(2,3,4), plot(T(:,2),all(22,:));
164 xlabel('${t}$','Interpreter','latex','FontSize',20);
165 ylabel('${p}$','Interpreter','latex','FontSize',20);
166
167 subplot(2,3,5), plot(T(:,2),all(23,:));
168 xlabel('${t}$','Interpreter','latex','FontSize',20);
169 ylabel('${q}$','Interpreter','latex','FontSize',20);
170
171 subplot(2,3,6), plot(T(:,2),all(24,:));
172 xlabel('${t}$','Interpreter','latex','FontSize',20);
173 ylabel('${r}$','Interpreter','latex','FontSize',20);
174 ti = supitle('Translational Velocity in EFF and Angular Velocity in BFF');
175 set(ti,'FontSize',20);
176 saveas(fig6,[model,'Dimensional.EFF_Velocity.fig'])
177 end

```

## Animation

```

1 function plotmoving (T,all,a,b,tstep,model)

```

```

2 % input arguments
3 % T:    ditional time series n by 1
4 % all:  ditional position vector in EFF
5 % a:    major axis
6 % b:    minor axis
7 % tstep: time step
8 % model: name of video created
9 ski = 300; % number of time steps skipped
10 %% make video
11 FV = VideoWriter(model);
12 FV.Quality = 100;
13 FV.FrameRate = 1/(tstep*ski)/20;
14 open(FV);
15 % initialization
16 parrow1 = [a+0.05;0;0];
17 parrow2 = [0;a;0];
18 parrow3 = [0;0;a];
19 fg7=figure(7);
20 set(fg7,'Position',[50 30 1270 630]);
21 %% subplot
22 xup = 0.3;  xlow = -0.3;
23 ylow = -0.3;  yup = 0.3;
24 zup = 0.5;  zlow = -0.2;
25 %%
26 q1 = subplot(1,2,2);
27 %set(q1,'position',[ 0.5703,0.1100,0.2638,0.8150]);
28 axis([xlow,xup,ylow,yup,zlow,zup])
29 view([0,-1,0])
30 set(q1,'ZDir','reverse'); % reverse z axis
31 set(q1,'yDir','reverse'); % reverse y axis
32 axis equal
33 axis([xlow,xup,ylow,yup,zlow,zup])
34 set(q1,'FontSize',12,'FontWeight','bold')
35 % xlabel ylabel zlabel
36 hx = annotation('textbox',[0.7 0.05 0.2 0.1], 'FontSize',16,'FontWeight','bold',...
37             'EdgeColor','none');
38 set(hx,'str','x(m)');
39 hz = annotation('textbox',[0.5 0.5 0.2 0.1], 'FontSize',16,'FontWeight','bold',...
40             'EdgeColor','none');
41 set(hz,'str','z(m)');
42 view([0,-1,0])
43 axis tight
44 opengl('software')
45 %%
46 q2 = subplot(1,2,1);
47 axes(q2)
48 %set(q2,'position',[0.1300,0.1100,0.3347,0.8150]);
49 set(q2,'ZDir','reverse'); % reverse z axis
50 set(q2,'yDir','reverse'); % reverse y axis
51 axis equal
52 axis([xlow,xup,ylow,yup,zlow,zup])
53 q2 = gca;
54 set(q2,'FontSize',12,'FontWeight','bold')
55 % xlabel ylabel zlabel
56 hx = annotation('textbox',[0.37 0.05 0.2 0.1], 'FontSize',16,'FontWeight','bold',...
57             'EdgeColor','none');
58 set(hx,'str','x(m)');
59 hy = annotation('textbox',[0.14 0.1 0.2 0.1], 'FontSize',16,'FontWeight','bold',...
60             'EdgeColor','none');

```

```

61 set(hy,'str','y(m)');
62 hz = annotation('textbox',[0.065 0.50 0.2 0.1], 'FontSize',16,'FontWeight','bold',...
63     'EdgeColor','none');
64 set(hz,'str','z(m)');
65 axis tight
66 opengl('software')
67 % for loop to create
68 for i=1:ski:length(T)*1.8/3 ;
69     pg = all(1:6,i);
70     t = T(i);
71     k=floor(i/ski+1);
72     n=30; % points in one dimension
73     [X,Y,Z]=ellipsoid(0,0,-0,a,b,b,n); % points on a ellipsoid
74     Tt=transform(pg(4:6)); % transformation matrix
75     for ii=1:n+1;
76         for j=1:n+1;
77             mm=Tt\[X(ii,j);Y(ii,j);Z(ii,j)];
78             X(ii,j)=mm(1)+pg(1);
79             Y(ii,j)=mm(2)+pg(2);
80             Z(ii,j)=mm(3)+pg(3);
81         end
82     end
83 parrowl1 = (Tt\parrow1)';
84 parrowl2 = (Tt\parrow2)';
85 parrowl3 = (Tt\parrow3)';
86 %%
87 axes(q1)
88 %set(q1,'position',[ 0.5703,0.1100,0.2638,0.8150]);
89 view([0,-1,0])
90 ff = mesh(X,Y,Z,'EdgeColor',[0 0 0.7],'FaceColor',[0 0 0.7]);
91 set(ff,'FaceAlpha',0.2)
92 set(ff,'EdgeAlpha',0.2)
93 ax = arrow3d(pg(1:3)',pg(1:3)'+parrowl1,20,cylinder,[0.15,0.1],[20,10],[1,0,0]);
94 ay = arrow3d(pg(1:3)',pg(1:3)'+parrowl2,20,cylinder,[0.15,0.1],[20,10],[1,0,1]);
95 az = arrow3d(pg(1:3)',pg(1:3)'+parrowl3,20,cylinder,[0.15,0.1],[20,10],[0,0,1]);
96 % "arrow3d" function from Matlab central
97 % http://www.mathworks.com/matlabcentral/fileexchange/8396-draw-3d-arrows
98 set(gca,'ZDir','reverse');
99 set(gca,'yDir','reverse');
100 axis equal
101 axis([xlow,xup,ylow,yup,zlow,zup])
102 view([0,-1,0])
103 legend([ax(1),ay(1),az(1)], 'x_h', 'y_h', 'z_h', 'best')
104 set(gca, 'FontSize', 12, 'FontWeight', 'bold')
105 %%
106 axes(q2)
107 %set(q2,'position',[0.1300,0.1100,0.3347,0.8150]);
108 ff = mesh(X,Y,Z,'EdgeColor',[0 0 0.7],'FaceColor',[0 0 0.7]);
109 set(ff,'FaceAlpha',0.2)
110 set(ff,'EdgeAlpha',0.2)
111 arrow3d(pg(1:3)',pg(1:3)'+parrowl1,20,cylinder,[0.15,0.1],[20,10],[1,0,0]);
112 arrow3d(pg(1:3)',pg(1:3)'+parrowl2,20,cylinder,[0.15,0.1],[20,10],[1,0,1]);
113 arrow3d(pg(1:3)',pg(1:3)'+parrowl3,20,cylinder,[0.15,0.1],[20,10],[0,0,1]);
114 set(gca,'yDir','reverse');
115 set(gca,'ZDir','reverse');
116 axis equal
117 axis([xlow,xup,ylow,yup,zlow,zup])
118 set(gca, 'FontSize', 12, 'FontWeight', 'bold')
119 % time

```

```
120 tm = annotation('textbox',[0.45 0.75 0.1 0.2], 'FontSize',16,'FontWeight','bold',...
121     'EdgeColor','none');
122 set(tm,'str',['t=',num2str(t,3),'(s)']);
123 %%
124 gf = getframe(fg7,[70 30 1160 600]);
125 frame(:,k) = gf;
126 delete(tm);
127 end
128 % output video
129 writeVideo(FV,frame(1:end));
130 close(FV)
131 end
132 % Transformation matrix
133 function [T,Tt]=transform(alpha)
134 %% Transformation from EFF to BFF
135 % Effect of phi
136 Tphi = [1,      0,      0;
137         0,cos(alpha(1)),sin(alpha(1));
138         0,-sin(alpha(1)),cos(alpha(1))];
139 % Effect of theta
140 Ttheta = [cos(alpha(2)), 0, -sin(alpha(2));
141          0,      1,      0;
142          sin(alpha(2)), 0, cos(alpha(2))];
143 % Effect of psi
144 Tpsi = [cos(alpha(3)),sin(alpha(3)),0;
145        -sin(alpha(3)),cos(alpha(3)),0;
146         0,      0,      1];
147 % Transfor mation
148 T = Tphi*Ttheta*Tpsi;
149 % Transformation from dalpha to omega
150 T1 = Tphi*Ttheta;
151 Tt = [Tphi(:,1),T1(:,2),T(:,3)];
152 end
```

DEPARTMENT OF MECHANICAL ENGINEERING

UNIVERSITY OF CALIFORNIA - BERKELEY

\*\*\*\*\*

LIBRARY PERMISSION FORM

MASTER'S PLAN II

Last Name:  First Name:  Middle Name:

SID :  Major Field Area :  Degree Goal:

Phone Number  Email :  Submission Date:

Report Title:

IMMEDIATE RELEASE

I authorize the Department of Mechanical Engineering to release my report to the UC Berkeley Library and have it made available to the public electronically through the library catalog as soon as is feasible after my report has been filed.

EMBARGO FOR 2 YEARS

I wish my report to be withheld for 2 years following the date of filing after which time it will be released to the UC Berkeley Library and made available to the public electronically through the library catalog.

EMBARGO FOR LESS/MORE THAN 2 YEARS

I wish my report to be withheld for \_\_\_\_\_ year(s) following the date of filing after which time it will be release to the UC Berkeley Library and made available to the public electronically through the library catalog.

Explanation required if more than 2 years:

Student Signature: Bo Yang

Date: 5/14/2015

MS Committee Chair Signature: Ronald W. Jensen Prof

Date: 5/14/2015